ROLE OF OXYGEN AND SALINITY ON BIOGEOCHEMICAL PROCESSES CONTROLLING MERCURY AND MONOMETHYLMERCURY FLUX FROM ESTUARINE SEDIMENTS

Joshua S. Vinson

A Thesis Submitted to the
University of North Carolina Wilmington in Partial Fulfillment
Of the Requirements for the Degree of
Master of Chemistry

Department of Chemistry and Biochemistry

University of North Carolina Wilmington

2008

Approved by

Advisory Committee

Dr. Stephen Skrabal
Chair

Dr. G. Brooks Avery

Dr. Robert Kieber

Dr. Joan Willey

Accepted by

Robert D. Roer

Digitally signed by Robert D. Roer
DN: cn=Robert D. Roer, o=UNCW, ou=Dean of the Graduate School & Research, email=roer@uncw.edu, c=US
Date: 2008.09.16 09:12:53 -04'00'

Dean, Graduate School

TABLE OF CONTENTS

ABSTRACT

Estuarine sediments are complex biogeochemical microenvironments that play an important role in the transformation and redistribution of mercury and methylmercury (MeHg) to overlying waters. The presence of sulfate-reducing bacteria is widely accepted to be a critical factor in mercury methylation. As freshwater contains typically low concentrations of sulfate and seawater is sulfate-rich, salt water intrusion to freshwater sediments by sea level rise or anthropogenic causes may significantly increase MeHg production and release by sediments. This study used high-resolution (millimeter-scale) pore water profiling of redox-active analytes, combined with simultaneous measurement of benthic fluxes, to discern how biogeochemical processes affect sediment-water exchange of dissolved mercury and MeHg in predominantly tidal freshwater and estuarine wetlands. Sediment incubations and manipulations of oxygen and salinity conditions were performed using sediment cores from two contrasting sites in the Cape Fear and White Oak estuaries.

The dominance of manganese reduction in Cape Fear sediments in February and June apparently inhibited the expected thermodynamic progression toward sulfate reduction and subsequent MeHg fluxes. Maximum MeHg fluxes of 29-36 pmol m^{-2} d^{-1} were observed in early fall (September) under anoxic, low salinity conditions and were coincident with of Fe^{2+} and Mn^{2+} pore water accumulation at the sediment-water interface (SWI) and low concentrations of H_2S (5-40 μM) below the SWI. Presence or absence of Mn^{2+} and Fe^{2+} at the SWI was consistently associated with MeHg fluxes, suggesting the reduction of metal oxyhydroxides in conjunction with sulfate reduction are factors controlling sediment-water exchange of MeHg. Variable fluxes of MeHg (0, -6, 6

pmol m^{-2} d^{-1}) during summer in White Oak sediments was observed in the presence of sulfate reduction under low salinity, suggesting the presence of other methylation-inhibiting mechanisms. These data suggest increasing salinities of freshwater sediments due to sea level rise or human activities promote sulfate reduction and associated MeHg production resulting in elevated concentrations of MeHg in the Cape Fear River sediments. In addition, Fe and Mn oxyhydroxides, which are effective barriers against the diffusion of MeHg to overlying water, are reduced during periods of anoxia and release MeHg to the overlying waters.

ACKNOWLEDGMENTS

Thank you to all my friends and family for all their moral support over the past few years. It's been a long, muddy, sometimes depressing, often frustrating, but always educational three years and I'm lucky to have had great friends and family to help see me through it.

I would also like to thank my committee and Carrie Miller, without whom many frustrations and complications with mercury analysis would have been far greater. Of course thank you to Dr. Skrabal for always being there to lend a hand, be it creating home-made microelectrodes or interpreting data.

Lastly I would like to thank the University of North Carolina at Wilmington, the department of chemistry and biochemistry, and Sut Ahuja for the financial support of this project.

LIST OF TABLES

Table Page

LIST OF FIGURES

Table Page

INTRODUCTION

Mercury (Hg) is a pervasive pollutant that enters the environment from a variety of natural and anthropogenic sources. Anthropogenic sources are estimated to be twofold greater than natural sources and have resulted in elevated environmental concentrations around the world due to the potentially long residence time of gaseous Hg(0) in the atmosphere (Fitzgerald et al., 1998, Lamborg et al., 2002). Monomethylmercury (MeHg) is the most toxic of Hg species and exists in aquatic environments primarily as CH_3HgOH or CH_3HgCl. Its high toxicity is a result of its ability to freely diffuse across cell membranes and bioaccumulate in higher trophic levels (Spry, 1991; Mason et al., 1996; Morel et al., 1998). Elevated concentrations of MeHg in fish caught along US coastline have led to health advisories for fish consumption in 65% of Atlantic waters, 100% of Gulf coast waters, and 37% of Pacific coast waters (USEPA, 2006).

The primary sources of Hg to estuarine and coastal sediments are atmospheric and river inputs (Horvat et al., 1999). Nearly all atmospheric Hg emissions occur as inorganic Hg(II) species (Morel, 1998). Microbiological processes are responsible for methylation, degradation, and reduction of Hg(II) to Hg(0) in sediments, and these processes ultimately control the speciation of Hg (Barkay, 1992). Wetland and estuarine sediments play a critical role in the transformation and flux of MeHg released into aquatic and estuarine ecosystems. Studies by Holmes and Lean (2006) found levels of MeHg in rivers to be correlated to the percentage of wetlands within the drainage basin. The Cape Fear river drainage basin drains over 45,000 acres of wetlands (Mallin 2008), making it a potentially significant source of MeHg to the estuary.

Estuarine sediments present very complex biogeochemical environments. Vertical fluctuations in the redoxicline, variable salinities, variable amounts and types of organic matter, and seasonality are just a few of the many factors that critically impact these microenvironments. Due to typically high levels of labile organic matter in estuarine sediments oxygen is often rapidly depleted near the sediment-water interface (SWI). Under reduced oxygen conditions microbial respiration shifts to alternate electron acceptors for the oxidation of carbon. Bacterial populations in sediments have been found to use the electron acceptor that produces the greatest free energy change upon oxidation of organic matter (Froelich et al., 1979). Free energies associated with the various electron acceptors are listed in Table 1. Under ideal conditions, aerobic respiration is expected to be carried out until oxygen levels are depleted at which time nitrate reduction takes over but is typically limited to a narrow zone below the depth of O_2 penetration, and contributes very little to sediment organic matter remineralization (Canfield et al., 1993). At depths below oxygen penetration manganese reduction becomes the thermodynamically favorable mode of organic matter oxidation. Upon depletion of manganese, iron reduction is predicted to take place, followed by sulfate reduction and then methanogenesis. This sequence of processes for carbon remineralization is often observed in surficial sediment layers (Luther et al., 1998) and is often seen to occur sequentially with sediment depth as depicted in Fig 1. It is now widely accepted that Hg methylation occurs under anoxic or suboxic conditions (Olson and Cooper, 1974; Compeau and Bartha, 1984) primarily by microbial sulfate reducers (Compeau and Bartha, 1985; Gilmour et al., 1992; King et al., 1999, 2001), although more recent studies have also implicated iron reducing bacteria in Hg methylation (Flemming, 2006).

Table 1. Free energy changes for bacterial oxidation reactions of organic matter. Adapted from Froelich et al. (1979).

Reaction	ΔG° kJ/mol Glucose
Aerobic Respiration	-3190
$(CH_2O)_{106}(NH_3)_{16}(H_3PO_4) + 138O_2 \rightarrow 106CO_2 + 16HNO_3 + H_3PO_4 + 122H_2O$	
Manganese Reduction	-3090
$(CH_2O)_{106}(NH_3)_{16}(H_3PO_4) + 236MnO_2 + 472H^+ \rightarrow 236Mn^{2+} + 106CO_2 + 8N_2 + H_3PO_4 + 366H_2O$	
Nitrate Reduction	-3030
$(CH_2O)_{106}(NH_3)_{16}(H_3PO_4) + 94.4HNO_3 \rightarrow 106CO_2 + 55.2N_2 + H_3PO_4 + 177.2\ H_2O$	
Iron Reduction	-1410
$(CH_2O)_{106}(NH_3)_{16}(H_3PO_4) + 212Fe_2O_3 + 848H^+ \rightarrow 424Fe^{2+} + 106CO_2 + 16NH_3 + H_3PO_4 + 530H_2O$	
	-1330
$(CH_2O)_{106}(NH_3)_{16}(H_3PO_4) + 424FeOOH + 848H^+ \rightarrow 424Fe^{2+} + 106CO_2 + 16NH_3 + H_3PO_4 + 742H_2O$	
Sulfate Reduction	-380
$(CH_2O)_{106}(NH_3)_{16}(H_3PO_4) + 53SO_4^{2-} \rightarrow 106CO_2 + 16NH_3 + 53S^- + H_3PO_4 + 106H_2O$	
Methanogenesis	-350
$(CH_2O)_{106}(NH_3)_{16}(H_3PO_4) \rightarrow 53CO_2 + 53CH_4 + 16NH_3 + H_3PO_4$	

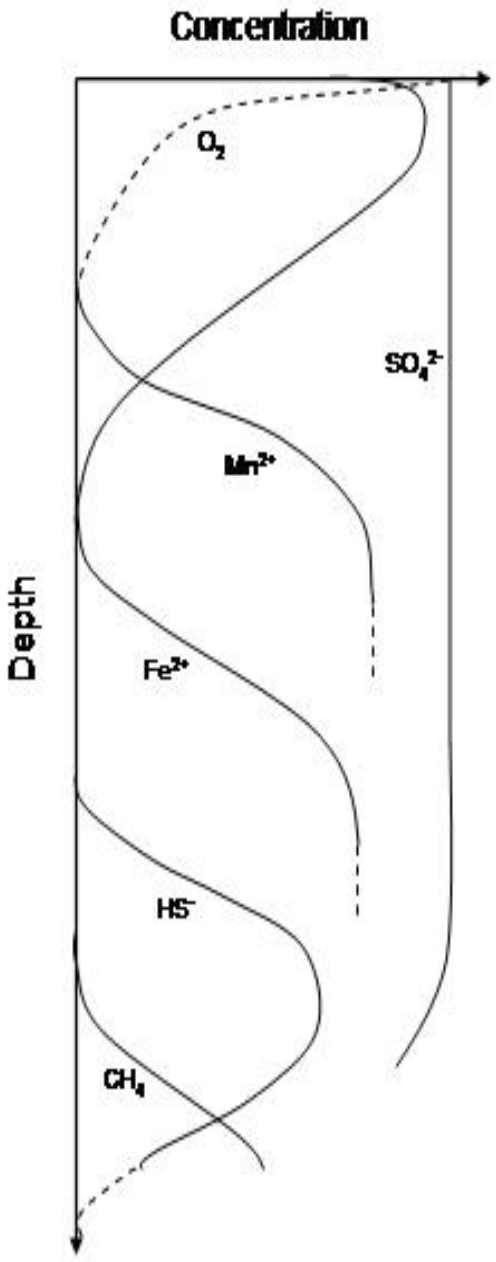

Figure 1. Hypothetical pore water profiles predicted by the successive utilization of inorganic compounds as terminal electron acceptors in sedimentary organic matter decomposition (modified from Froelich et al., 1979).

The majority of Hg(II) that enters water systems and is not photo-reduced to volatile Hg(0) binds to particulate matter and is deposited in bottom sediments (Morel et al., 1998), so estuaries are often considered a sinks for inorganic mercury. As sulfate reduction is thought to be chiefly responsible for Hg methylation and because estuaries are a sink for inorganic mercury, sea level rise, or salt water intrusion due to anthropogenic activities, and the associated introduction of higher concentrations of sulfate, may increase the amount of Hg methylated and potentially released from the sediments.

Sediments play a critical role in the amount of MeHg produced and released into the water column. Two general factors affect the amount of MeHg released into the water column by sediments: rates of Hg methylation and the potential for methylated Hg to escape the sediments and enter the water column (flux) by any combination of free diffusion, bioirrigation, and resuspension (Morel et al. 1998). Factors controlling sediment Hg methylation, transformation, and complexation have been studied extensively (Gilmour et al., 1992; King et al., 2001;Hines et al., 2006; Hammerschmidt and Fitzgerald, 2005). These studies indicate that active sulfate reducers are largely responsible for the methylation of inorganic Hg.

Recent studies have examined fluxes of Hg and MeHg in freshwater (Holmes et al., 2006; Goulet et al., 2007), estuarine (Choe et al., 2004; Gill et al, 1999; Mason et al, 2006) and marine sediments (Covelli et al. 1999). These studies have found that fluxes of MeHg generally increase with decreasing oxygen concentration (Covelli et al., 1999; Gill et al., 1999). Despite growing interest in the factors affecting fluxes of Hg and MeHg from sediments, few studies have examined how biogeochemistry and redox conditions in the surface sediment (top 10 cm) may impact the transport of mercury, especially

MeHg, across the SWI. Studies by Goulet et al. (2007) and Holmes and Lean (2006) used low resolution dialysis membranes (peepers) to examine pore waters and only measured sulfate and sulfide levels and not other redox active analytes. Beutal et al. (2008) monitored fluxes of Hg while also monitoring fluxes of redox-active analytes and found a direct relationship between the concentrations of Mn and Hg in the overlying water, but this study did not report any pore water profiles. Gill et al. (1999) found that estimated diffusional fluxes are often not closely related to actual flux, suggesting factors controlling Hg and MeHg flux are processes occurring directly at the SWI. To better understand the biogeochemical factors affecting rates of Hg and MeHg flux from sediments, high resolution pore water profiles of redox-active analytes are needed. Development of a gold amalgam voltammetric microelectrode by Brendel and Luther (1995) has allowed for millimeter-scale resolution of pore water Fe, Mn, and sulfide.

This study used the microelectrode method developed by Brendel and Luther (1995) to generate high-resolution pore water profiles of redox-active analytes, while simultaneously using sediment incubation chambers to monitor Hg and MeHg sediment fluxes under varying conditions. Because active sulfate-reducing bacteria are largely responsible for methylation of Hg and oxygen levels have been reported to affect MeHg flux (Covelli et al., 1999,; Gill et al. 1999, Gagnon,1996), this study examined the flux of Hg and MeHg under manipulated “oxic” and “anoxic” conditions. In addition, effects of changing salinity on sulfate reduction and subsequent changes in sediment biogeochemistry and MeHg exchange were examined.

METHODS

Overview

Two approaches were utilized to better understand how salinity and estuarine sediment biogeochemistry affect Hg sediment flux dynamics. These two approaches were benthic flux measurement by sediment incubation chambers and sediment depth profiles of the redox-active analytes Measurements of TDHg and MeHg, Reducible Fe (R-Fe) and reducible Mn (R-Mn) in sediments from sectioned cores, and sulfate/chloride sediment fluxes were incorporated for the last two experiments.

Sediment cores from two freshwater-dominated estuarine sites were taken and transported intact to the laboratory where they were incubated under either anoxic or oxic conditions for 7-18 days. At the end of this time the overlying water was replaced with water containing sulfate for another 7-18 days. Due to drought, by experiment IV one site had become increasingly saline and the experiment was carried out in reverse (saline followed by freshwater). At representative time points the overlying water was sampled and analyzed for MeHg, TDHg, dissolved organic carbon (DOC), and in the last two experiments sulfate and chloride. Sediment depth profiles of the redox-active analytes, Mn^{2+}, Fe^{2+}, and H_2S were measured using a gold amalgam voltammetric microelectrode on the same days as flux samples were taken. Dissolved oxygen was measured in experiments II and IV by a Unisense OX100 microsensor. Sediment cores were sectioned at the beginning and end of each incubation treatment and samples frozen until analysis.

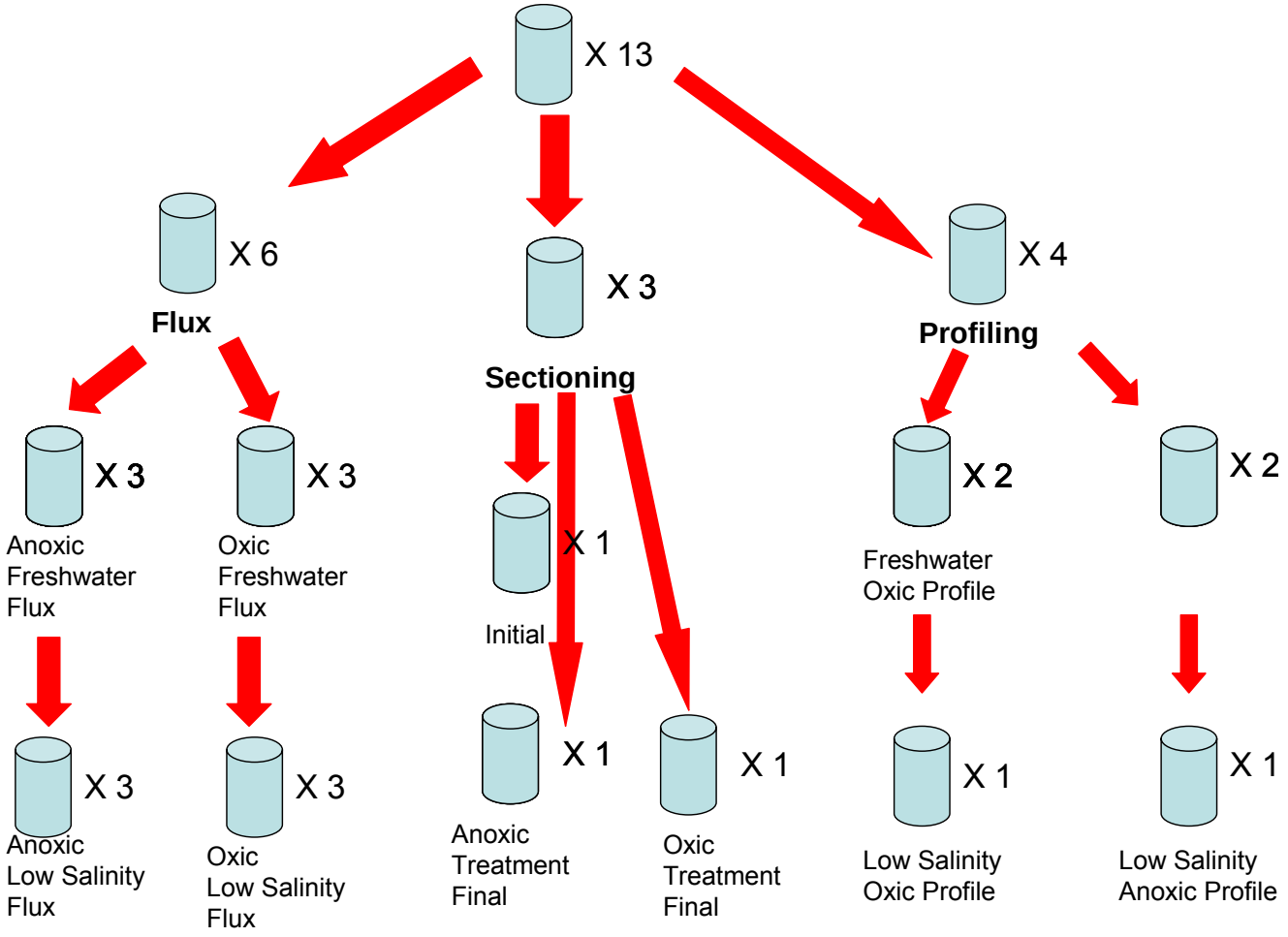

Figure 2. Flow chart of experimental procedures, depicting how sediment incubation cores were distributed for flux measurements, analysis of sediment content by core sectioning, and pore water profiling by microelectrode. Numbers represent those used in experiments III&IV and were slightly different for experiments I&II. Core sectioning was only carried out in experiments III&IV.

Study Sites

Eagle Island

This study site was located on Eagle Island (34°15'31" N, 77°58'43" W) in the Cape Fear River in North Carolina (Fig. 3). This site coincides with station P6 of the Wilmington Harbor Monitoring Program (WHMP) (Figure 2; Hackney et al., 2003). Monthly monitoring of this site as part of a US Army Corps of Engineers project provides extensive geochemical data. The site represents a transition between saline and fresh-dominated stations providing a variety of salinity conditions and geochemical variations for comparison. This section of the Cape Fear River has been impacted by historical imputs of Hg form a defunct manufacturing plant and provides an opportunity to study mercury sediment dynamics in a saline to freshwater transition zone.

Intact sediment cores, along with overlying surface water (when present), were collected at low tide from the intertidal mud flats within one meter of the marsh edge. Three experiments were carried out with Eagle Island sediments in June, October, and February.

White Oak River Site

The section of the White Oak River examined in this study (Station GI) has been previously described by Martens and Goldhaber (1978), Kelley (1993), Chanton et al., (1989) and Kelley et al., (1995). Briefly, it is a tidal freshwater section of an eastern North Carolina estuary located approximately 20 km from the Atlantic Ocean (Fig. 4). The diurnal tides are approximately 70 cm in amplitude (Chanton and Martens, 1988) with water depths ranging from about 5 cm to 1 m. The sediments have been previously

Figure 3. Satellite image of Eagle Island study site on the Cape Fear River north-west of Wilmington (map from Google Earth).

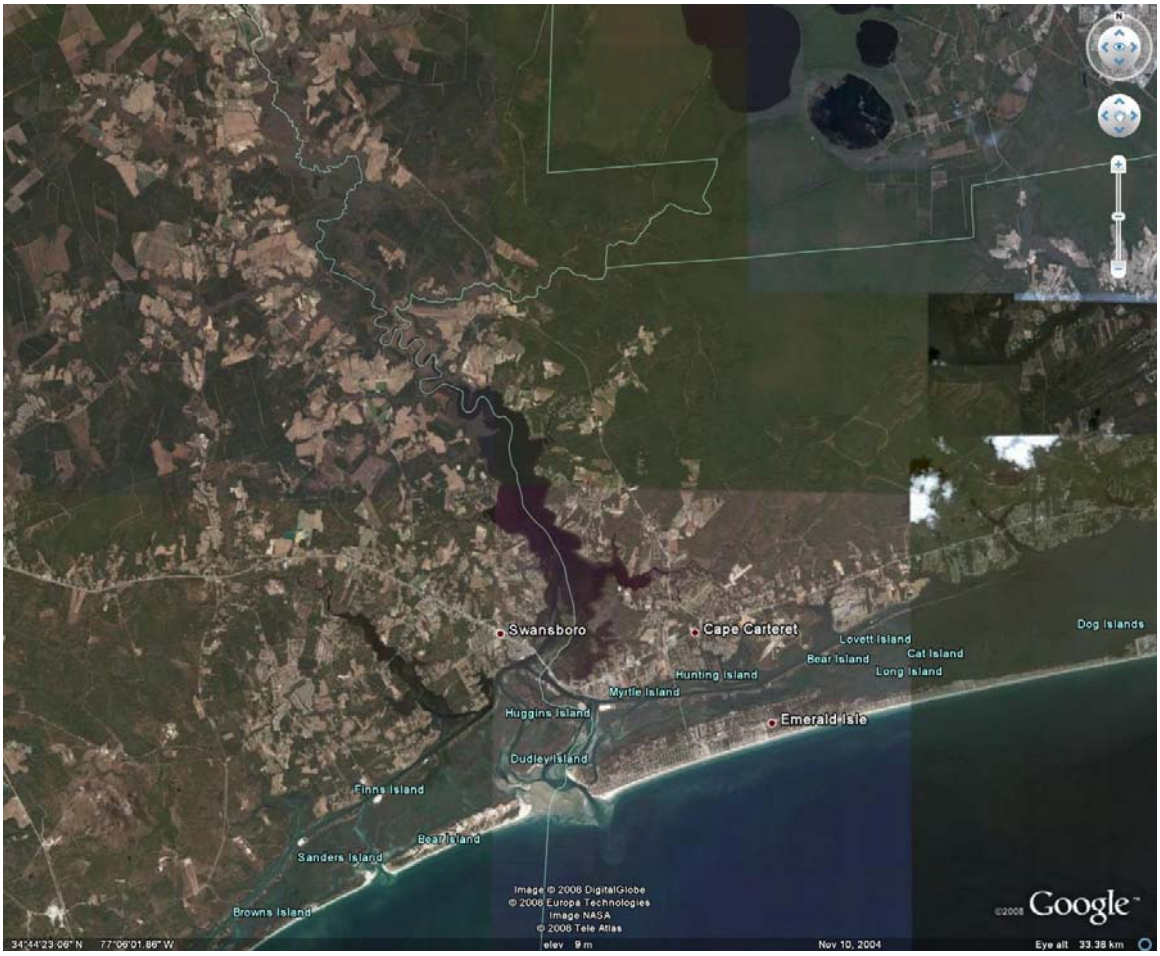

Figure 4. Satellite image of White Oak River study site (map from Google Earth)

described as Dorovan muck (Barnhill, 1992) and are underlain by sand. The sediments contain approximately 18% organic carbon which consists largely of macrophyte detritus (Avery, 2002 and references therein). The main flora contributing organic material to the sediments are the submerged macrophytes *Ceratophyllum* and *Najas*, as well as several blue-green algal species (Kelley, 1993). Intact sediment cores, along with overlying surface water (when present), were taken from a boat when possible to avoid disturbing the sediments.

Field Sampling

Cores were collected during low tide using trace-metal clean acrylic cores with dimensions 3 mm thick x 14.5 cm diameter x 25 cm long. To transport the cores back to the laboratory, they were sealed on the top and bottom with trace metal clean polyethylene caps and externally sealed with rubber gaskets on the bottom to prevent pore water leakage. Cores were transported, as quickly as possible, to the lab where they were incubated at temperatures similar to that in the field until beginning the experiments.

Experimental Design

Four sediment core incubation experiments were carried out as follows. Experiments I, II, IV were conducted with sediments and water taken from Eagle Island in June 2006, October 2006, and February 2008, respectively. Experiment III was conducted with sediments and water taken from the White Oak River study site in September 2007. Over the course of the four experiments minor adjustments to the number of cores taken were made. All experiments contained the following: 1 core

maintained under anoxic conditions for profiling redox-sensitive analytes; 1 core maintained under oxic conditions for profiling redox-sensitive analytes; 2 replicate cores maintained under anoxic conditions for monitoring sediment fluxes; and 2 replicate cores maintained under oxic conditions for monitoring sediment fluxes, for a total of six cores. In addition to these cores for experiments III & IV, an additional 7 cores were taken: 2 cores each for anoxic and oxic profiling of redox analytes; triplicate cores for both anoxic and oxic flux monitoring; 1 core for initial sediment sectioning; and 2 cores for sectioning at the end of first treatment (2 of the flux cores were sacrificed and sectioned at the end of the second treatment) for a total of 13 sediment cores (see fig. 2)

Forty liters of fresh river water (<0.5) was collected at or near the sample site and used to fill two acrylic cylinders with dimensions 3 mm thick x 14.5 cm diameter x 88 cm long. Anoxic and oxic recharge waters were bubbled with trace metal tested N_2 and compressed air, respectively for ~2 h to remove oxygen from the anoxic recharge and saturate the oxic recharge with oxygen. Overlying water in sediment cores was pumped out and replaced with treated recharge water three times to ensure complete water replacement, after which the sediment core was filled with treated recharge water and the water level recorded (water level ranged from 8-12 cm above sediment surface). In experiments III & IV one core was sectioned immediately and sediments frozen for further analysis (described further under Analytical Methods). All cores were fitted with trace-metal clean lids with Teflon sampling apparatus and gas bubblers. Anoxic cores were bubbled with Hg-tested N_2 and oxic cores were bubbled with Hg–tested compressed air.

Benthic fluxes were measured using core incubation techniques described by Burdige and Homestead (1994), modified for trace metals as described by Skrabal et al. (1997). Briefly, samples of recharge water and overlying water in cores were removed as a function of time (ranging from 3-6 times over the course of 7-18 days per treatment) using a peristaltic pump fitted with trace metal clean C-Flex® tubing and Teflon connectors. Samples were filtered inline during collection through Meissner 0.2 μM polyethersulfone filter cartridges during experiment I&II and through 0.2 μM polysulfone membrane set in a Teflon casing for experiments III&IV. Volumes of water removed during sampling were replaced with water from recharge cylinders. MeHg samples (100 mL) from experiments I&II were treated with 200 μL of 9 M H_2SO_4 (trace-metal grade) and stored in 125 mL trace metal clean FEP-Teflon bottles in a refrigerator. MeHg samples (100mL) from experiments III&IV were treated with 500 μL of 12 M HCl (trace-metal grade, Fisher) and stored in 125 mL trace metal clean polyethylene bottles in a refrigerator. TDHg samples (100mL) from experiments I & II were treated with 0.5 mL of 0.2 N bromine monochloride and stored in 125 mL trace metal clean FEP-Teflon bottles at room temperature. TDHg samples (100mL) from experiments III&IV were treated with 0.5 mL of 12 M HCl (trace-metal grade) and stored in 125 mL trace metal clean polyethylene bottles at room temperature. DOC samples (50 mL) were treated with 50 μL of 6 M HCl and stored in glass vials in a refrigerator. Sulfate samples (5 mL) were acidified with 50 μL of 10% HCl and stored in polyethylene vials in a refrigerator. Chloride samples (5 mL) were untreated and stored in polyethylene vials in a refrigerator. After sufficient time had passed to observe flux trends, the overlying water was removed, flushed 3 times as before, and replaced with sulfate-treated (1.6 mM) river water

(experiment I), or low salinity (3-5) river water (experiments II & III). Experiment IV was carried out in reverse (saline treatment followed by freshwater treatment) due to drought and increased salinity of the Eagle Island study site.

Core sectioning was accomplished by one of two ways depending on the consistency of sediments. Eagle Island sediments were more consolidated and could be extruded from the acrylic core and sliced at 1-2 cm intervals with a knife. White Oak sediments had higher water content and 1-2 cm sections had to be scraped of with a plastic spoon. pH was measured for the surface and bottom sections of the core. Cores were sectioned at 0-1, 1-2, 2-4, 4-6, 6-8, and 8-10 cm intervals and stored in 150 mL trace-metal tested polyethylene cups and kept frozen until analysis.

Analytical Techniques

Sediment Depth Profiles

Depth profiles of redox active analytes were generated using a gold amalgam voltametric microelectrode method described by Brendel and Luther (1995). The Au/Hg electrodes were assembled using the guidelines outlined in Brendel (1995). After construction, the surface of the electrode was roughly polished using 400 grit sandpaper to remove all major scratches and to ensure an even electrode surface. A series of diamond polishes (15, 6, 1, and 0.05 μm) in succession were then used to obtain a mirror finish on the electrode surface. To check that the surface was flat and smooth, the tips of the electrodes were examined with a bench top microscope. Once an adequate surface was confirmed, the electrode was plated with Hg. The polished electrode and a saturated calomel electrode were placed in a 0.1 M ACS grade $Hg(NO_3)_2 \cdot H_2O$ (Baker) solution

acidified to a pH of 1.5 with nitric acid and purged with nitrogen for 5 minutes. The plate was formed by electroreducing Hg(II) at a potential of -0.1 V for 4 min. After sitting for 24 h the amalgam was polarized to ensure reproducible peak positions and sensitivities necessary for analysis. This was accomplished by attaching the Au/Hg electrode to the negative terminal and a Pt wire to the positive terminal of a 9 V battery, and placing them both in 1 M NaOH solution for 90 s. Allowing the amalgam to set overnight prior to polarization reduced the electrical noise of the scans.

Prior to electrode measurements, a calibration curve for Mn^{2+} was obtained using a standard solution. Analytical grade chemicals $MnSO_4 \cdot H_2O$ (Fisher) and deionized water provided by A Milli-Q Plus Ultra-pure water system (Millipore, Bedford, MA) acidified to pH 2 were used to make standard solutions. All calibrations were performed using 0.45 μm filtered Wrightsville Beach seawater as a supporting electrolyte. Deionized water was used to dilute the seawater when salinities under 32 were required. N_2 gas was bubbled through the seawater for 30 minutes prior to calibration to purge the water of O_2; bubbling was continued through the scanning process.

The polarographic peak for sulfide is characterized as total H_2S, which represents the sum of the H_2S, HS^-, and polysulfide species (Luther et al., 1998). Under the standard scanning parameters used in this study the total sulfide peak begins to split into two distinct peaks at concentrations above 100 μM. Calibrations were performed for concentrations below this point; experimental concentration never reached concentrations above 80 uM.

A standard three-electrode configuration, consisting of the Au/Hg working electrode, a saturated calomel reference electrode with a salt bridge filled with 3 M KCl,

and a Pt wire counter electrode, was used in obtaining all electrochemical measurements. The reference and counter electrodes were inserted and fixed in the surface of the core approximately 1 to 2 cm from the insertion point of the working electrode. The Au/Hg electrode was inserted into the sediment core using a micromanipulator. All voltammetric scans for Fe^{2+}, Mn^{2+}, and S^{2-} were performed using an Analytical Instrument Systems DLK-60 and DLK-100 potentiostat using accompanying AIS software loaded onto a laptop. The potentiostat and laptop were electrically grounded to each other, and powered by a marine battery in order to decrease external electrical noise. The whole system was grounded to the cold water pipe in the building for additional noise reduction.

The voltammetric technique used in this study was square wave voltammetry (SWV). In SWV, the square wave form consists of a symmetrical square wave pulse of the potential applied to the Au/Hg electrode, where the amplitude and step height are defined by the user (Kounaves, 1997). The resultant current, or the net current, is the difference between the forward and reverse currents and is centered on the redox potential of the analyte of interest. The peak height at these potentials is directly proportional to the concentration of the electroactive species reduced or oxidized at the working electrode. This method is ideal because it has the ability for low detection limits, fast scan rates, and exclusion of background noise (Brett and Brett, 1998).

The standard parameters used for SWV were as follows: pulse height 15 mV, step increment 2 mV, frequency 100 Hz, scan rate 200 mV sec^{-1}. The voltage range scanned was generally from -0.1 to -1.8 V. As described in Brendel and Luther (1995), the microelectrode is conditioned at each scan by applying a potential that removes any

previously deposited redox-active species. For the purpose of this study, the potential applied was -0.8 V for the duration of 2 min due to the possible presence of reduced species. After conditioning, the electrode was allowed to equilibrate for 5 s before applying the wave form.

Prior to taking measurements in the cores, the electrode was calibrated for Mn under the same environmental conditions (salinity and temperature) in which the cores were collected. The "pilot ion method" (Meites 1965) was used, based on published calibration slopes generated for Mn, Fe, H_2S (Brendel and Luther 1995), to obtain calibration curves for all analytes on a given day since the relative slopes for these curves are constant. Mn was chosen as our standard for calibration because it is relatively stable at seawater pH.

After calibration, measurements were then obtained from the sediment cores. Each core was sectioned into 4 quadrants, each reserved for different time points. For each profile, the working electrode was placed in the center of the quadrant so that it was away from the side of the core tube and from locations where subsequent profiles would be obtained. Voltammetric measurements were taken over a total depth 0 to 9 cm. Oxygen measurements were taken 1 cm above the SWI to a depth of 0.7 cm. One anoxic and one oxic core were each profiled on days coinciding with sampling of flux cores.

Data collected with the DLK-60 and DLK-100 software was converted into Excel spreadsheets and imported to the program PeakFit v.4.12 (Jandel Scientific) for peak height measurements. This software has demonstrated the ability to measure an accurate baseline and high resolution for all analytes studied, but especially for Fe when Mn is

present (Brendel, 1995). Where more than one redox-species was present, distinct baselines were drawn and each peak was calculated independent of the others.

Oxygen concentrations were determined using a Unisense OX100 microsensor. Calibrations for the microsensor were conducted following the manufacturers instructions before obtaining any data. Microsensors were calibrated using the same river water as that in the incubated cores, and at similar environmental temperatures. Nitrogen gas was bubbled through the river water for at least 10 minutes to remove O_2, and an aquarium pump was used to achieve O_2 saturation for calibrations.

Total Dissolved Mercury Analysis

TDHg was analyzed according to EPA method 1631 with some adjustments. Reagents used for TDHg analysis were reagent grade materials from VWR, J.T. Baker, Aldrich Chemical, and Fisher Scientific, unless otherwise noted. Milli-Q water was used for all analyses, reagent and standard preparations. The stock Hg standard, (Fluka) contained 4.99 mM mercury as $Hg(NO_3)2{\cdot}H_2O$ and remains stable for one year or until the expiration date (USEPA Method 1631). The secondary Hg standard (4.99 μM) is a dilution of 100 μL of the stock Hg standard with 500 μL BrCl solution diluted to 100 mL, gravimetrically in a Teflon bottle, with Milli-Q. Working Hg standards of 49.9 nM and 0.499 nM were prepared by diluting the secondary Hg standard. Both working standards were prepared monthly.

The calibration curve for total Hg was made using both working standards. Calibration blanks were made by adding 250 μL BrCl and 75 μL NH_2OH to 50 mL of Milli-Q. All calibration standards were made by adding 50 mL of Milli-Q and 250 μL

BrCl (to oxidize all the Hg in the sample to Hg(II)) to each 50 mL polypropylene autosampler vial. The first sets of standards were prepared by sequential addition of 0.100, 0.250, and 1.0 mL dilute working standard producing concentrations of 1.0, 2.5, and 10 pM. The next set of standards were prepared by addition of 0.025, 0.075, and 0.125 mL of concentrated working standard to produce concentrations of 25, 75, and 125 pM. Bottles containing the standards were capped and inverted to mix the solutions and allowed to react for a minimum of 30 min. Finally, 75 μL of NH_2OH was added to each bottle and mixed until the excess BrCl was destroyed and the yellow color disappeared.

The day before analysis samples preserved with HCl (experiments III & IV) were treated with 0.5 mL of 0.2 N BrCl and allowed to oxidize overnight. Prior to analysis the preserved sample was reduced with the addition of $NH_2OH{\cdot}HCl$, at approximately 30% of the volume of BrCl, in order to destroy all remaining BrCl.

TDHg was analyzed by USEPA Method 1631, by oxidation, reduction to Hg(0), purge and trap, thermal desorption and cold vapor atomic fluorescent spectrometry (CVAFS), using a Tekran Model 2600 Mercury Analysis System with a Tekran model 2620 auntosampler. A calibration curve with standards ranging from 0 to 125 pM was constructed prior to sample analysis with consistent correlation coefficients greater than 0.99.

Dissolved Monomethylmercury Analysis

Dissolved MeHg in water was analyzed according to EPA method 1630. Water samples were distilled at 125 ± 3^0C and the distillate collected. Four heating blocks accommodating three distillation vials each were placed in a frying skillet and brought to

a temperature of 125 ± 3^0C. 45 mL aliquots of samples were poured into pre-weighed distillation vials and exact masses recorded. 200 uL of 1 % APDC solution was added to vials and distillation caps securely fastened. 5 mL of Milli-Q was added to pre-weighed receiving vials with a 40 mL mark engraved and caps securely fastened. Distillation vials were placed in heating block and connected to receiving vials with an argon gas flow of 60 ± 20 mL/min. Receiving vials were held in a Styrofoam cooler filled with ice. Samples were distilled until each of the twelve receiving vials was filled to the engraved 40 mL line. Upon complete distillation FEP-Teflon tubing on the receiving vials is looped around to close off the second port of the cap and samples stored at room temperature until analysis (no longer than 48 h later). Distillations vials and receivers were weighed after distillation and percent distilled and percent recovered calculated.

Immediately before analysis 0.5 mL of 2 M acetate buffer and the 40 mL distilled sample were added to a glass reaction vessel/bubbler. 80 µL of freshly thawed $NaBEt_4$ was added to bubbler and allowed to react for 17min to convert all CH_3Hg to volatile methylethylmercury. After ethylation, a graphitic carbon Carbotrap® was attached to each bubbler with a fluoropolymer fitting. The sample was then purged with argon for 17 min at 200 mL/min. Absorbed water was dried from the Carbotrap® by connecting the argon line directly to the trap and allowing it to dry for 7 min. According to USEPA Method 1630 dried traps are stable for up to 6 h.

Samples were analyzed by connecting Carbotraps® to the GC column using a FEP-Teflon fitting. A nichrome wire coil was placed around the Carbotrap®, centered over, and extending beyond, the packing material. Argon gas lines with flow rates of 40 mL/min were connected to the other end of Carbotrap® and gas allowed to flow for 30 s.

Sample was then thermally desorbed from trap by heating of the nichrome wire and MeHg gas was carried through a pyrolytic decomposition column, which converted organo mercury forms to elemental Hg(0), and then into the cell of a cold-vapor atomic fluorescence spectrometer (CVAFS) for detection (USEPA Method 1630).

Calibration blanks were analyzed by adding 80 µL freshly thawed $NaBEt_4$ to 50 mL of Milli-Q buffered with .5 mL of 2 M acetate buffer in a glass bubbler and following the above steps for purging and sample analysis. Calibration standards were prepared by sequential addition of 10, 20, 40, 60, and 100 µL of working MeHg standard to 50 mL of buffered Milli-Q. Standard were treated with 80 µL freshly thawed $NaBEt_4$, allowed to react for 17 minutes, then purged onto Carbotrap®, dried for 7 min and analyzed. Calibration curves were plotted as total MeHg in picograms to be able to account for variability in distillation sample volume. Total MeHg of samples was then divided by the distilled sample volume to calculate concentrations in pM. Sample duplicates, spike addition, and distillation blanks were run every 10 samples.

Dissolved Organic Carbon Analysis

Dissolved organic carbon was determined by high temperature combustion (HTC) using a Shimadzu TOC 5000 total organic carbon analyzer equipped with an ASI 5000 autosampler (Shimadzu, Kyoto, Japan). Standards were prepared from reagent grade potassium hydrogen phthalate (KHP) in Milli-Q Plus Ultra Pure Water. Samples and standards were acidified to pH 2 with 2 M HCl and sparged with carbon dioxide free carrier gas for 5 min at a flow rate of 125 ml min-1 to remove inorganic carbon prior to injection onto a heated catalyst bed (0.5% Pt on alumina support, 680°C, regular

sensitivity). A nondispersive infrared detector measured carbon dioxide gas from the combusted carbon. Each sample was injected 4 times. The relative standard deviation was < 3%. The detection limit for this instrument is 5 μM. All samples were run in triplicate.

Sediment Mercury Analysis

Frozen sediment samples from sectioned cores were placed in the refrigerator overnight to thaw. A mass of 0.5 to 1.5 g of wet sediment was weighed into a 30 mL trace metal clean FEP-Teflon vial. In a fume hood 8.0 mL of HCl (trace metal grade) was added followed by 2.0 mL of HNO_3 (trace metal grade). Vials were capped and allowed the sediment allowed to digest at room temperature overnight. After digestion the samples were diluted to 25 mL with Milli-Q, shaken vigorously and sediment allowed to settle until supernatant became clear. A volume of 250 μL of diluted digestate was pipetted to a polypropylene auto sampler vial and diluted to 50 mL with Milli-Q. Sample was treated with 250 μL of 0.2 N BrCl, capped, inverted, and allowed to oxidize for 30 min. Resulting samples were then analyzed by the method described previously for total TDHg. Sample duplicates, spike additions, blanks and SRMs were run a minimum of every 15 samples. Wet sediment samples were weighed and placed in drying oven on day of analysis to determine wet-dry ratios.

Sediment MeHg content was analyzed according to methods proposed by Horvat et al. (1993) with some modifications. Eight frozen sediment samples from sectioned cores were placed in the refrigerator overnight to thaw. A mass of 0.5 to 2.0 g of wet sediment was weighed into a pre-weighed FEP-Teflon distillation vial. A volume of 0.3

mL of 20 % KCl and .750 mL 9M H_2SO_4 was added to distillation vial and then diluted to 30 mL with Milli-Q gravimetrically. A volume of 5.0 mL of Milli-Q was added to the Teflon receiving vials. Samples were distilled for 3-4 h, as described previously for dissolved MeHg in water, in heating blocks set in a frying skillet at 145 ^{0}C. Due to greater concentrations of MeHg in sediments only a portion of the distillate was analyzed. Specifically 50, 30, and 30% of distillate from samples, Spike additions, and SRMs, respectively, was diluted and analyzed. Calibration standards were prepared as described previously for MeHg with calibration standards ranging from 10 to 250 pg MeHg. The partial volumes analyzed were corrected by calculating concentrations from total picograms based on a calibration curve. With this exception samples were analyzed in the same method previously described for dissolved MeHg in water. Duplicate samples, spike additions, blanks and SRMs were run every 8 samples. Wet sediment samples were weighed and placed in drying oven on day of analysis to determine wet-dry ratios.

Reducible Fe and Mn in Sediments Analysis

Solid phase Mn and Fe were determined for sediment samples following the dithionite extraction methods desribed by Kostka and Luther (1994). Prior to analysis, frozen sediment samples from sectioned cores were thawed and homogenized with a plastic spatula. Triplicate 0.4 to 0.6 g wet sediment samples were placed into 15 ml centrifuge tubes containing 0.5 g sodium dithionite in 10 ml of 0.35 M acetate/0.2 M sodium citrate (pH 4.8). These samples were placed onto a water bath rotary shaker at 60 °C and at a speed sufficient to maintain constant suspension for 4 hours. The supernatant was removed and analyzed for Mn and Fe on a Perkin Elmer Atomic Absorption

Spectrometer Model 3110. Matrix matched calibration curves were prepared for both Fe and Mn with 0.0, 10, 25, 50, and 100 µL standards.

Mercury Quality Assurance

All Teflon bottles, vials and distillation caps were soaked in 2 % citranox overnight, rinsed three times with DIW, placed in concentrated hot nitric acid bath over night, rinsed three times with DIW, and then rinsed three times with Milli-Q prior to analysis to remove trace metals. New polyethylene bottles were used for each Hg sample and blanks collected every other sampling day. Replicates, spikes, and blanks were regularly analyzed for TDHg, MeHg, sediment THg, and sediment MeHg. SRM were also tested for sediment THg, and MeHg. Bottle blanks ranged from -2.7 to 2.4 pM TDHg with and average of 0.2 pM. Dissolved MeHg bottle blanks ranged from -0.3 to 0.3 pM with an average of 0.1 pM. TDHg samples were analyzed in replicate as often as possible with relative standard deviations (RSDs) ranging from 1 to 28 % with an average RSD of 13 %. Replicate dissolved MeHg samples had a RSD range from 2 to 28 % with an average of 14 %. TDHg spike recoveries ranged from 95 to 128 % with an average of 102 %. MeHg spike recoveries ranged from 61 to 158 % with an average of 96 %. Distillation blanks for sediment MeHg ranged from 0 to 5 pM with an average of 2 pM. System blanks for sediment TDHg ranged from -13.9 to 10.6 pM with an average of 1 pM. Replicate sediment THg samples had an RSD range of 0.1 to 25.7 % with an average of 6.9 %. Sediment MeHg replicates had an RSD range of 0.2 to 21.9 % with an average of 9.0 %. Sediment MeHg spike recoveries ranged from 58 to 128 % with an average recovery of 105 %. Standard reference materials (SRMs) were analyzed for sediment

THg and MeHg. THg SRMs were anayzed only twice and in the last experiment and were 87 and 95 %. MeHg SRMs were analyzed more frequently with recoveries ranging from 68 to 137 % with an average of 98 %. Detection limits were determined as three times the standard deviation of the calibration blanks. Detection limit for TDHg was determined to be 1.3 pM, and for dissolved MeHg it was 0.2 pM.

In addition to quality testing of the analytical methods all sediment incubation chambers and associated sampling apparatus underwent numerous blank tests where incubation chambers (after trace metal cleaning) were filled with either Milli-Q or river water and incubated for 3-4 days with water samples taken each day (see fig. 5). Concentrations of MeHg were below detection limit (0.2 pM) in all time points.

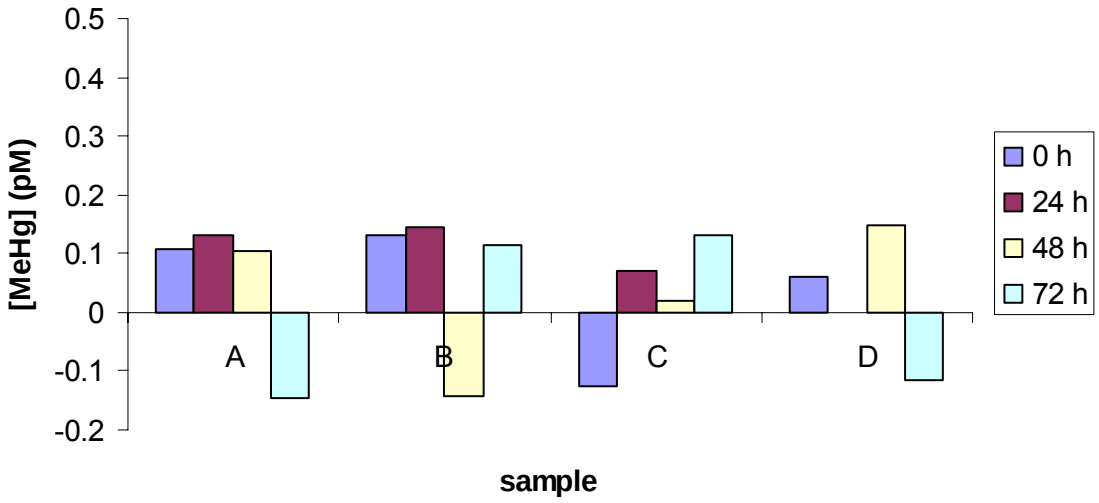

Figure 5. MeHg concentrations in four replicate sediment incubation chamber blanks tested using Milli-Q.

RESULTS

Experiment I: Eagle Island, June 2006.

Estuarine sediments on the intertidal mudflat of the Eagle Island study site are light grey in color and composed primarily of fine-grained clay. The semi-diurnal tidal range at the site in 2006 was 1.31 m ± 15% (Hackney et al., 2007). The sediments, though dominated by freshwater, are frequently subjected to salt water exposure during times of drought or abnormally high tides. This salinity transition zone provides a unique opportunity to study the biogeochemical impacts that saltwater intrusion may have on the flux dynamics of MeHg.

Total percent of reducible iron, total percent of reducible manganese, percent water content, and percent organic carbon were measured for sediment cores from this site from July 2006 through Febuary 2007 by Shaughnessy (2007) (Table 2). Reducible iron (R-Fe) ranged from 22 (±2) to 169 (±20) μMol/g dwt with a nine month mean of 56 (±60) μMol/g dwt. Reducible manganese (R-Mn) ranged from 0.2 (±0.03) to 4.6 (±0.02) μMol/g dwt with a nine month mean of 1.6 (±1.5). Percent water content was 49 to 89 with a nine month mean of 66 (±12). Percent organic carbon ranged from 12 to 19 with a nine month mean of 16 (±3). Salinity values ranged from 0.09 to 5.03 with a 13 month average of 1.85 (±1.93) and correspond to the WHMP data set, site P6, S1-1 (Hackney et al., 2006; Hackney et al., 2007).

Table 2. Chemical and physical characterization of Eagle Island Site

	Mar-06	Apr-06	May-06	Jun-06	Jul-06	Aug-06	Sept-06	Oct-06	Nov-06	Dec-06	Jan-07	Feb-07	Mean
% OC	n/a	n/a	n/a	n/a	17	17	17	19	16	13	12	14	16 ± 3
% H_2O	n/a	n/a	n/a	n/a	63	49	65	72	89	64	58	62	66 ± 12
R-Fe (µMol/g dwt)	n/a	n/a	n/a	n/a	145 ± 100	169 ± 20	30 ± 2	36 ± 1	22 ± 2	53 ± 1	26 ± 2	23 ± 1	56 ± 60
R-Mn (µMol/g dwt)	n/a	n/a	n/a	n/a	2.5± 0.2	1.4± 0.1	0.9± 0.1	0.2± 0.03	2.9± 0.2	4.6± 0.2	0.9± 0.3	1.2± 0.06	1.6± 1.5
Salinity	2.17	5.03	0.18	5.01	0.03	1.79	0.38	4.32	0.07	1.61	0.09	1.55	1.9 ± 1.9

Organic carbon (% OC), water content (% H_20), percent reducible iron (% R-Fe), and percent reducible manganese (% R-Mn) data was determined by Shaughnessy, 2007 . Data was unavailable for March 2006-June 2006. Salinity data is from P6 (S1) of the WHMP (Hackney et al., 2006; Hackney et al., 2007).

Sediment Redox Characterization

Sediment cores taken from this site were incubated and monitored at a temperature between 23 and 25 ^{0}C with freshwater, under oxic and anoxic conditions for approximately two weeks. Water was collected from a boat yard dock located several hundred meters up stream from the study site. “Oxic” and “anoxic” conditions refers to cores bubbled with compressed air and nitrogen, respectively, and not the measured concentrations of oxygen. Therefore, it is possible, and in fact probable, that the “oxic” core was dominated by sub-oxic or even anoxic conditions near the sediment-water interface (SWI). Conversely it is possible, but not probable, that the “anoxic” core had areas of low oxygen concentration. After two weeks the overlying freshwater was flushed and replaced with 1.6 mM sulfate spiked river water and the cores were monitored for an additional two weeks. Cores were incubated between 23 and 25 ^{0}C under freshwater and profiled by microelectrode after approximately one and two weeks (Figure 2).

Table 3 summarizes the concentration maximuma of Fe^{2+}, Mn^{2+}, and ΣH_2S and their respective depths. After approximately one week (186 h) under oxic conditions Mn^{2+} was detected at depths greater than 7.5 cm with a concentration maximum of 109 μM occurring at a depth of 7.4 cm. Fe^{2+} was detected at depths greater than 7.5 cm with a concentration maximum of 44 μM occurring at a depth of 8.6 cm. ΣH_2S was detected at just above the detection limit of 1 μM at 9.4 cm. Under anoxic conditions Mn^{2+} was detected at depths greater than 2.5 cm with a maximum concentration of 75 μM occurring at a depth of 6.2 cm. Fe^{2+} and H_2S were at or below the detection limit throughout the core. After approximately two weeks (354 h) under oxic conditions Mn^{2+} was detected

with a maximum concentration of 105 μM at the SWI and remained detectable throughout the core. Fe^{2+} was detected with a maximum concentration of 205 μM at the SWI and remained detectable throughout the core. H_2S was detected at the lower limit of the profile (9.0 cm) with a concentration of 1.2 μM. After approximately two weeks (354 h) under anoxic conditions Mn^{2+} was detected at depths greater than 0.8 cm with a concentration maximum of 406 μM occurring at the lower limit of the profile (9.0 cm). Fe^{2+} and H_2S were undetectable throughout the core.

After the 354 h profile, the overlying water of the cores was replaced with 1.6 mM sulfate spiked river water to mimic sea level rise and incubated under the same conditions for another two weeks. Profiling was carried out at intervals of 190 and 336 h (approximately 1 and 2 weeks), similar to the previous treatment. The last profile of the previous treatment served as the initial profile for the new treatment. After approximately one week (190 h) under oxic conditions Mn^{2+} was detected at depths greater than 0.8 cm with a concentration maximum of 425 μM occurring at the lower limit of the profile (9.0 cm). Fe^{2+} had a maximum concentration of 161 μM at a depth of 0.1 cm and diminished to below detection limit by a depth of 1.0 cm. H_2S was undetectable throughout the core. Under anoxic conditions Mn^{2+} was ephemerally detected at a depth of 5.8 cm with a concentration of 53 μM. Fe^{2+} was detected between depths of 0.7 and 1.8 cm with a maximum of 166 μM occurring at 1.4 cm depth. ΣH_2S was undetectable throughout the core. After approximately two weeks (336 h) under oxic conditions Mn^{2+} was sporadically detected with a concentration maximum of 61 μM at a depth of 0.1 cm. Fe^{2+} was maximally detected with a concentration of 375 μM at the SWI and diminished to below detection by a depth of 1.0 cm. ΣH_2S was detected between depths of 1.1 and 4.9

cm with a concentration maximum of 34 μM occurring at a depth of 1.9 cm. Under anoxic condition Mn^{2+} was detected at the SWI only with a concentration of 128 μM. Fe^{2+} was maximally detected with a concentration of 449 μM at the SWI and diminished to below detection by a depth of 0.3 cm. ΣH_2S was detected between the SWI and 4.9 cm depth with a concentration maximum of 16 μM occurring at a depth of 0.4 cm.

In summary, over the two weeks of incubation under freshwater conditions the oxic core displayed in increase in both Fe^{2+} and Mn^{2+} at the SWI and at depth, whereas ΣH_2S remained at or near the detection limit throughout. The anoxic core displayed an increase in Mn^{2+} at lower depths with no detectable concentrations ever reaching the SWI, whereas Fe^{2+} and ΣH_2S remained below detection throughout. Over the two weeks of incubation under 1.6 mM sulfate spiked conditions the oxic core displayed a steady increase in Fe^{2+} at the SWI. Mn^{2+} was depleted at the SWI while increasing at lower depths and ΣH_2S remained below detection limits after one week, but by the second week appeared in relatively low concentrations just below the SWI. The anoxic core displayed an increase of Fe^{2+}, and sporadic concentrations of Mn^{2+} at the SWI, whereas ΣH_2S increased to relatively low concentrations just below the SWI by the second week.

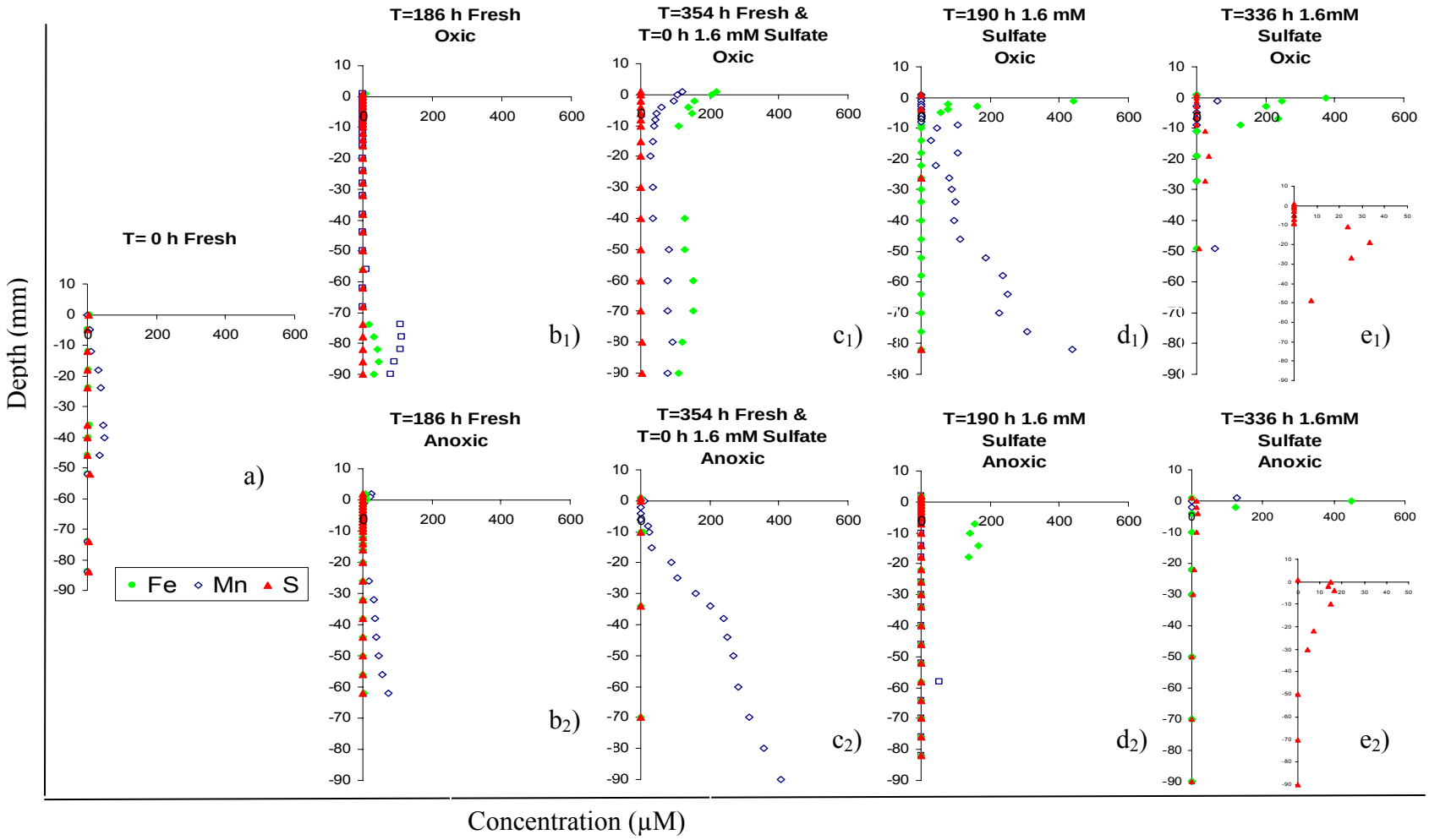

Figure 6. Depth profiles of redox active analytes: Fe^{2+}, Mn^{2+}, and ΣH_2S from experiment I. Profile prior to incubation (a). Freshwater profiles after 7 and 14 days (b and c). Profiles approximately 0, 7, and 14 days after overlying water was replaced with 1.6 mM sulfate spiked river water (c, d, and e).

Table 3. Maximum redox-active analyte concentrations and maximum concentration depths from experiment I pore water profiles.

Analyte	Conc Max (μM) / Depth of Conc. Max. (cm)		
Oxic Freshwater	0 Hours	186 Hours	354 Hours
Fe^{2+}	8 / 0.0	44 / -8.6	205 / 0.0
Mn^{2+}	50 / -0.4	109 / -7.4	105 / 0.0
ΣH_2S	6 / -0.5	2 / -9.4	2 / -9.0
Anoxic Freshwater	0 Hours	186 Hours	354 Hours
Fe^{2+}	8 / 0.0	12 / 0.0	0
Mn^{2+}	50 / -0.4	75 / -6.2	406 / -9.0
ΣH_2S	6 / -0.5	1 / 0.0	0
Oxic 1.6 mM Sulfate Water	0 Hours	190 Hours	336 Hours
Fe^{2+}	205 / 0.0	161 / -0.1	375 / 0.0
Mn^{2+}	105 / 0.0	425 / -9.0	61 / -0.1
ΣH_2S	2 / -9.0	0	34 / -1.9
Anoxic 1.6 mM Sulfate Water	0 Hours	190 Hours	336 Hours
Fe^{2+}	0	166 / -1.4	449 / 0.0
Mn^{2+}	406 / -9.0	53 / -5.8	128 / 0.0
ΣH_2S	0	0	16 / -0.4

Sediment-Water Fluxes

Filtered (0.2 μM) samples were taken from incubated sediment cores five times over each two week treatment. Resultant concentrations were calculated to account for dilution of the overlying water in the core with recharge water to maintain constant water volumes over the sediment. Figures 3a-c show the corrected concentrations of MeHg, TDHg, and DOC as a function of time. Sediment fluxes of MeHg, TDHg, and DOC were calculated based on the slope of the regression line for the dilution-corrected concentrations of the analyte studied (table 4). A negative flux represents a net flux from overlying water into the sediments and a positive flux represents a net flux from the sediments into the overlying water. The t-test was performed on the slopes of the regression lines to determine significance.

Under oxic freshwater no fluxes of MeHg, TDHg or DOC were observed. Under anoxic freshwater conditions MeHg showed a significant flux from overlying water into the sediment in replicate cores at equal rates of -5.8 pmol m^{-2} d^{-1} ($p \leq 0.001$, $p \leq 0.02$). TDHg, under these conditions, had significant fluxes into the sediment at rates of -179 and -183 pmol m^{-2} d^{-1} ($p \leq 0.005$, $p \leq 0.001$). DOC displayed significant fluxes into the sediment at rates of -7.6 and -2.2 mmol m^{-2} d^{-1} ($p \leq 0.001$, $p \leq 0.001$).

Under oxic, 1.6 mM sulfate-spiked water conditions a flux of MeHg into the sediments at a rate of -5.4 pmol m^{-2} d^{-1} ($p \leq 0.02$) was measured in the first core and a zero flux measured in the second. Fluxes of -331 and 203 pmol m^{-2} d^{-1} ($p \leq 0.001$, $p \leq 0.001$) into the sediments were measured for TDHg under these conditions. Contrasting fluxes of DOC at rates of -1.4 mmol m^{-2} d^{-1} ($p \leq 0.05$) into the sediments and +0.6 mmol m^{-2} d^{-1} ($p \leq 0.05$) out of the sediment were measured for replicate cores.

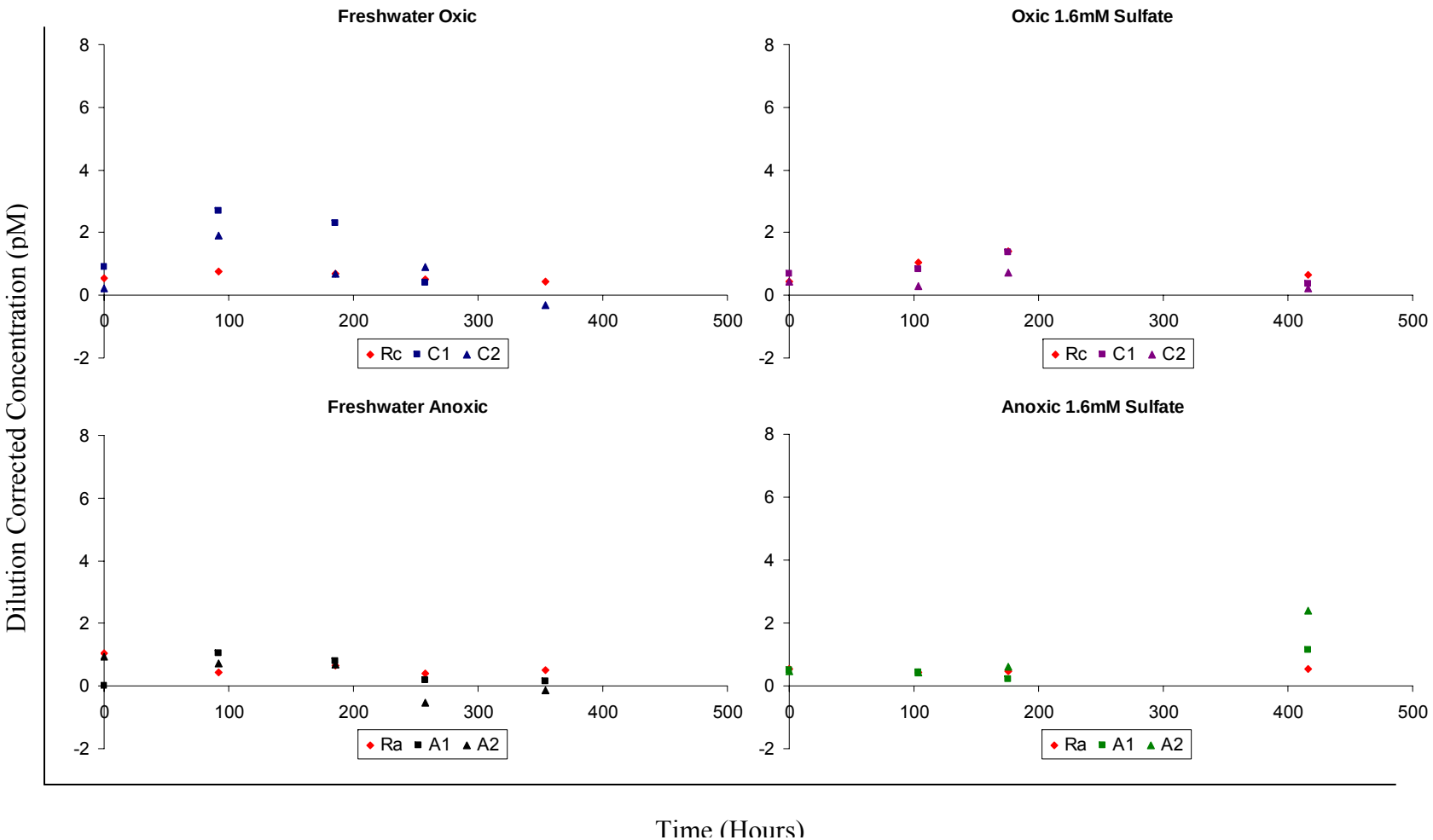

Figure 7a. Eagle Island experiment I, June 2006. Dilution-corrected concentrations of MeHg in overlying water of incubated sediment cores as a function of time.

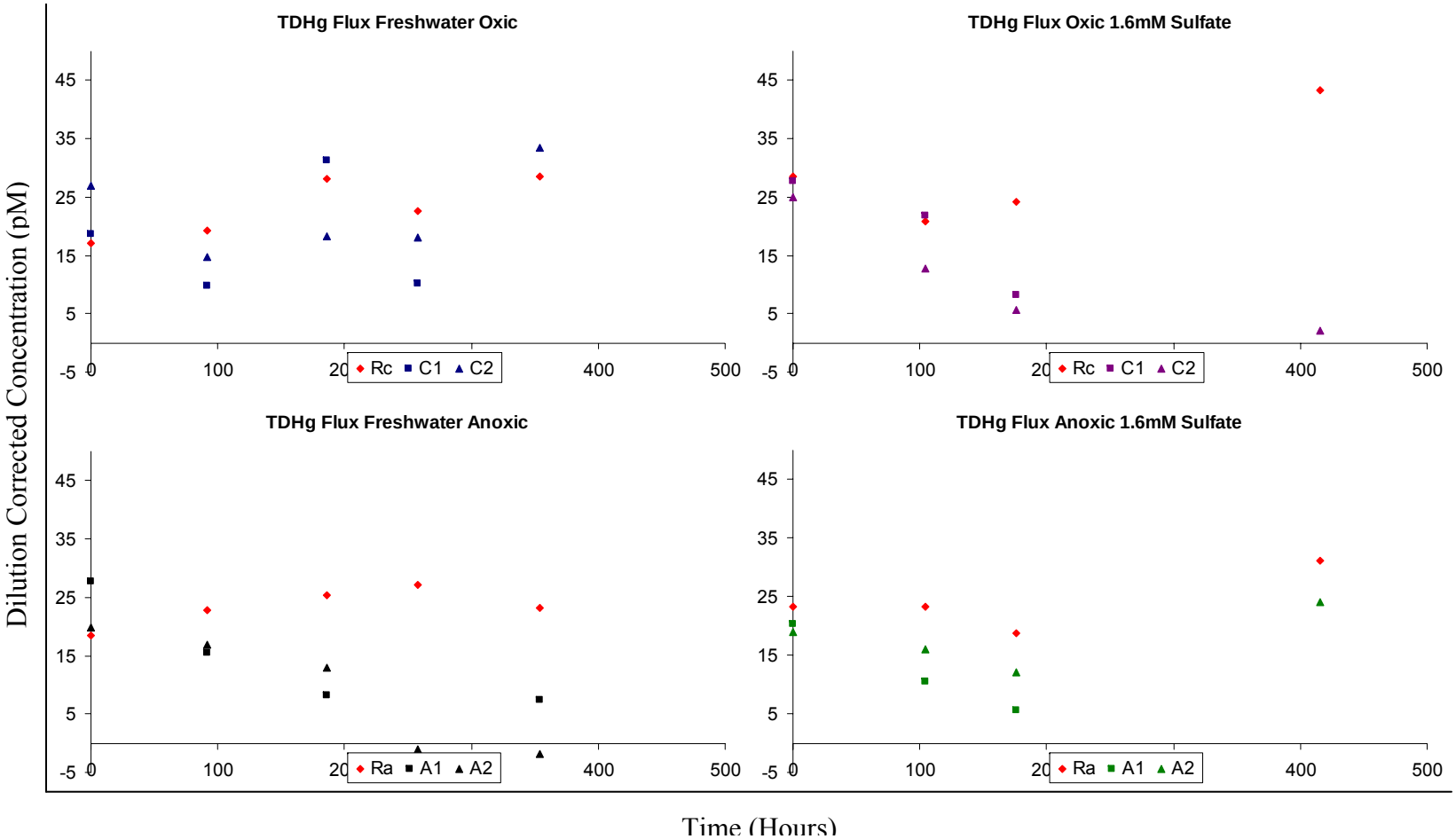

Figure 7b. Eagle Island experiment I, June 2006. Dilution-corrected concentrations of TDHg in overlying water of incubated sediment cores as a function of time.

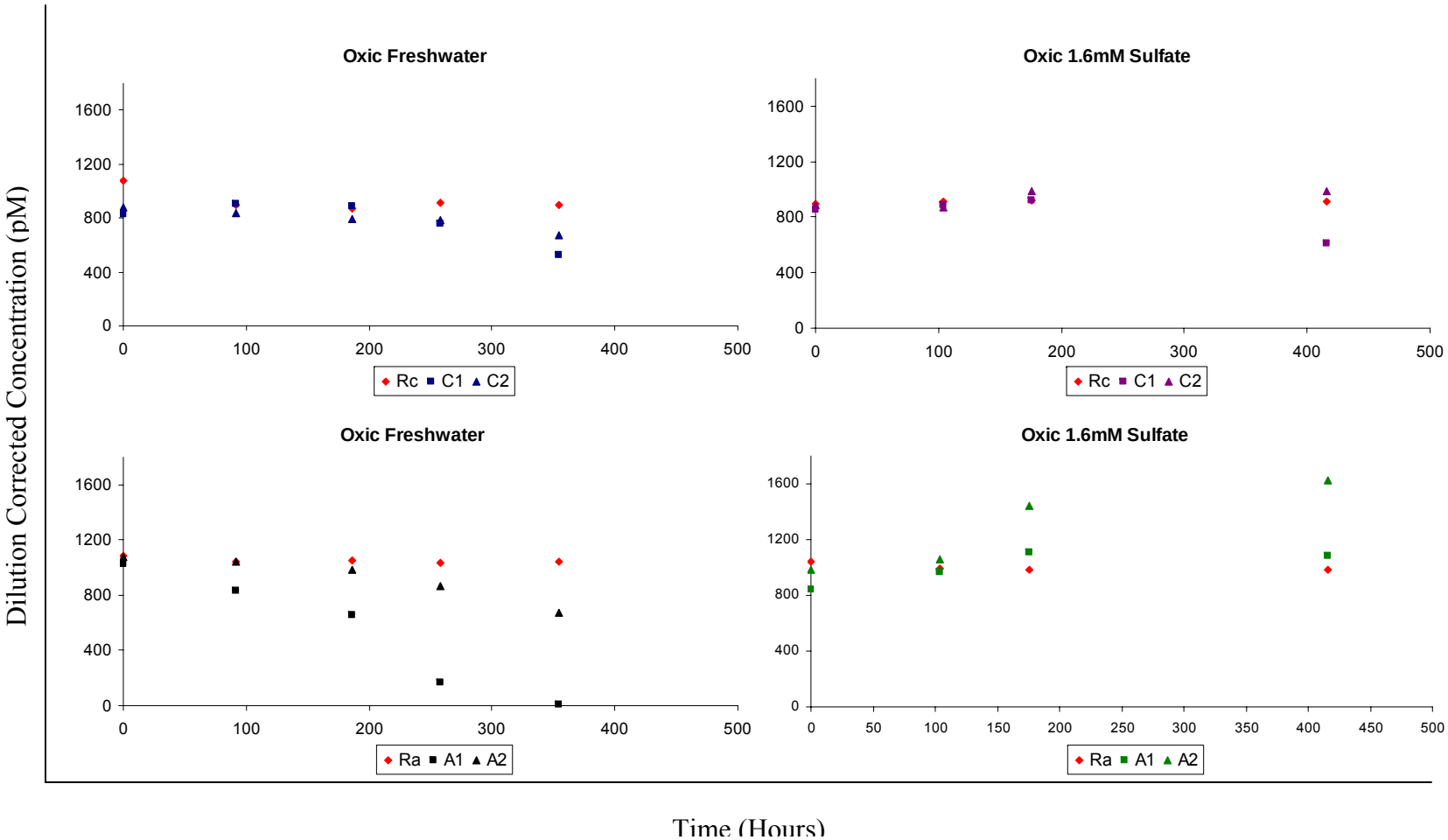

Figure 7c. Eagle Island, June 2006. Dilution-corrected concentrations of DOC in overlying water of incubated. sediment cores as a function of time.

Table 4. Flux summary of the three analytes studied in experiment I. T-test for the slope of the regression line, using the dilution corrected concentrations, was applied to determine significance. Negative values represent a net flux into the sediment and positive values represent a net flux from the sediment into the overlying water.

Treatment	MeHg (pmol m^{-2} d^{-1})	TDHg (pmol m^{-2} d^{-1})	DOC (mmol m^{-2} d^{-1})
Oxic Fresh	0.0	0.0	0.0
n=2	0.0	0.0	0.0
Anoxic Fresh	-5.8 ($p \leq 0.001$)	-178.6 ($p \leq 0.005$)	-7.6 ($p \leq 0.001$)
n=2	-5.8 ($p \leq 0.02$)	-182.9 ($p \leq 0.001$)	-2.2 ($p \leq 0.001$)
Oxic 1.6mM Sulfate	-5.4 ($p \leq 0.02$)	-330.7 ($p \leq 0.001$)	-1.4 ($p \leq 0.05$)
n=2	0.0	-203.3 ($p \leq 0.001$)	0.6 ($p \leq 0.05$)
Anoxic 1.6mM Sulfate	0.0	0.0	1.4 ($p \leq 0.05$)
n=2	10.7 ($p \leq 0.001$)	0.0	3.7 ($p \leq 0.001$)

Under anoxic, 1.6 mM sulfate-spiked water conditions a zero flux and a +11 pmol m^{-2} d^{-1} ($p \leq 0.001$) MeHg flux out of the sediment was measured. Under these conditions no flux of TDHg was measured , and a +1.4 and +3.7 mmol m^{-2} d^{-1} ($p \leq 0.05$ and $p \leq 0.001$) flux of DOC out of the sediments was measured. overlying water. A t-test was performed on the slopes of the regression lines to determine significance.

Experiment II: Eagle Island, October 2006.

Experiment two was carried out in exactly the same manner as experiment #1 with a few adjustments. First, a Unisense OX100 microsensor for oxygen measurements and depth profiling was used. Second, rather than spiking reagent sulfate into the overlying water, 2-5 salinity estuarine water from The Cape Fear River were used to add sulfate. Third, additional cores were taken to allow more frequent profiling (5-6 profiles per treatment). Salinity at the site the day of sampling was <1. Sediments were collected at the same site as in experiment I on 10 October 2006 at low tide and incubated for approximately two weeks under freshwater at 23-25 ^{0}C with one set of replicate cores bubbled with compressed air and another set bubbled with nitrogen After two weeks the overlying water was removed and replaced with water with a salinity of 5 taken from the Cape Fear estuary and incubated for approximately another two weeks.

Sediment Redox Characterization

Initial (T=0 h) sediment profiles were not obtained due to malfunction of the microelectrode the day of collection. Figure 4a shows the depth profiles for the remaining five profiles generated over the two week freshwater treatment. Table 5 lists the concentration maxima and respective depths of the analytes studied.

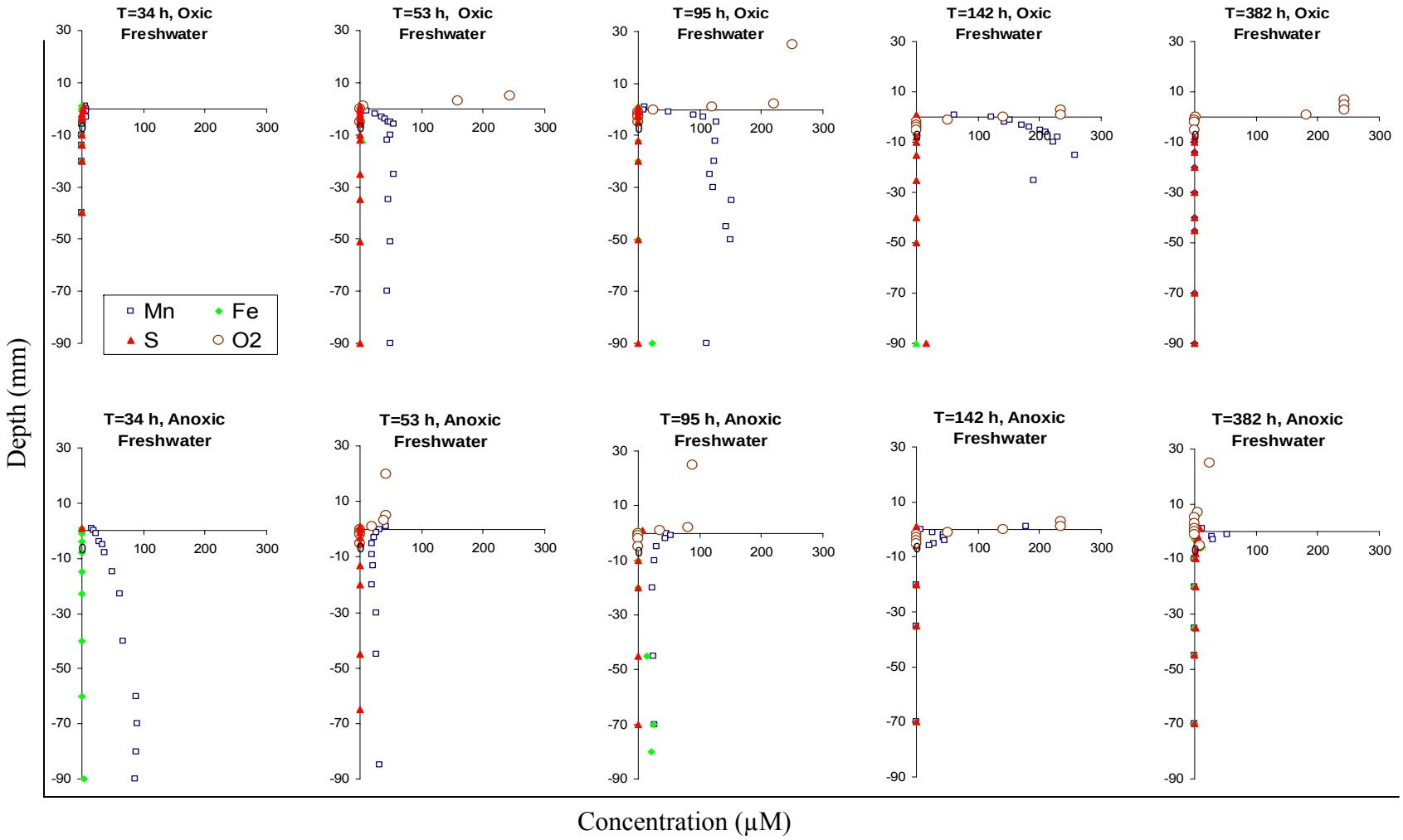

Figure 8a. Eagle Island sediment cores taken October 2006 incubated with freshwater for approximately two weeks at 22-23^{0}C. Sediment depth profiles of redox active analytes: O_2, Fe^{2+}, Mn^{2+}, and S^{2-} as a function of time.

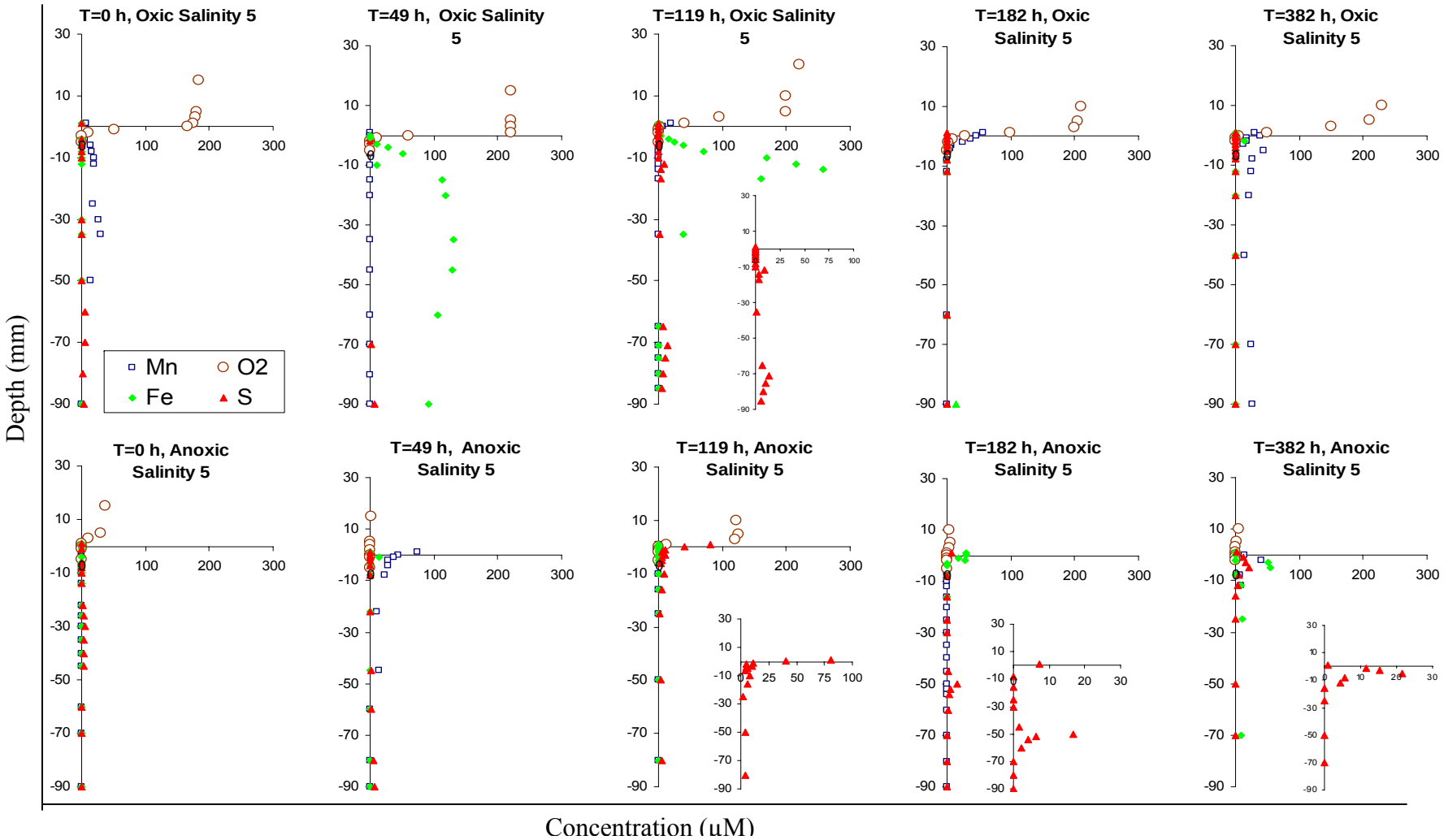

Figure 8b. Eagle Island sediment cores taken October 2006 incubated with 5ppt salinity water for approximately two weeks at 22-23^{0}C. Sediment depth profiles of redox active analytes: O_2, Fe^{2+}, Mn^{2+}, and S^{2-} as a function of time.

Table 5. Maximum redox-active analyte concentrations and max concentration depths from experiment II pore water profiles. Depths reported for O_2 indicate the deepest depth in which O_2 was detected and not the depth of the conc. max. (conc. maxima for O_2 were always in the overlying water.

Analyte	Conc Max (µM) / Depth of Conc. Max. (cm)*				
Oxic Freshwater	34 Hours	53 Hours	95 Hours	142 Hours	382 Hours
Fe^{2+}	0	3 / -1.2	22 / -9.0	0	0
Mn^{2+}	8 / -0.1	54 / -2.5	152 / -3.5	488 / -5.0	0
ΣH_2S	3 / 0.0	0	0	0	0
O_2	n/a	244 / -0.1	250 / 0.0	234 / -0.2	244 / 0.0
Anoxic Freshwater	34 Hours	53 Hours	95 Hours	142 Hours	382 Hours
Fe^{2+}	7 / -7.0	0	24 / -7.0	0	12 / -0.6
Mn^{2+}	91 / -7.0	32 / 0.0	53 / 0.1	179 / 0.0	53 / -0.1
ΣH_2S	0	0	7 / 0.0	0	9 / 0.0
O_2	n/a	43 / 0.1	89 / 0.1	33 / 0.1	25 / 0.5
Oxic Low Salinity water	0 Hours	49 Hours	119 Hours	182 Hours	382 Hours
Fe^{2+}	0	0	308 / -0.5	0	15 / -0.2
Mn^{2+}	6 / -0.6	0	7 / 0.1	99 / 0.0	45 / -0.5
ΣH_2S	30 / -3.5	8 / -9.0	14 / -7.1	0	0
O_2	183 / -0.2	220 / -0.0	220 / 0.0	210 / -0.2	195 / 0.1
Anoxic Low Salinity water	0 Hours	49 Hours	119 Hours	182 Hours	382 Hours
Fe^{2+}	0	14 / -0.1	0	30 / 0.0	55 / -2.5
Mn^{2+}	0	44 / 0.1	0	5 / 0.0	41 / -0.2
ΣH_2S	5 / -3.0	7 / -9.0	40 / 0.1	17 / -5.0	6 / -0.8
O_2	37 / 0.3	2 / 0.5	122 / 0.1	6 / 0.1	5 / 0.3

Both oxic and anoxic cores in this experiment displayed manganese reduction as the dominant form of carbon remineralization, with a concentration just above detection limits in the first profile gradually increasing, below the SWI, to a concentration of 488 μM by 142 h (~6 days) before disappearing completely by 382 h (~16 days). In the anoxic core a concentration maximum of 91 μM Mn^{2+}at 7.0 cm depth decreased at greater depths whereas Mn^{2+} at the SWI steadily increased to a concentration of 179 μM by 142 h.

In both oxic and anoxic cores Fe^{2+} remained at or below the detection limit for the experiment, with the exception of small concentration maxima of 22 and 24 μM at 95 h in lower depths of the oxic and anoxic cores, respectively. Similarly, ΣH_2S remained at or below detection limit throughout the experiment with two minor exceptions. At 34 h ΣH_2S was detected in low concentrations of 3 μm at the SWI of the oxic core and again at 95 h in the oxic core with a concentration of 7 μM at the SWI. O_2 concentrations in the oxic core were consistent and ranged from 183 to 250 μM in the overlying water and persisted as deep as 0.1 cm below the SWI. Concentrations of O_2 were less consistent in the anoxic core due to technical trouble with the compressed N_2 regulator sensitivity. These maximum concentrations ranged from 6 to 126 μM in the overlying water and persisted as deep as, but not below, the SWI.

After approximately ten days the freshwater was removed from all cores and replaced with river water of salinity 5. Due to the sequential nature of these treatments, the time values assigned to each data set refer to the overlying water and not the age of the core. For example, at 0 h anoxic under water with salinity of 5, the sediment had been under anoxic conditions for 382 h, but under saline conditions for 0 h. This is essential in

understanding the redox chemistry of the sediments. Figure 4b shows the five profiles generated over the course of the saline treatment. Maximum concentrations and their respective depths are listed in Table 5.

The oxic core under river water with salinity 5 initially had relatively low concentrations of Mn^{2+} and no detectable Fe^{2+} or ΣH_2S below the oxic zone. By 49 h these sediments were dominated by iron reduction as seen by the increase in Fe^{2+} concentrations throughout the core. At 95 h this zone of Fe reduction had migrated toward the SWI with an Fe^{2+} maximum concentration of 308 μM occurring just below the oxic zone at 0.5 cm. By 182 h Fe^{2+} fell below detection levels and Mn^{2+} appeared to dominate at the SWI with relatively low concentrations. O_2 concentrations were constant throughout this treatment, ranging from 183 to 230 μM and reaching a depth of 0.2 cm.

In the anoxic core under river water with a salinity of 5, virtually no trends were discernable. Fe^{2+} and Mn^{2+} display sporadic, low concentrations just below the SWI throughout the experiment except at 199 h. At this time point there was a pulse of H_2S with a concentration maximum of 40 μM just above the SWI. Interestingly, this H_2S pulse coincides with an inadvertent increase in O_2 concentration due to technical trouble with the N_2 regulator. O_2 concentrations were relatively constant at less than 10 μM throughout this treatment with the exception of 119 h where there was a concentration maximum of 126 μM at 0.5 cm above the SWI.

Sediment-Water Fluxes

Samples were taken from incubated sediment cores six times over each two week treatment. Figures 5a-c show the dilution-corrected concentrations of MeHg, TDHg, and

DOC as a function of time. Table 6 shows significant analyte fluxes as determined based on the slope of the regression of the dilution-corrected concentrations from Figures 5a-c. As in experiment I a negative flux represents a net flux from overlying water into the sediments and a positive flux represents a net flux from sediments into the overlying water.

Sediments under oxic freshwater conditions had fluxes of MeHg from the water into the sediments at rates of -12 and -10 pmol m^{-2} d^{-1} ($p \leq 0.01$, $p \leq 0.01$). TDHg fluxed at rates of -960 and -870 pmol m^{-2} d^{-1} ($p \leq 0.005$, $p \leq 0.01$) from the water into the sediments. DOC fluxed from the water into the sediments at rates of were -2.5 and -17.5 mmol m^{-2} d^{-1} ($p \leq 0.001$, $p \leq 0.001$). Under anoxic freshwater conditions the sediments had fluxes of MeHg of 0 and -39 pmol m^{-2} d^{-1} ($p \leq 0.001$) into the sediment. TDHg had fluxes of -1,000 and -490 pmol m^{-2} d^{-1} ($p \leq 0.001$, $p \leq 0.001$) into the sediments. DOC fluxes were -19.7 and -23.6 mmol m^{-2} d^{-1} ($p \leq 0.001$, $p \leq 0.001$).

Sediments under oxic river water with salinity 5 showed MeHg fluxes into the sediment of -11 and -13 pmol m^{-2} d^{-1} ($p \leq 0.05$, $p \leq 0.001$). TDHg fluxed into the sediments at rates of 0.0 and -39 pmol m^{-2} d^{-1} ($p \leq 0.05$) and DOC had flux rates of -13.0 and -21.1 mmol m^{-2} d^{-1} ($p \leq 0.001$, $p \leq 0.001$) into the sediments. Under anoxic salinity 5 conditions, the sediments had net MeHg fluxes into the overlying water at rates of +29 and +36 pmol m^{-2} d^{-1} ($p \leq 0.001$, $p \leq 0.001$). TDHg fluxed into the sediments at rates of -480 and 0 pmol m^{-2} d^{-1} ($p \leq 0.001$) and DOC fluxed into the sediment at rates of -1.4 and -10.5 mmol m^{-2} d^{-1} ($p \leq 0.05$, $p \leq 0.001$).

In summary, all significant fluxes of MeHg were in the direction of water to sediment (i.e. removal from water column) with the exception of the sediments under anoxic, sulfate-containing saline water which showed fluxes from sediment to the overlying water in replicate cores. TDHg consistently fluxed from the overlying water into the sediments regardless of treatment. DOC had positive fluxes under anoxic conditions and negative fluxes under oxic conditions.

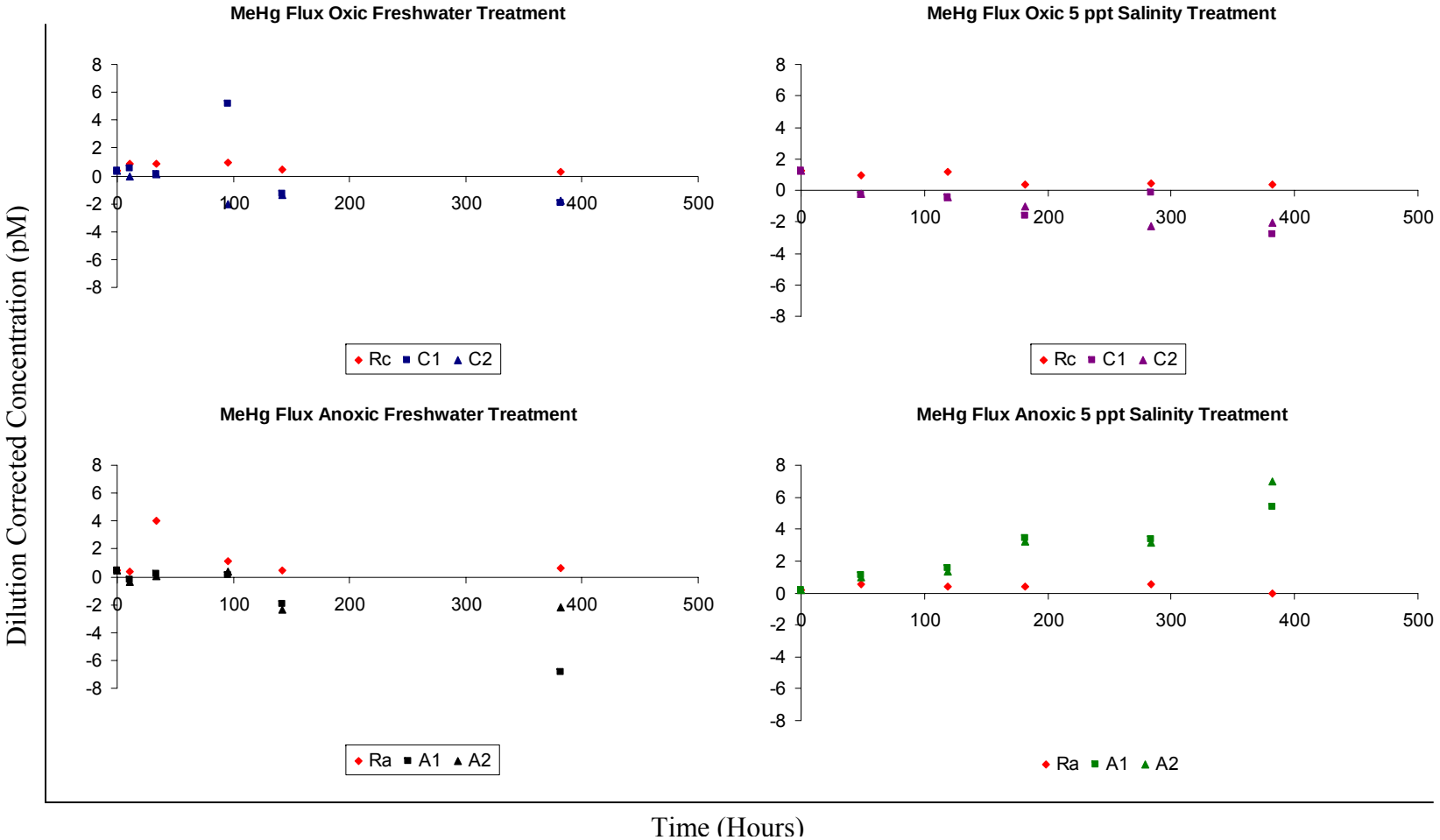

Figure 9a. Eagle Island, October 2006. Dilution-corrected concentrations of MeHg in overlying water of incubated sediment cores as a function of time.

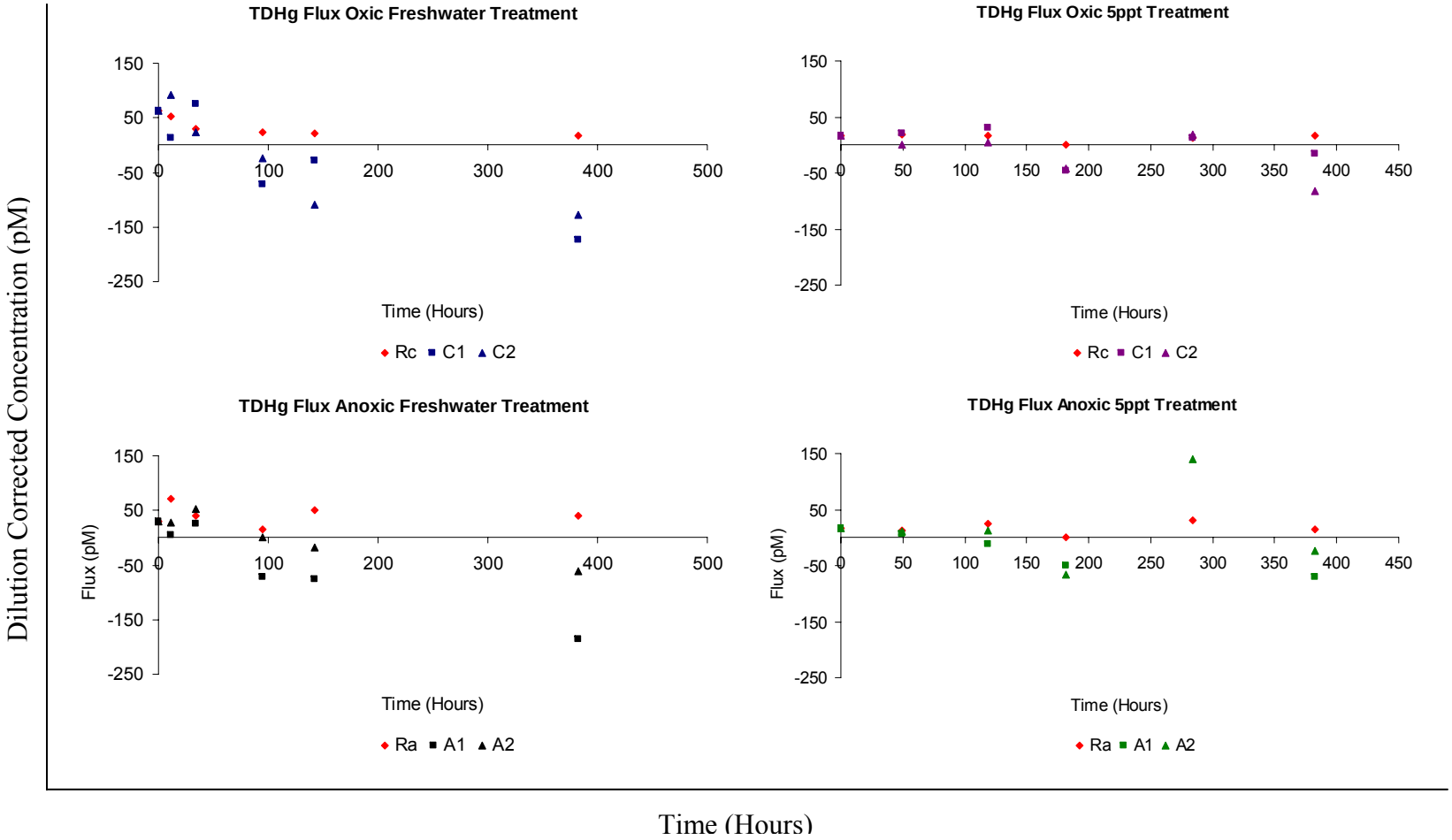

Figure 9b. Eagle Island, October 2006. Dilution-corrected concentrations of TDHg in overlying water of incubated. sediment cores as a function of time.

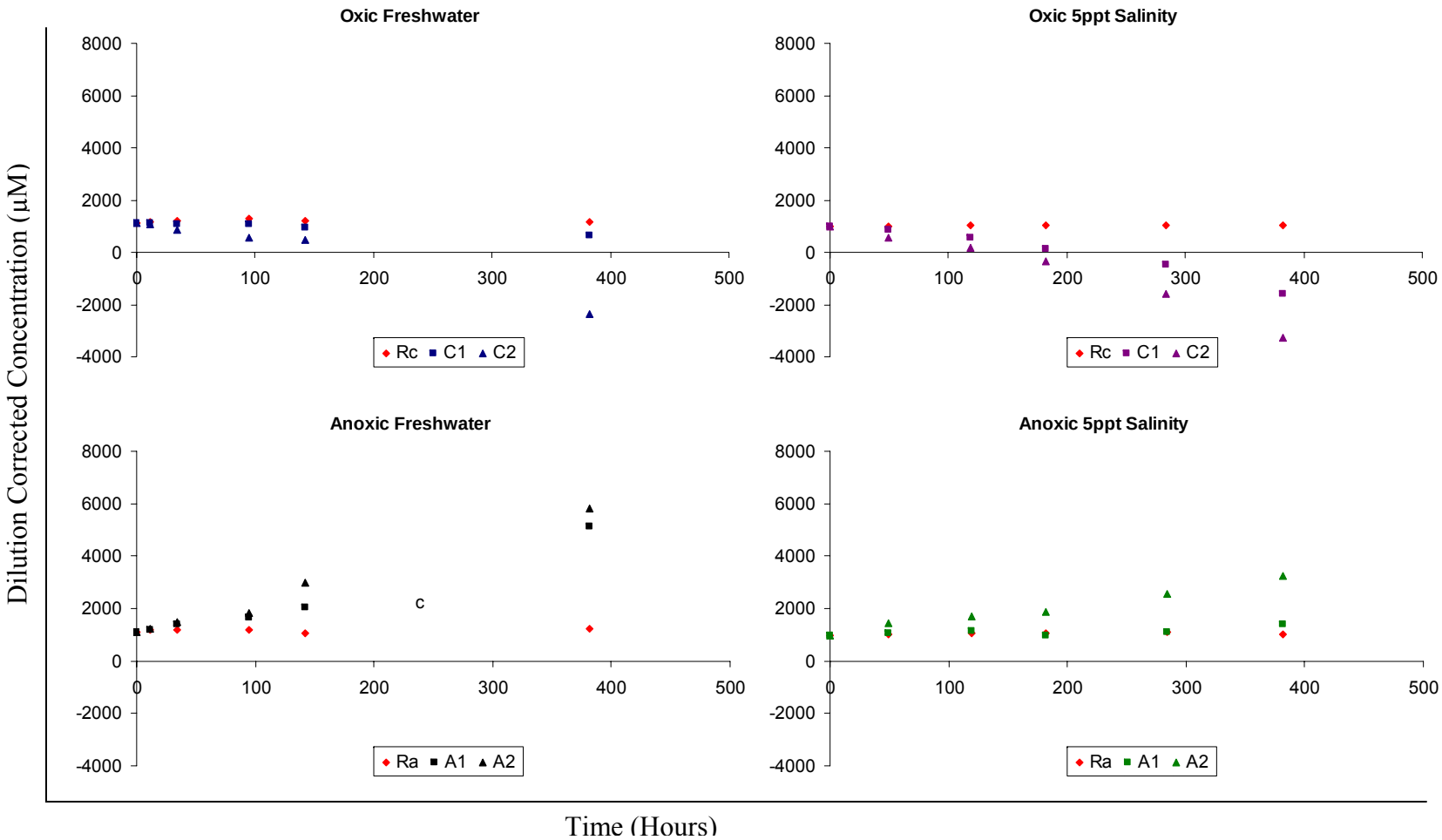

Figure 9c. Eagle Island, October 2006. Dilution-corrected concentrations of DOC in overlying water of incubated. sediment cores as a function of time.

Table 6. Flux summary of the four analytes studied in experiment II. T-test for the slope of the regression line, using the dilution corrected concentrations, was applied to determine significance for each experiment. Negative values represent a net flux into the sediment and positive values represent a net flux from the sediment into the overlying water.

Treatment	MeHg (pmol m^{-2} d^{-1})	TDHg (pmol m^{-2} d^{-1})	DOC (mmol m^{-2} d^{-1})
Oxic Fresh	-11.5 ($p \leq 0.01$)	-958.7 ($p \leq 0.005$)	-2.5 ($p \leq 0.001$)
n=2	-9.7 ($p \leq 0.01$)	-867.8 ($p \leq 0.01$)	-17.6 ($p \leq 0.001$)
Anoxic Fresh	-36.3 ($p \leq 0.001$)	-1044.1 ($p \leq 0.001$)	19.7 ($p \leq 0.001$)
n=2	0.0	-486.9 ($p \leq 0.001$)	23.6 ($p \leq 0.001$)
Oxic 5ppt Salinity	-11.2 ($p \leq 0.05$)	0.0	-13.0 ($p \leq 0.001$)
n=2	-12.7 ($p \leq 0.001$)	-38.5 ($p \leq 0.05$)	-21.0 ($p \leq 0.001$)
Anoxic 5ppt Salinity	28.7 ($p \leq 0.001$)	-477.0 ($p \leq 0.001$)	1.4 ($p \leq 0.05$)
n=2	35.6 ($p \leq 0.001$)	0.0	10.5 ($p \leq 0.001$)

Experiment III: White Oak, September 2007

Unlike the Eagle Island study site on the Cape Fear River, the White Oak River study site is not part of any ongoing monitoring project and therefore has fewer ancillary data. This site is in a tidal freshwater section of an eastern North Carolina estuary located approximately 20 km from the Atlantic Ocean. The sediments, which deposit over a sandy bottom, contain approximately 18% organic carbon which consists largely of macrophyte detritus (Avery et al., 2002 and references therein). Total reducible iron (R-Fe) in the top 10 cm averaged 87 μmol/g of dry sediment. Total reducible manganese (R-Mn), in the top 10 cm was 1.8 μmol/g of dry sediment. Unlike the sediments of Eagle Island which were compacted clays (45 % water by weight), these sediments are more organic-rich with a very high water content (85% water by weight). Intact sediment cores, along with overlying surface water (when present), were taken from the boat when possible to avoid disturbing the sediment.

Experimental parameters were similar to the previous two experiments with a few modifications. Due to warm temperatures and higher organic content it was assumed that less time would be required to observe flux and redox chemistry trends. The length of each treatment, therefore, was shortened to 9-11 days to allow more frequent profiling. Additional cores were taken to allow triplicates for flux treatments, and sectioning and sediment analysis of MeHg, TDHg, R-Mn, and R-Fe. In addition, samples of overlying water were taken at each time point for sulfate and chloride flux measurements. As in previously described experiments, upon termination of the freshwater treatment the overlying water was removed and replaced with low salinity (S = 4) river water. Due to

limited river access this water was a mixture taken from two sites of varying salinity on the White Oak River in order to achieve the desired salinity.

Sediment Redox Characterization

Initial sediment profiling of the redox-active analytes revealed significant heterogeneity of redox zones within the sediments. Figure 6a shows the six sediment profiles from the initial freshwater treatment. Cores were profiled upon returning to the lab before beginning the experiment. At 0 h neither anoxic nor oxic cores had been treated and therefore any heterogeneity seen at this time point was natural. As can be seen from Figure 6a the core designated as oxic was dominated by Fe and Mn reduction in the surface layers with some sulfate reduction at depth. The core designated as anoxic indicated no iron or manganese reduction and was dominated by ΣH_2S. Due to a damaged oxygen electrode, oxygen data were collected by using a linear sweep scan with the microelectrode (Brendel and Luther, 1995). Though useful in determining the presence or absence of oxygen, the accuracy of this method was found to be poor and the data unreliable.

Under freshwater conditions the oxic sediments demonstrated variability in the depth of Mn^{2+} concentration maxima, whereas the concentration maxima themselves varied only slightly. Mn^{2+} concentration maxima ranged between 8 and 66 μM at depth between 0.2 and 7.5 cm. Fe^{2+} concentrations increased in the initial 20 h to a maximum concentration of 75 μM at a depth of 0.1 cm, before falling below detection at 43 h. Small concentrations of Fe^{2+} were seen again in the near surface layers at 219 h.

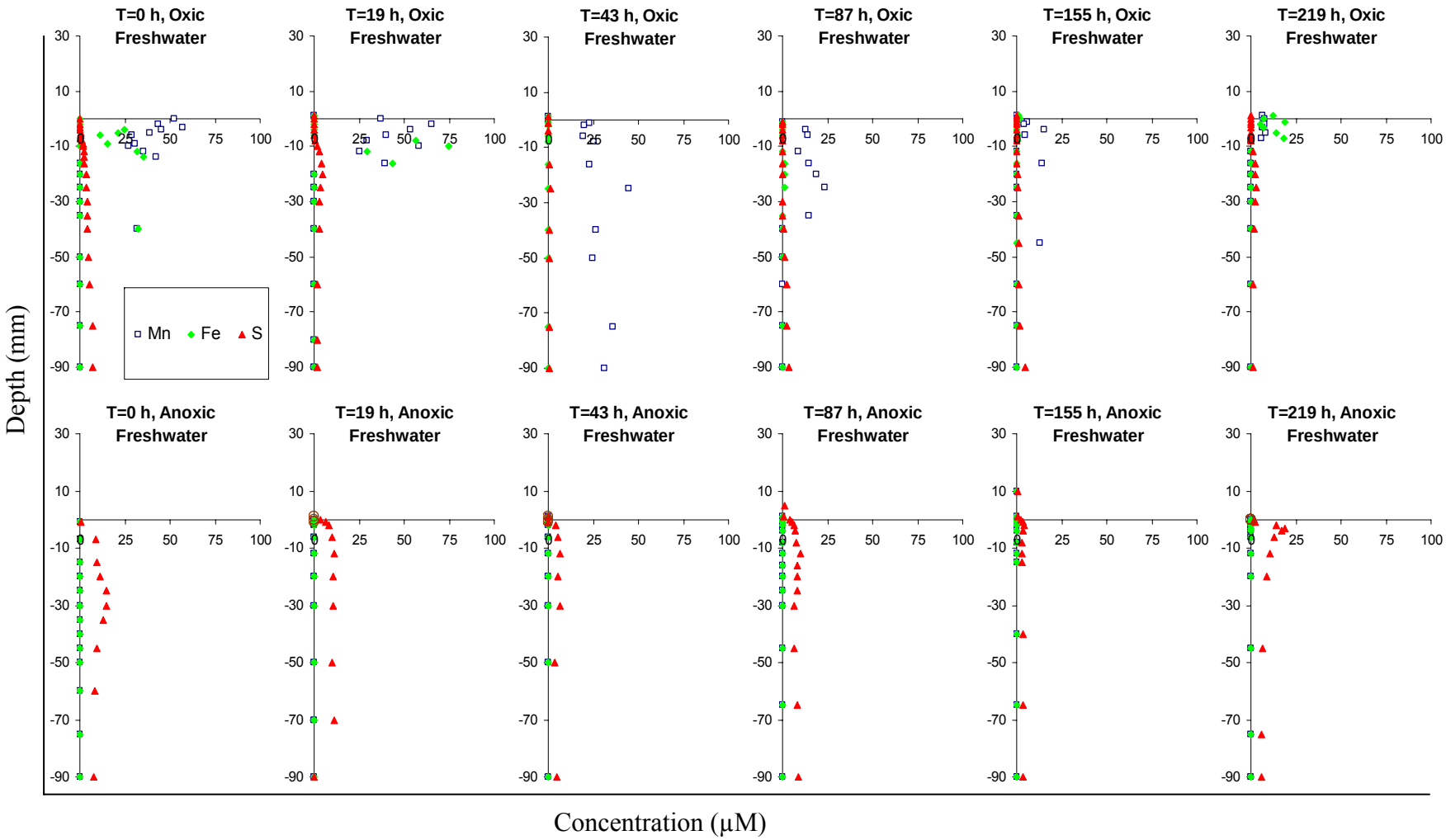

Figure 10a. White Oak river sediment cores taken September 2007 incubated with freshwater for approximately nine days at 22-23^{0}C. Sediment depth profiles of redox active analytes: Fe^{2+}, Mn^{2+}, and S^{2-} as a function of time.

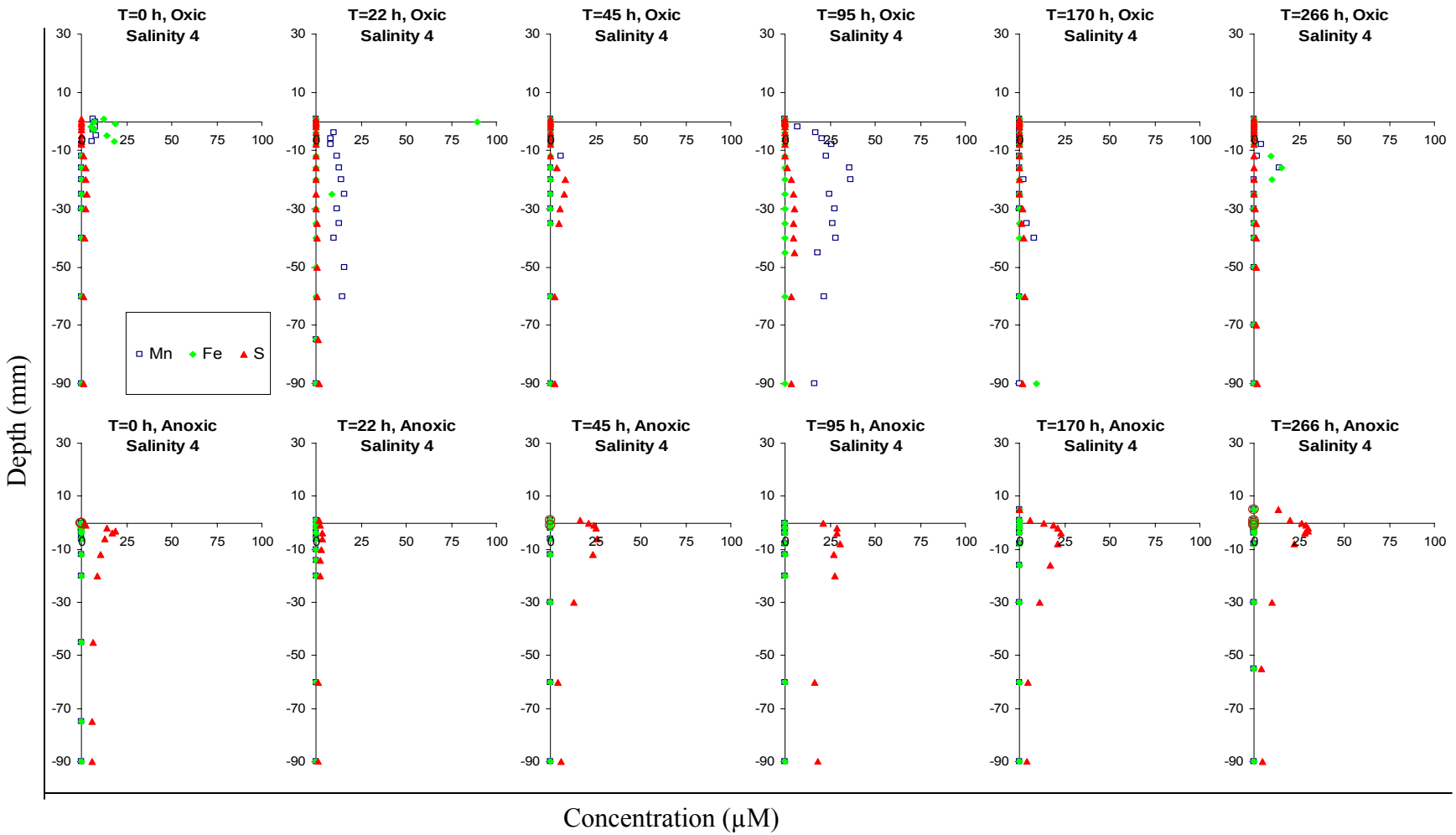

Figure 10b. White Oak river sediment cores taken September 2007 incubated with 4ppt salinity river water for nine days at 22-23^{0}C. Sediment depth profiles of redox active analytes: Fe^{2+}, Mn^{2+}, and S^{2-} as a function of time.

Table 7. Maximum redox-active analyte concentrations and maximum concentration depths from experiment III pore water profiles. Negative depth values indicate maximums below the sediment-water interface and positive values indicate above this interface.

Analyte	Conc Max (µM) / Depth of Conc. Max. (cm)*					
Oxic Freshwater	0 Hours	19 Hours	43 Hours	87 Hours	155 Hours	219 Hours
Fe^{2+}	35 / -1.4	75 / 0.0	0	37 / -2.5	36 / 0.0	19 / -0.1
Mn^{2+}	57 / -0.3	66 / -1.0	36 / -7.5	24 / -2.5	15 / -0.4	8 / -0.5
ΣH_2S	15 / -3.0	5 / -2.0	1 / -2.5	3 / -9.0	0	3 / -2.5
Anoxic Freshwater	0 Hours	19 Hours	43 Hours	87 Hours	155 Hours	219 Hours
Fe^{2+}	0	0	0	0	0	0
Mn^{2+}	0	0	0	0	0	0
ΣH_2S	10 / -1.5	11 / -1.2	6 / -1.2	10 / -1.2	4 / -0.2	19 / -0.3
Oxic Low Salinity water	0 Hours	22 Hours	45 Hours	95 Hours	170 Hours	266 Hours
Fe^{2+}	19 / -0.1	89 / 0.0	0	0	9 / -9.0	15 / -1.6
Mn^{2+}	8 / -0.5	16 / -5.0	6 / -0.6	37 / -2.0	8 / -4.0	14 / -1.6
ΣH_2S	3 / -2.5	2 / -9.0	8 / -2.0	5 / -3.0	3 / -6.0	2 / -9.0
Anoxic Low Salinity water	0 Hours	49 Hours	119 Hours	182 Hours	382 Hours	266 Hours
Fe^{2+}	0	0	0	0	0	0
Mn^{2+}	0	0	0	0	0	0
ΣH_2S	19 / -0.3	4 / -0.4	26 / -0.6	31 / -0.8	23 / -0.4	30 / -0.3

After the initial profile ΣH_2S remained near or below the detection limit for the remainder of the treatment. The anoxic sediments changed very little from the initial time point. The ΣH_2S concentration maximum of 15 μM at 0 h migrated gradually toward the SWI and was detectable in the overlying water by 87 h. Maximum ΣH_2S concentration varied between 4 and 19 μM. Fe^{2+} and Mn^{2+} remained below detection levels for the duration of the treatment.

Under low salinity conditions the oxic sediments showed few discernable trends. Mn^{2+} showed variable detection course of the treatment, likely due to heterogeneity within the core. By 22 h Fe^{2+} increased to a maximum concentration of 89 μM at the SWI and then remained undetectable for the remainder of the treatment. At 45 hours ΣH_2S increased to a concentration maximum of 8 μM at a depth of 2.0 cm and then diminished to near detection limit by 266 h. Under anoxic conditions ΣH_2S persisted as the only detectable analyte. Increasing in concentration slightly at the SWI until becoming detectable in the overlying water at 45 hours, it reached a concentration maximum of 31μM at 95 h.

Reducible Iron and Manganese

In this experiment a core was sectioned immediately upon returning to the lab. Sections of 1-2 cm were immediately frozen until analysis. Two additional cores were taken and kept under the same conditions with one oxic and one anoxic and these were sectioned at the end of the first treatment in 1-2 cm increments and frozen. At the end of the low salinity treatment one oxic and one anoxic intact flux core was sectioned in 1-2 cm increments and frozen. These sections were thawed and analyzed for dithionite-

reducible Fe and Mn, as described previously. Depth profiles of R-Fe and R-Mn are shown in Figure 7a and 7b, respectively. Little difference was seen in oxic and anoxic profiles of R-Fe. In both cases the maximum R-Fe concentration shifts from 1-2 cm depth at 0 h to the surficial 0-1 cm section at the end of the freshwater treatment. After the low salinity treatment this concentration maximum migrated down to 1-2 cm depth. Interestingly, there is an abundance of R-Fe throughout the cores despite very little detectable Fe^{2+}, indicating either some factor inhibiting the reduction of Fe^{3+} oxides or complexation of Fe^{2+} by sulfides or organics to form species undetected by the microelectrode. Sediment Mn concentrations ranged from 1 to 6 μmol g^{-1} dry sediment, displaying no discernable correlations with changing conditions of the overlying waters.

Sediment-Water Fluxes

Dilution corrected concentrations of MeHg, TDHg, DOC, and sulfate for the six time points as a function of time are shown in Figures 8a-c. Table 8 summarizes fluxes for these analytes based on the slopes of these corrected concentrations. Negative values represent water to sediment fluxes and positive values represent sediment to water fluxes.

In the oxic freshwater cores no net MeHg fluxes were observed in triplicate cores. TDHg fluxed into the sediments in two of the three cores at rates of -12 and -6 pmol m^{-2} d^{-1} ($p \leq 0.001$, $p \leq 0.001$). DOC had positive fluxes into the overlying water in triplicate cores of this treatment and at rates of 3.2, 2.5, and 2.5 mmol m^{-2} d^{-1} ($p \leq 0.001$, $p \leq 0.001$, $p \leq 0.05$, respectively). Sulfate fluxes were into the sediment in triplicate cores at rates of -0.61, -0.84, and -1.4 mmol m^{-2} d^{-1} ($p \leq 0.05$, $p \leq 0.001$, $p \leq 0.001$, respectively).

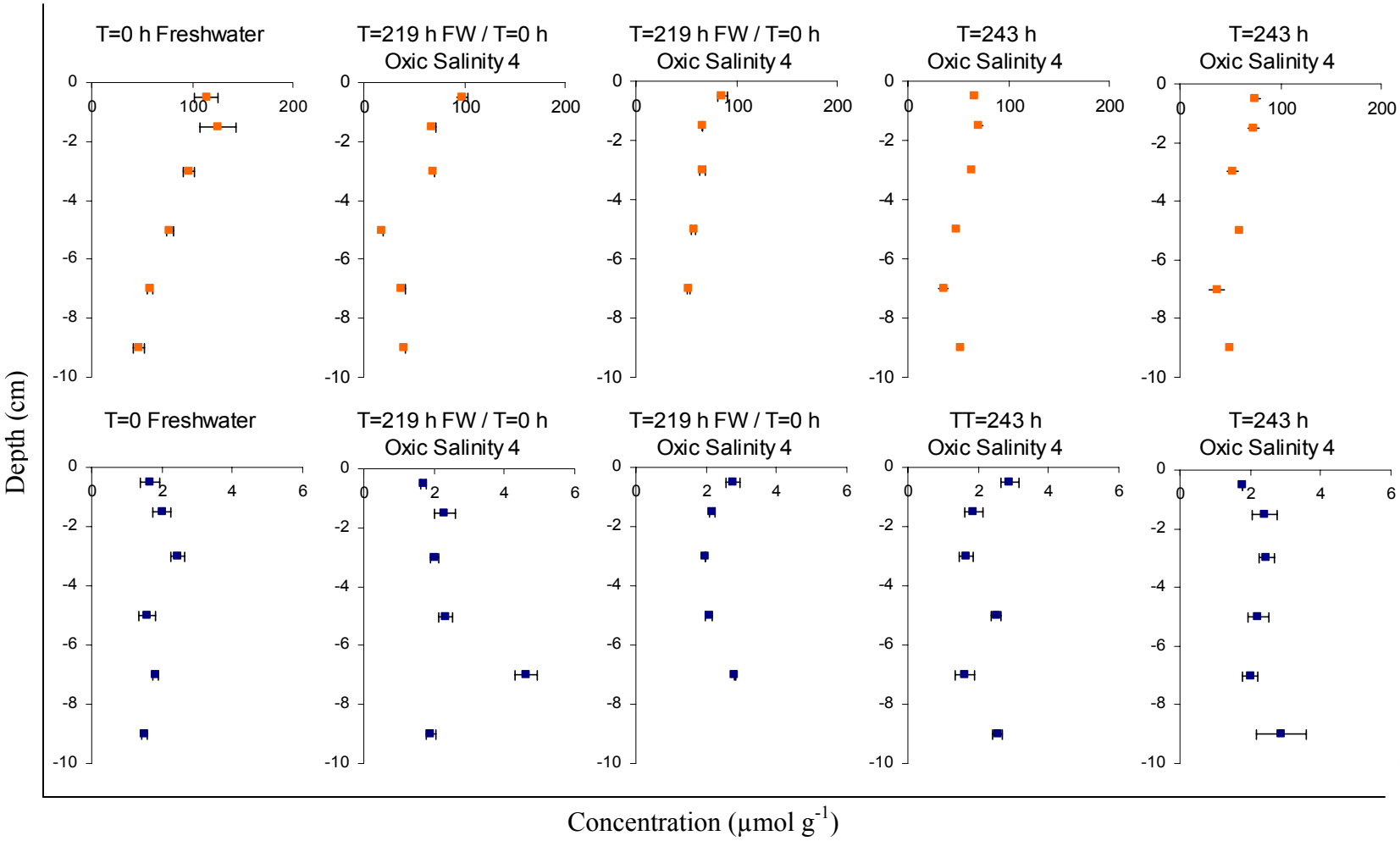

Figure 11. Sediment R-Fe and R-Mn profiles. a) R-Fe in µmol/g of dry sediment. b) R-Mn in µmol/g of dry sediment. Sediment cores were sectioned and analyzed before incubation (a1, b1), after freshwater treatment (a2-a3, b2-b3) , and after lowt salinity treatment (a4-a5, b4-b5).

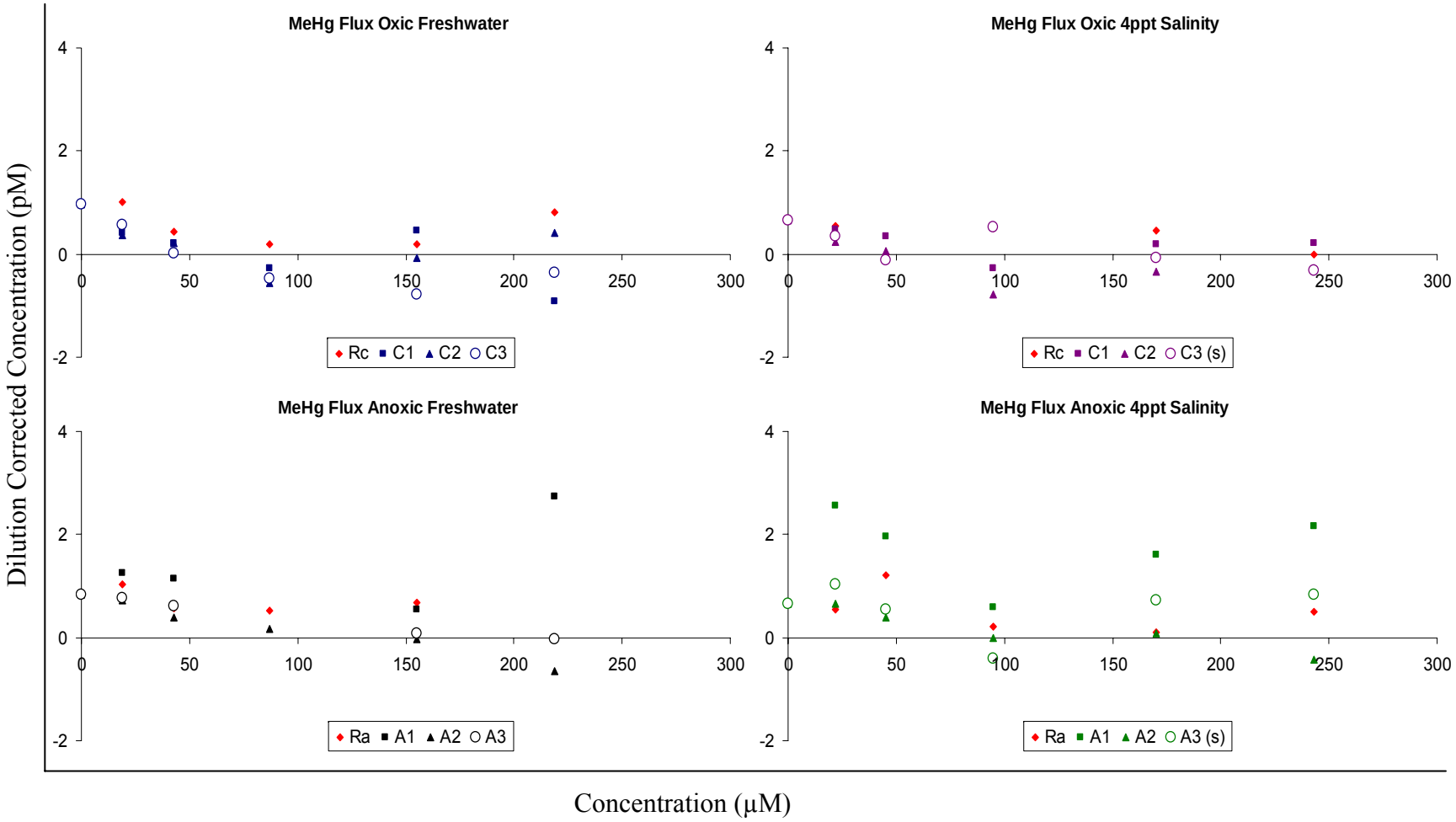

Figure 12a. White Oak River. Dilution-corrected concentrations of MeHg in overlying water of incubated sediment cores as a function of time.

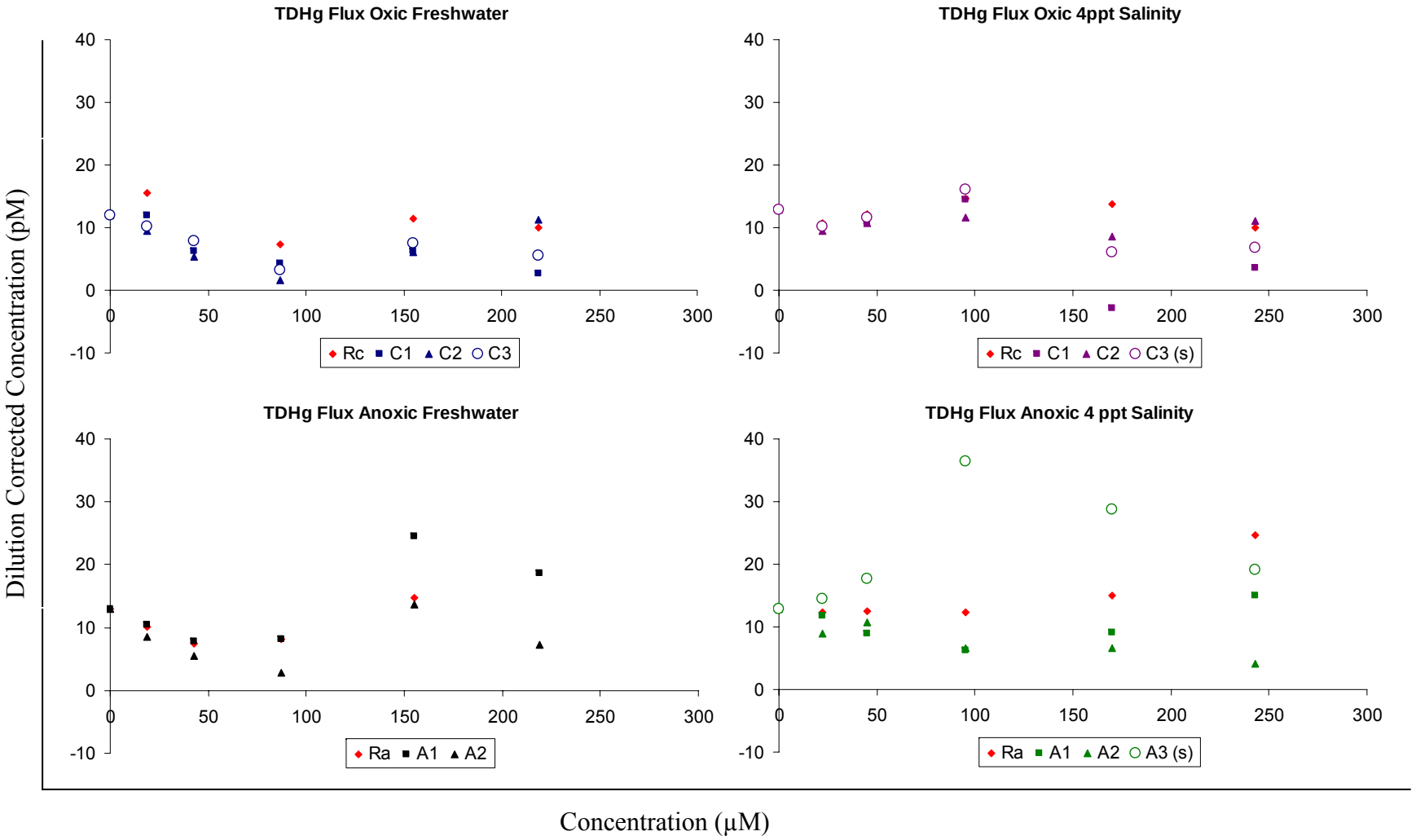

Figure 12b. White Oak River. Dilution-corrected concentrations of TDHg in overlying water of incubated sediment cores as a function of time.

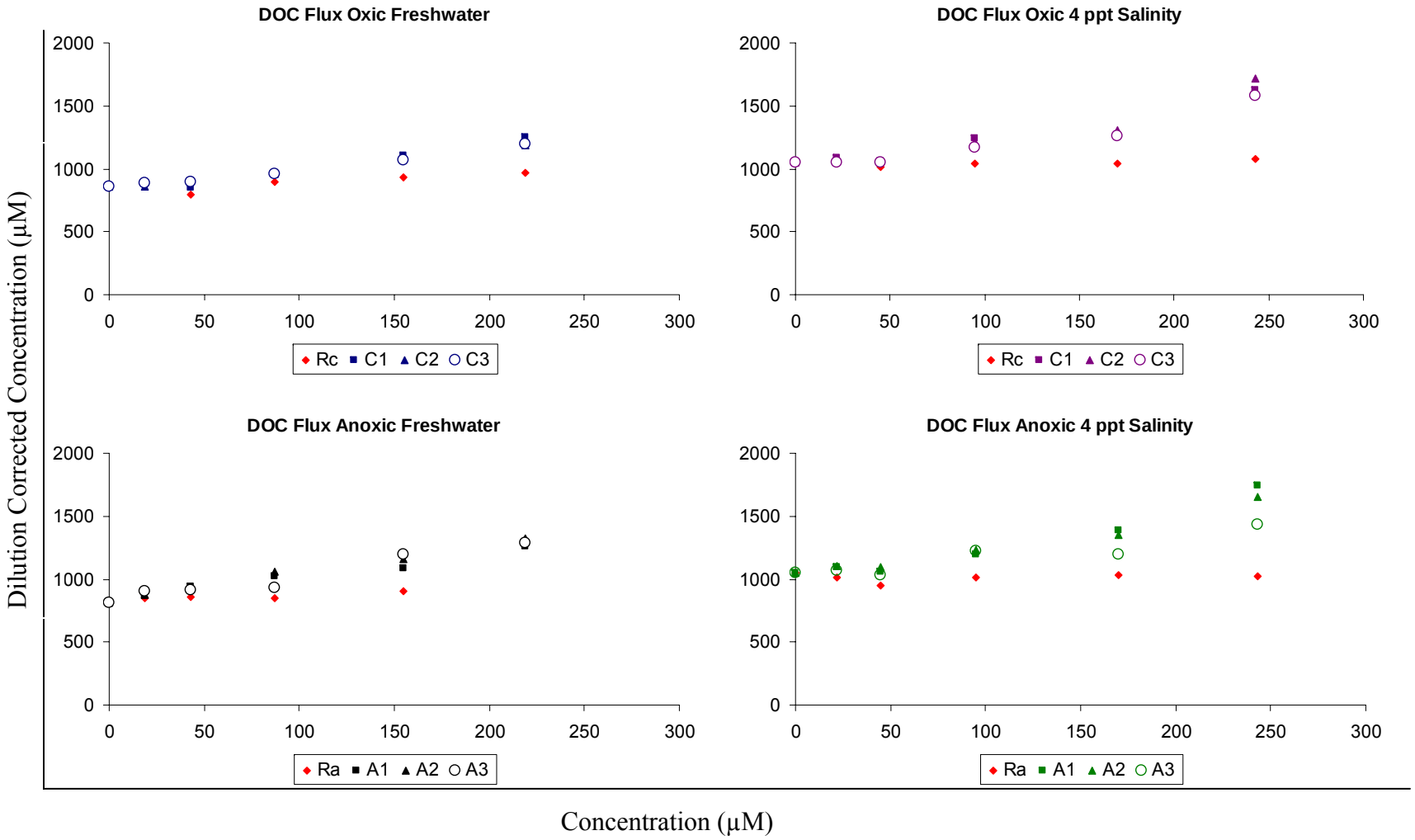

Figure 12c. White Oak River. Dilution-corrected concentrations of DOC in overlying water of incubated sediment cores as a function of time.

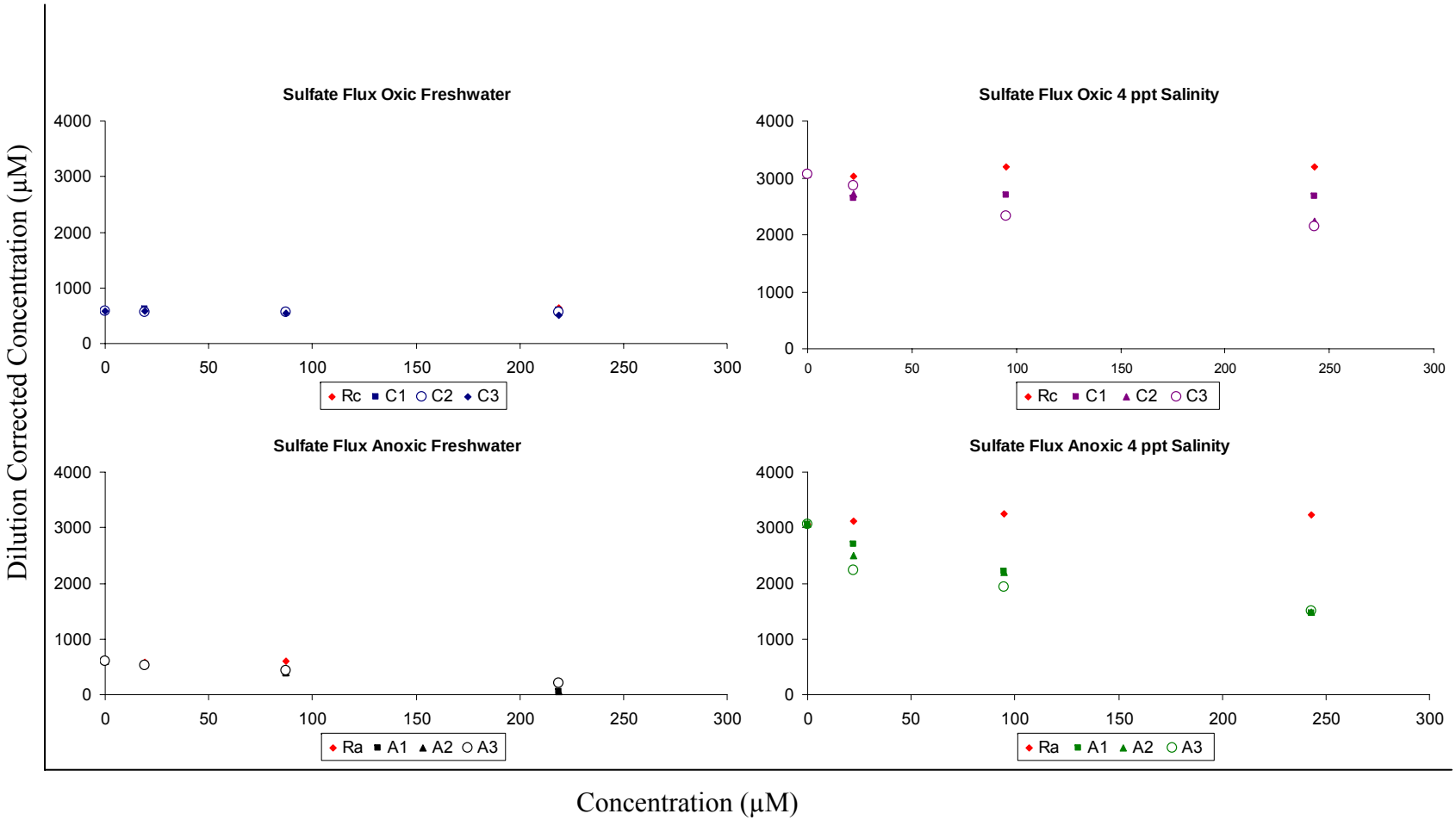

Figure 12d. White Oak River. Dilution-corrected concentrations of sulfate in overlying water of incubated sediment cores as a function of time.

Table 8. Flux summary of the four analytes studied in experiment III. The t-test for the slope of the regression line, using the dilution corrected concentrations, was applied to determine significance.

Treatment	MeHg (pmol m^{-2} d^{-1})	TDHg (pmol m^{-2} d^{-1})	DOC (mmol m^{-2} d^{-1})	Sulfate (mmol m^{-2} d^{-1})
Oxic Fresh	0.0	-72.0 ($p \leq 0.05$)	3.3 ($p \leq 0.001$)	-0.6 ($p \leq 0.05$)
n=3	0.0	0.0	2.5 ($p \leq 0.001$)	-0.8 ($p \leq 0.001$)
	0.0	0.0	2.5 ($p \leq 0.005$)	-1.4 ($p \leq 0.001$)
Anoxic Fresh	0.0	0.0	3.8 ($p \leq 0.001$)	-6.9 ($p \leq 0.001$)
n=3	-11.9 ($p \leq 0.001$)	0.0	4.7 ($p \leq 0.001$)	-7.1 ($p \leq 0.001$)
	-6.3 ($p \leq 0.001$)	-995.5 ($p \leq 0.005$)	4.7 ($p \leq 0.005$)	-5.1 ($p \leq 0.001$)
Oxic 4ppt Salinity	0.0	-124.5 ($p \leq 0.05$)	6.3 ($p \leq 0.001$)	0.0
n=3	0.0	0.0	6.4 ($p \leq 0.001$)	-9.4 ($p \leq 0.02$)
	0.0	0.0	5.2 ($p \leq 0.005$)	-11.3 ($p \leq 0.005$)
Anoxic 4ppt Salinity	0.0	0.0	7.2 ($p \leq 0.001$)	-18.2 ($p \leq 0.001$)
n=3	-6.3 ($p \leq 0.001$)	-114.0 ($p \leq 0.001$)	6.1 ($p \leq 0.001$)	-16.9 ($p \leq 0.001$)
	5.5 ($p \leq 0.05$)	0.0	3.9 ($p \leq 0.005$)	-15.6 ($p \leq 0.02$)

Two of the three cores under anoxic freshwater, showed fluxes of MeHg into the sediments at -12 and -6.3 pmol m^{-2} d^{-1} ($p \leq 0.001$, $p \leq 0.001$). A negative TDHg flux was measured into the sediments in one of the three cores at a rate of -1000 pmol m^{-2} d^{-1} ($p \leq 0.005$). DOC fluxes into the overlying water were measured in all cores of this treatment at rates of 3.8, 4.7, 4.5 mmol m^{-2} d^{-1} ($p \leq 0.001$, $p \leq 0.001$, $p \leq 0.005$, respectively). Negative fluxes of sulfate were measured in all cores of this treatment at rates of -6.9, -7.1, -5.1 mmol m^{-2} d^{-1} ($p \leq 0.001$, $p \leq 0.001$, $p \leq 0.001$, respectively).

Sediments under oxic low salinity water displayed no MeHg fluxes in any of the three cores. One of these three cores had a negative flux of TDHg into the sediments of -125 pmol/m^2/day ($p \leq 0.05$). All three of these cores had positive DOC fluxes of 6.3, 6.6, 5.2 mmol/m^2/day ($p \leq 0.001$, $p \leq 0.001$, $p \leq 0.005$, respectively). Two of these three cores had negative sulfate fluxes, into the sediments, of -9.4 and -11.3 mmol/m^2/day ($p \leq 0.02$, $p \leq 0.005$).

Two of the three cores under anoxic low salinity water measured MeHg fluxes, but in opposite directions. One showed a flux into the sediments of -6.3 pmol/m^2/day ($p \leq 0.001$) and the other a flux into the overlying water at 5.5 pmol/m^2/day ($p \leq 0.05$). One of three cores under this treatment showed a TDHg flux into the sediments at a rate of -115 pmol/m^2/day ($p \leq 0.001$). DOC fluxes under these condition were all positive and measured 7.2, 6.1, 3.9 mmol/m^2/day ($p \leq 0.001$, $p \leq 0.001$, $p \leq 0.005$, respectively). In all three cores sulfate fluxed into the sediments at rates of -18, -17, and -16 mmol/m^2/day ($p \leq 0.001$, $p \leq 0.001$, $p \leq 0.002$, respectively).

Sediment Mercury Content

Cores at the beginning and end of each treatment were sectioned at 1-2 cm intervals and analyzed for sediment MeHg and TDHg content. Figure 13 shows the MeHg (a) and TDHg (b) sediment content as a function of depth. Interestingly, the effect of salinity on the maximum concentration of MeHg was less significant than oxygen concentration. Maximum concentrations of MeHg were relatively constant between the oxic freshwater and oxic low salinity water sediments. Under both freshwater and low salinity water the maximum concentration of MeHg just below the SWI increased by > 500 pg g^{-1} when the overlying water had been bubbled with air. It is unfortunate there is no oxygen data for this experiment, because it is likely this zone of maximum MeHg concentration in the "oxic" cores occurred in the sub-oxic layer as suggested by(Holmes and Lean, 2006; Merrit and Amirbahman). If this is in fact the case it would appear that since there is little change in the maximum concentration of MeHg as a function of salinity that either there is already sufficient sulfate present in these freshwater sediments for sulfate reduction and we are seeing maximum MeHg production or the bacterial populations are slower to switch to sulfate reduction than expected and the experiment was not of sufficient length to see MeHg concentrations increase as a result of sulfate reduction.

TDHg concentration in the sediment changed little over the course of the experiment and showed no correlation with the treatment of the overlying water.

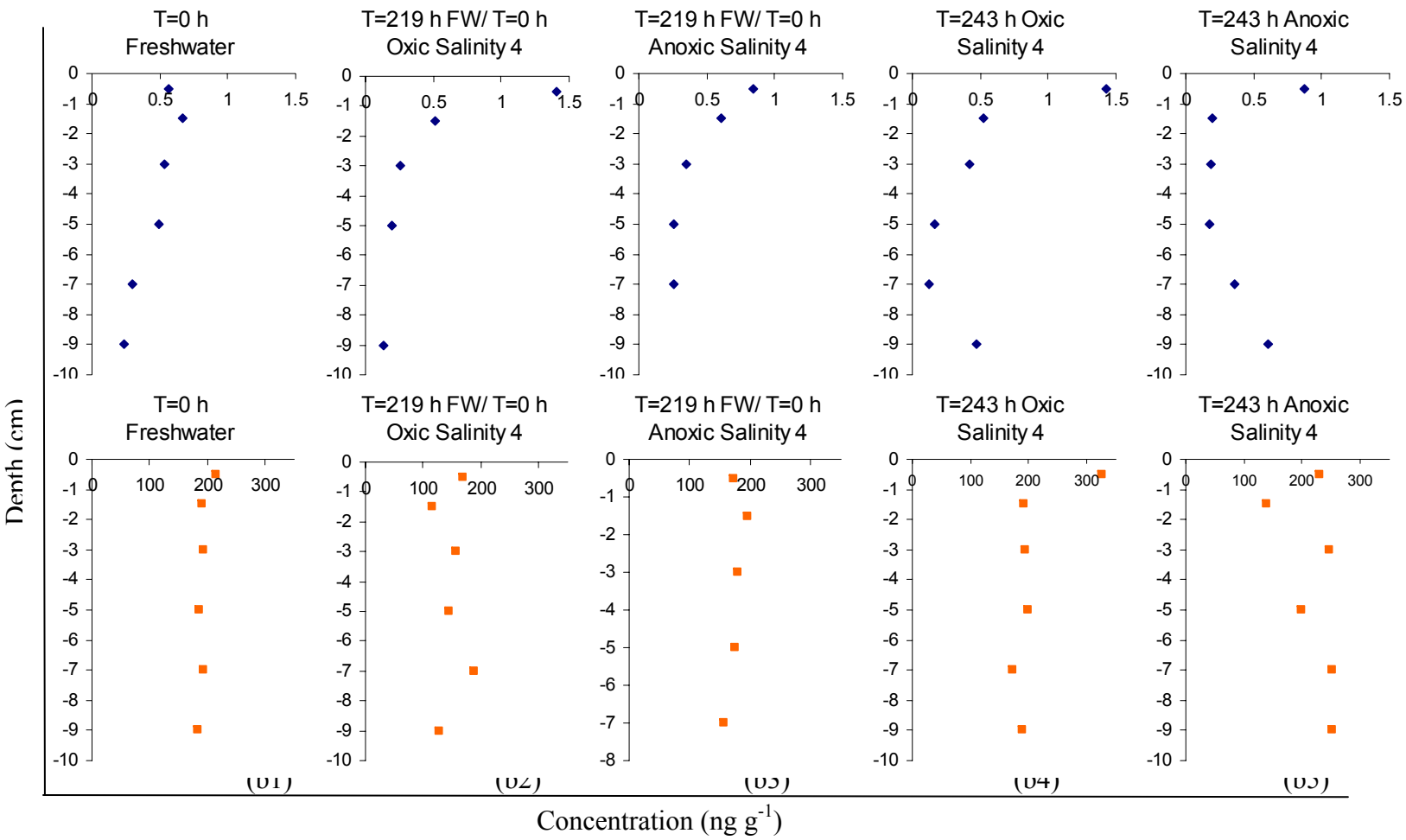

Figure 13. Sediment Hg profiles. a) MeHg in ng g^{-1} of dry sediment. b) TDHg in ng g^{-1} of dry sediment. Sediment cores were sectioned and analyzed before incubation (a1, b1), after freshwater treatment (a2-a3, b2-b3) , and after low salinity treatment (a4-a5, b4-b5).

Experiment IV: Eagle Island, February 2008

To examine potential variations of sediment biogeochemistry due to seasonality Eagle Island sediments for experiment IV were collected in February of 2008 and incubated in a temperature controlled cold room at 5^0C. Treatments were incubated and monitored for 17-18 days as oppose to the 9-11 day long treatment of experiment III. This was done because, due to slower rates of organic matter remineralization at colder temperatures, flux and redox chemistry trends may take longer to observe. Additionally, due to severe drought in 2007 the waters adjacent to Eagle Island had risen to a salinity of 5. For this reason the experiment had to be carried out in reverse (i.e. low salinity treatment followed by the freshwater treatment). This complicates comparisons as it is not possible to remove the sulfate from the sediments before the freshwater treatment. So although the overlying water of the freshwater treatment should have been very low in sulfate, the sediment likely still contained more than threshold concentrations for sulfate reduction. All other parameters of the experiment were the same as in experiment III. Triplicate cores for each water treatment were used for flux measurements, two cores were used, and maintained under the same conditions as flux cores, for depth profiling, and additional cores were taken, and maintained under the same conditions as flux cores, for sectioning and analyzing sediment contents. Fluxes were measured for MeHg, TDHg, DOC, and sulfate.

Sediment Redox Characterization

As in the previous experiments the initial time point profiles were measured before treating and incubating the cores. Therefore, the "oxic" and "anoxic" designation refers not to their current condition but to the treatment they underwent. Initially both cores were dominated by Fe and Mn reduction with no detectable sulfide in either core. Sediment depth profiles of Fe^{2+}, Mn^{2+}, ΣH_2S, and O_2 are shown in Figures 14a and 14b. Table 9 lists the concentration maxima of the analytes and their respective depths. The core designated as oxic had initial oxygen penetration to 0.2 cm followed by a small zone of iron reduction. Mn^{2+} was first detected at 1.2 cm and had a maximum concentration of 33 μM at 6.0 cm. The core designated as anoxic had initial oxygen penetration to a depth of 0.1 cm, overlapping with initial detection of Fe^{2+} and Mn^{2+}. Maximum concentrations of Fe^{2+} and Mn^{2+} were 32 and 51 μM, respectively with both occurring at 0.4 cm.

Under the oxic low salinity conditions Fe^{2+} exhibited a gradual concentration increase and migration toward to the SWI, despite oxygen penetration to 0.3 cm. Mn^{2+}, under this treatment, had concentration increases both at depth and at the surface (288 h) indicating either diffusion of Mn^{2+} into the sediments at the surface, which is unlikely as it undetected in the overlying water, or two distinct zones of manganese reduction. ΣH_2S was not detected throughout this entire treatment. O_2 concentrations remained fairly constant between 330 and 375 μM in the overlying water, penetrating to 0.3 cm.

Under anoxic low salinity conditions Mn^{2+} dominated the sediments with a concentration increase upon incubation and variable depth of maximum concentration

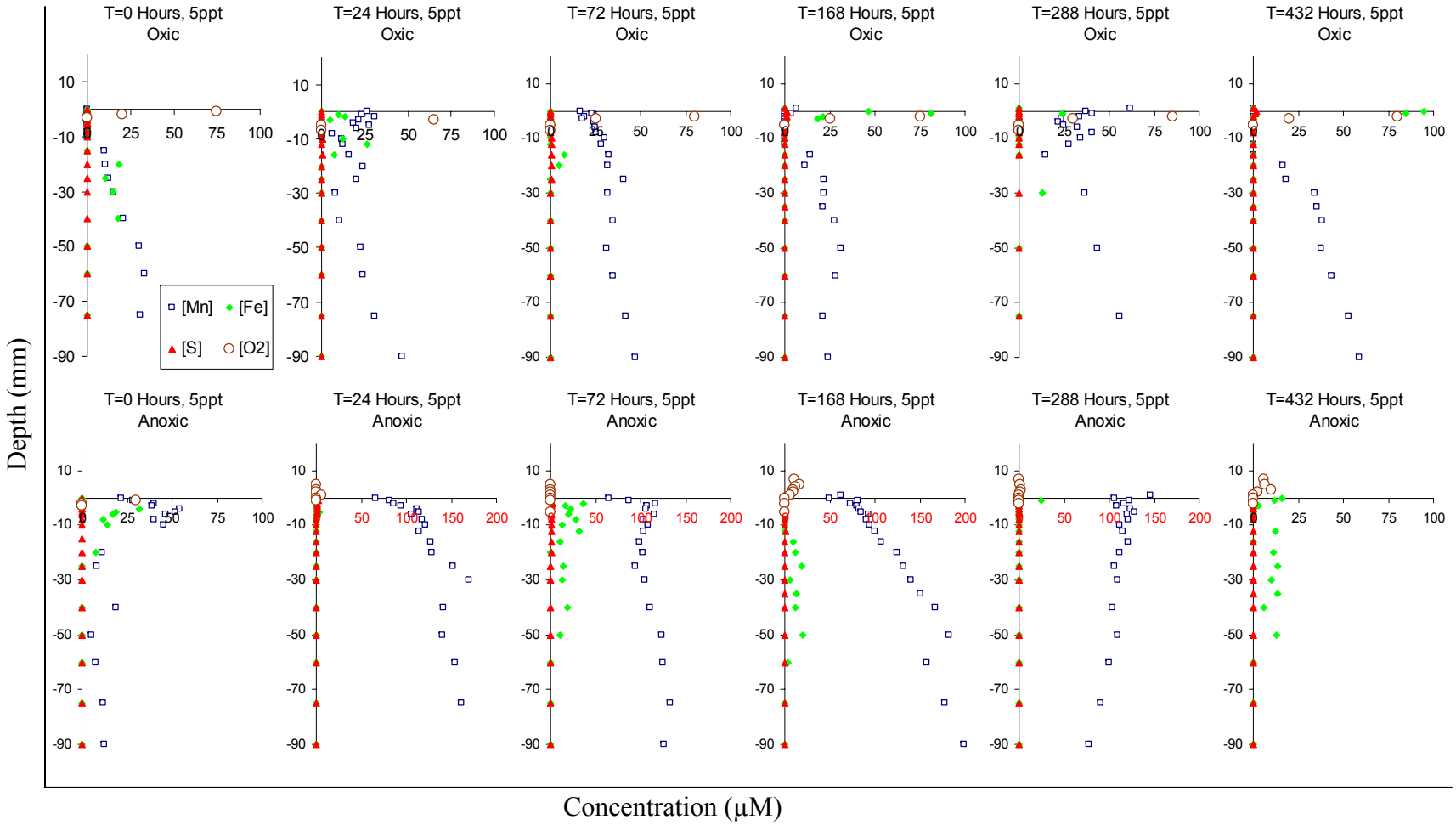

Figure 14a. Experiment IV: Eagle Island river sediment cores taken February 2008 incubated with salinity 5 river water for approximately two weeks at 5-8 ^{0}C. Sediment depth profiles of redox active analytes O_2, Fe^{2+}, Mn^{2+}, and ΣH_2S as a function of time. Note the scale of the x-axis between 24 and 288 h anoxic is doubled.

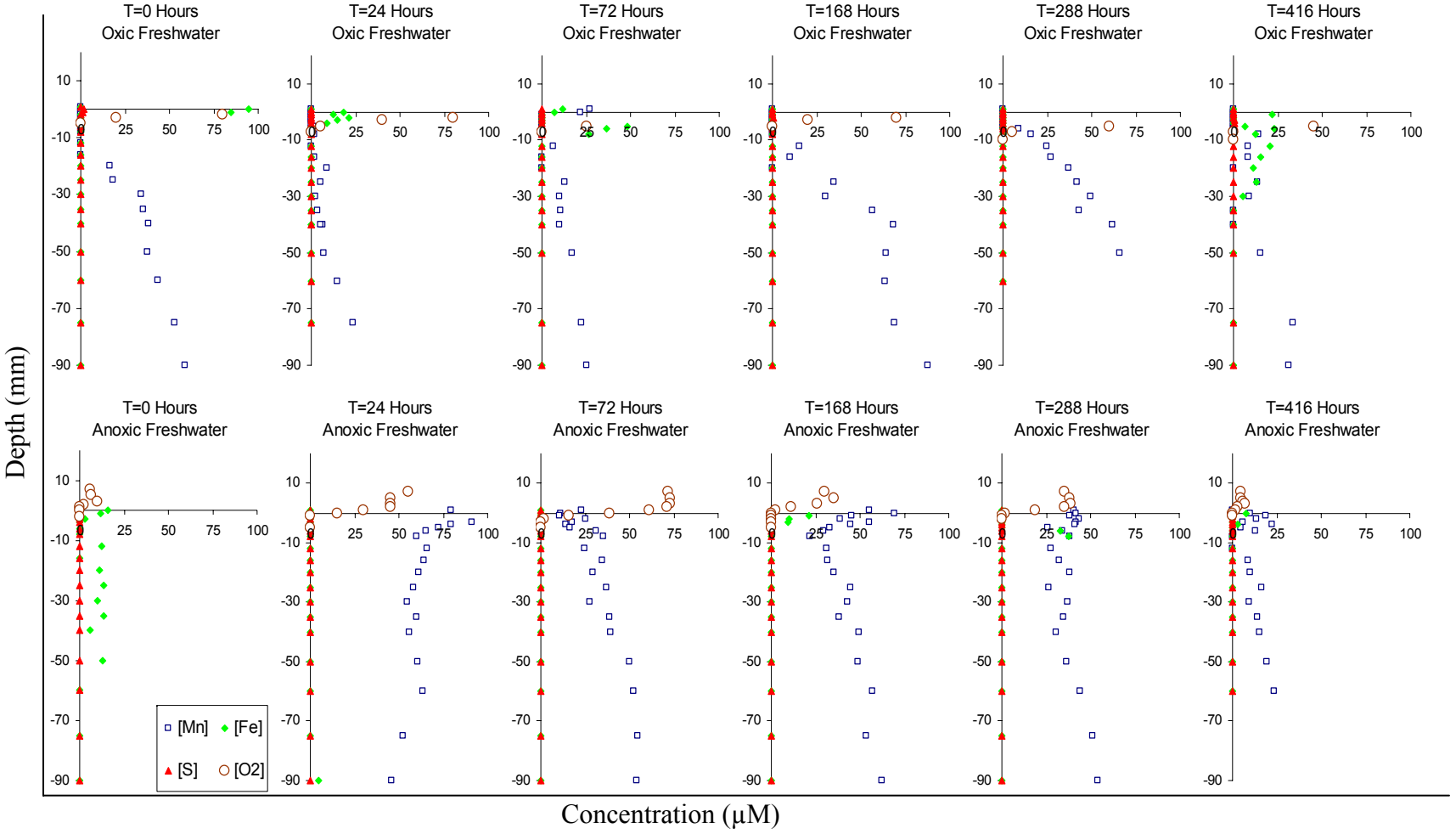

Figure 14b. Expeimentn IV: Eagle Island river sediment cores taken February 2008 incubated with freshwater for approximately two weeks at 5-8^{0}C. Sediment depth profiles of redox active analytes O_2, Fe^{2+}, Mn^{2+}, and ΣH_2S as a function of time.

Table 9. Maximum redox-active analyte concentrations and respective maximum concentration depths from depth profiles of experiment IV. Negative depth values indicate maximums below the sediment-water interface and positive values indicate above this interface. a) 5 ppt salinity treatment, b) freshwater treatment. O_2 depth refers not to depth of concentration maximum as this was always occurred in the overlying water, but to the last depth at which O_2 was detected in sediments

Analyte	Conc Max (µM) / Depth of Conc. Max. (cm)*					
Oxic Low Salinity water	0 Hours	24 Hours	72 Hours	168 Hours	288 Hours	432 Hours
Fe^{2+}	18 / -2.0	26 / -1.2	7 / -1.6	81 / -0.2	24 / -0.1	95 / 0.0
Mn^{2+}	33 / -6.0	47 / -9.0	47 / -9.0	31 / -5.0	56 / -7.5	60 / -9.0
S^{2-}	0	0	0	0	0	2 / 0.0
O_2	190 / -0.2	375 / -0.3	350 / -0.3	345 / -0.3	330 / -0.3	340 / -0.3
Anoxic Low Salinity water	0 Hours	19 Hours	43 Hours	87 Hours	155 Hours	219 Hours
Fe^{2+}	32 / -0.4	37 / -0.2	37 / -0.2	20 / -5.0	25 / -0.1	16 / 0.0
Mn^{2+}	54 / -0.4	234 / -9.0	133 / -7.5	199 / -9.0	128 / -0.5	191 / 0.0
S^{2-}	0	2 / 0.0	2 / -0.2	0	0	0
O_2	130 / -0.1	0	0	0	2.7 / 0.2	10 / 0.2
Oxic Freshwater	0 Hours	22 Hours	45 Hours	95 Hours	170 Hours	266 Hours
Fe^{2+}	95 / 0.0	21 / 0.2	48 / -0.5	0	0	23 / -0.6
Mn^{2+}	59 / -9.0	24 / -7.5	25 / -9.0	88 / -9.0	165 / -6.0	34 / -7.5
S^{2-}	2 / 0.0	0	0	0	0	0
O_2	340 / -0.3	400 / -0.5	375 / -0.5	400 / -0.3	385 / -0.7	400 / -0.5
Anoxic Freshwater	0 Hours	49 Hours	119 Hours	182 Hours	382 Hours	266 Hours
Fe^{2+}	16 / 0.0	5 / -9.0	0	21 / -0.1	38 / -0.8	7 / 0.0
Mn^{2+}	191 / -9.0	108 / 0.0	55 / -7.5	70 / 0.0	54 / -9.0	24 / -6.0
S^{2-}	0	0	0	0	0	0
O_2	10 / 0.2	55 / 0.0	72 / -0.1	30 / 0.1	35 / 0.0	7.2 / 0.1

over the treatment period, likely due to sediment heterogeneity. Fe^{2+}, under these conditions, remained at relatively low concentrations and displayed no discernable trends over the course of the treatment. ΣH_2S, in this treatment, remained at or below detection limits. O_2 concentrations were typically below detection with a maximum concentration of 10 μM occurring in the overlying water at 432 h and 0.2 cm above the SWI.

Under oxic freshwater conditions Mn^{2+} dominated the sediments with maximum concentrations ranging from 24 to 165 μM and occurring typically at depths below 6.0 cm. Fe^{2+} under these conditions, was inconsistent and was detected only sporadically at the surface. ΣH_2S remained at or below detection limit throughout this treatment. O_2 concentrations were between 375 and 400 μM in the overlying water and reached maximum depths of 0.7 cm.

Under anoxic freshwater conditions the sediments were again dominated by manganese reduction with concentration maxima ranging from 24 to 191 μM at depths of > 6.0 cm. Fe^{2+} was again sporadic with concentration maximuma never exceeding 40 μM and usually occurring within the top 1 cm. O_2 concentrations were consistently higher than in the anoxic low salinity treatment, ranging from 7.2 to 72 μM and reaching a maximum depth of 0.1 cm below SWI at 72 h.

Reducible Fe and Mn

Figure 11 shows the depth profiles of R-Fe and R-Mn at the beginning and end of each treatment, generated as described above for experiment III. R-Fe concentration maxima ranged between 25 and 200 μg g^{-1} but it is unclear if this variability is due to the conditions of the overlying water or the heterogeneity of the sediments. It is evident,

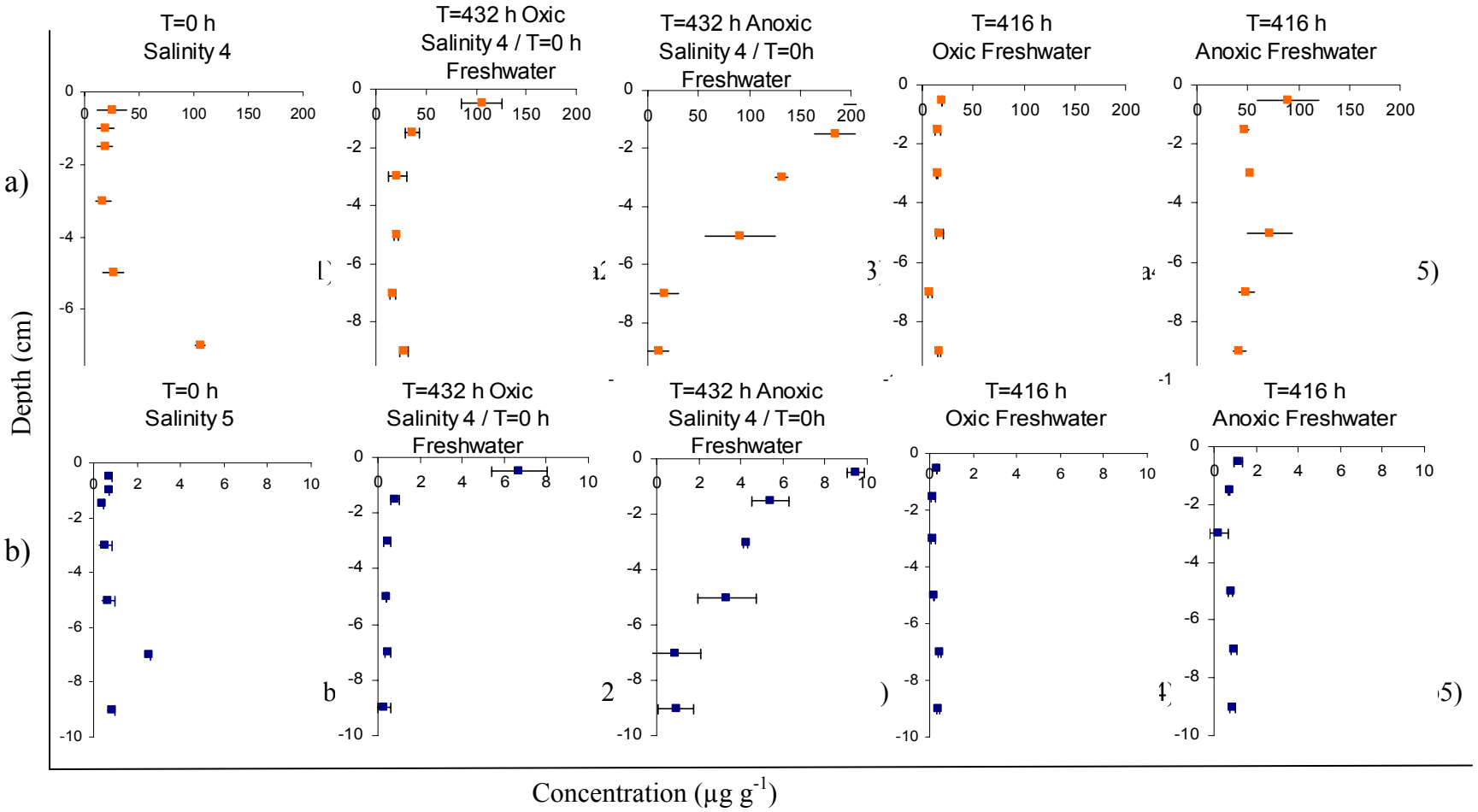

Figure 15. Sediment Fe and Mn profiles from experiment IV. A) R-Fe in µg/g of dry sediment. b) R-Mn in µg/g of dry sediment. Sediment cores were sectioned and analyzed before incubation (a1, b1), after 5ppt salinity treatment (a2-a3, b2-b3) , and after freshwater treatment (a4-a5, b4-b5).

that as in experiment III there is an abundance of reducible iron available, despite detecting only small and sporadic concentrations of Fe^{2+} with the electrode.

R-Mn had initial concentrations between 0.5 and 4.0 μg g^{-1} with a concentration maximum occurring between 6 and 8 cm. After approximately 18 days this concentration maximum increased to greater than 6 and 8 μg g^{-1} in the oxic and anoxic low salinity treatments, respectively and occurred at the uppermost interval. By the end of the freshwater treatment these R-Mn concentration maxima were reduced to less than 2.0 μg g^{-1}.

Sediment-Water Fluxes

The dilution corrected concentrations of MeHg, TDHg, DOC, and sulfate for the six time points as a function of time are shown in Figs. 12a-c. Table 10 summarizes the significant flux rates for these analytes based on the slopes of these corrected concentrations. As before, negative values represent water to sediment fluxes and positive values represent sediment to water fluxes.

Under oxic low salinity conditions MeHg showed a flux of -4.8 pmol m^{-2} d^{-1} ($p \leq 0.01$) in one of three cores. TDHg had a flux of -56 pmol m^{-2} d^{-1} ($p \leq 0.005$) in one of the three cores. A single DOC flux was measured, under these conditions, of 0.8 mmol m^{-2} d^{-1} ($p \leq 0.05$). Two of the three cores measured positive sulfate fluxes of 7.2 and 3.0 mmol m^{-2} d^{-1} ($p \leq 0.05$, $p \leq 0.05$)

Under anoxic low salinity conditions MeHg fluxed into the sediments in each of three replicates at rates of 2.2, 3.4, and 3.4 pmol m^{-2} d^{-1} ($p \leq 0.02$, $p \leq 0.02$, and $p \leq 0.02$, respectively). Under these conditions TDHg had measured fluxes of -34 and -49

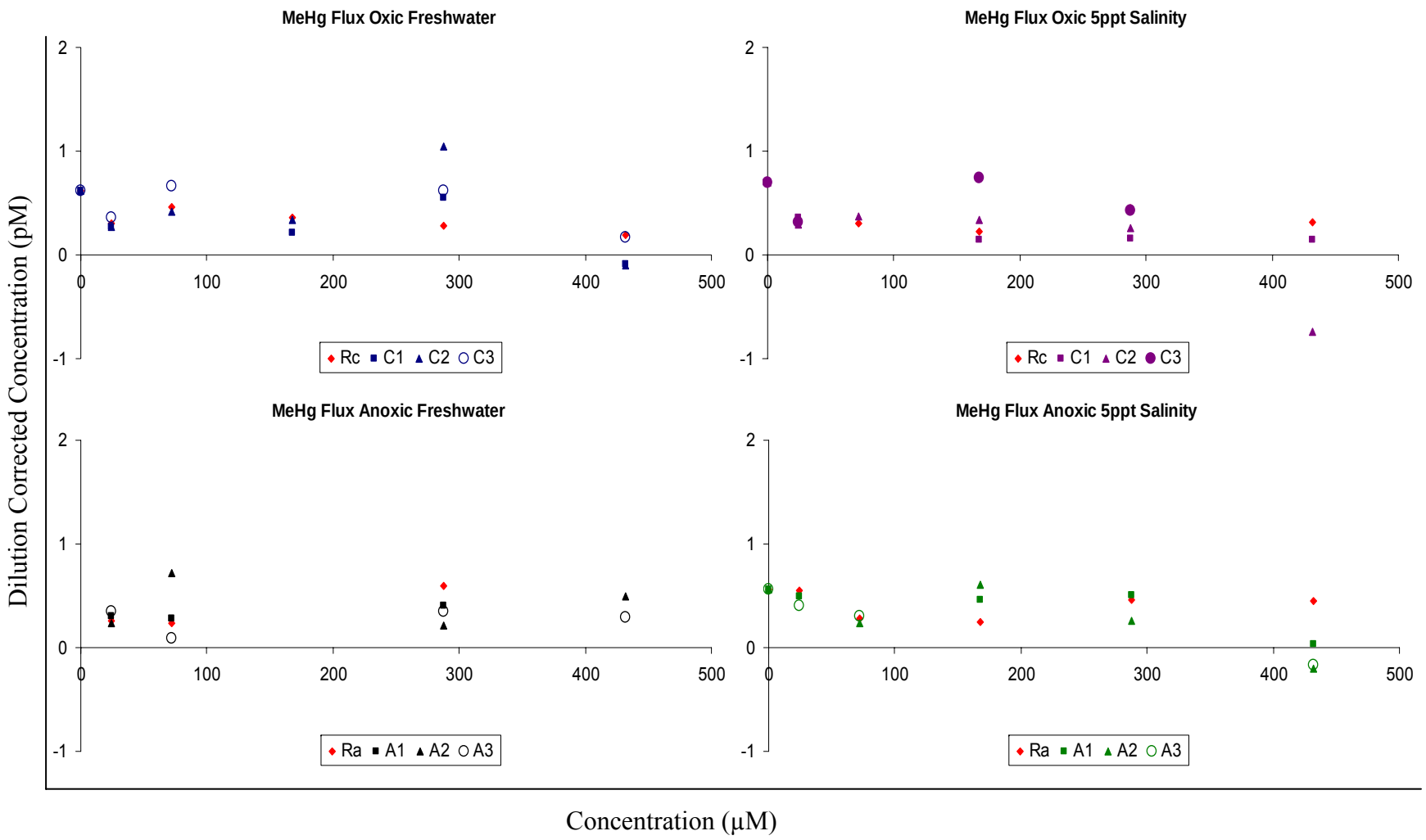

Figure 16a. Eagle Island experiment IV. Dilution-corrected concentrations of MeHg in overlying water of incubated sediment cores as a function of time.

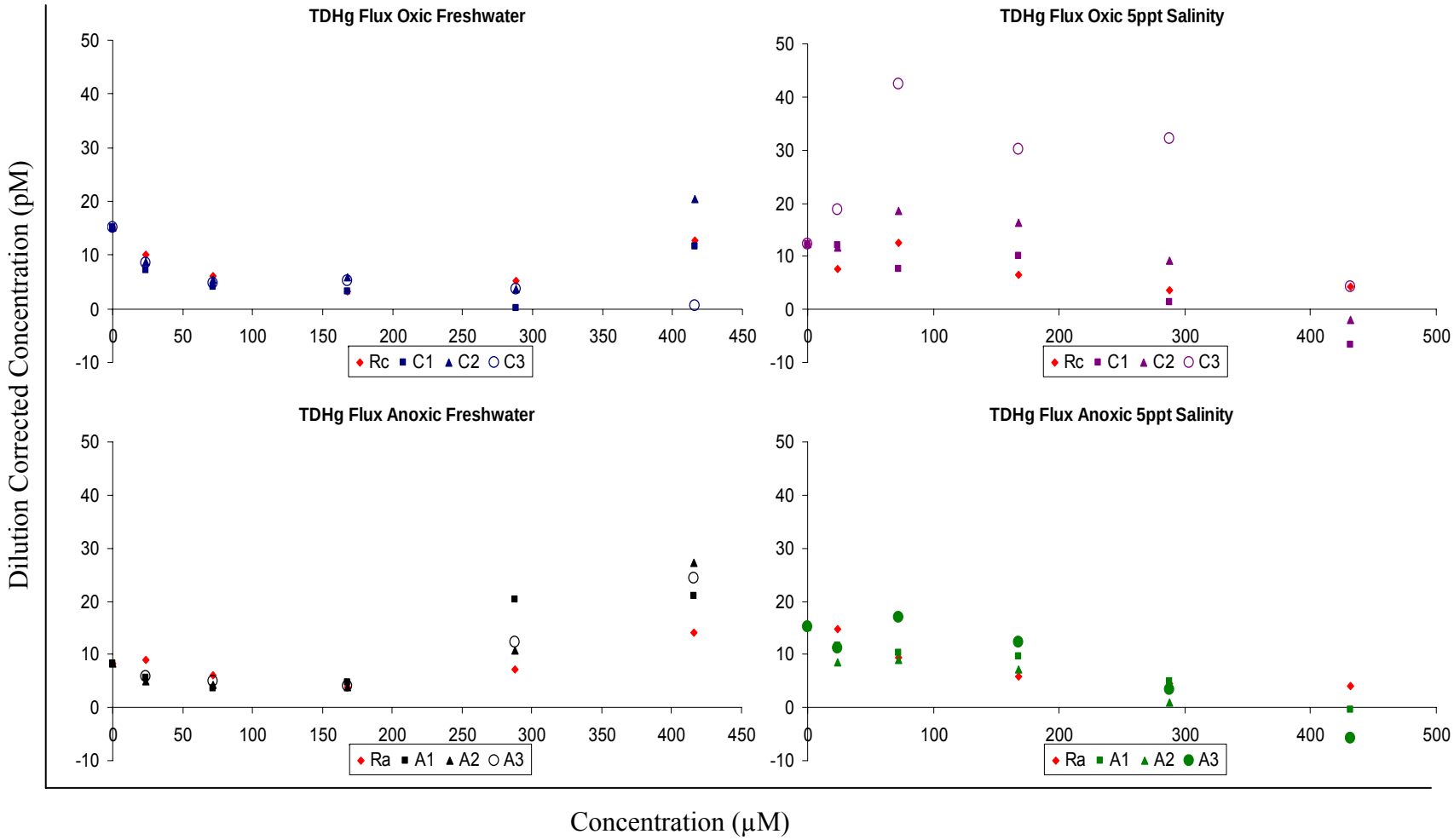

Figure 16b. Eagle Island experiment IV. Dilution-corrected concentrations of TDHg in overlying water of incubated sediment cores as a function of time.

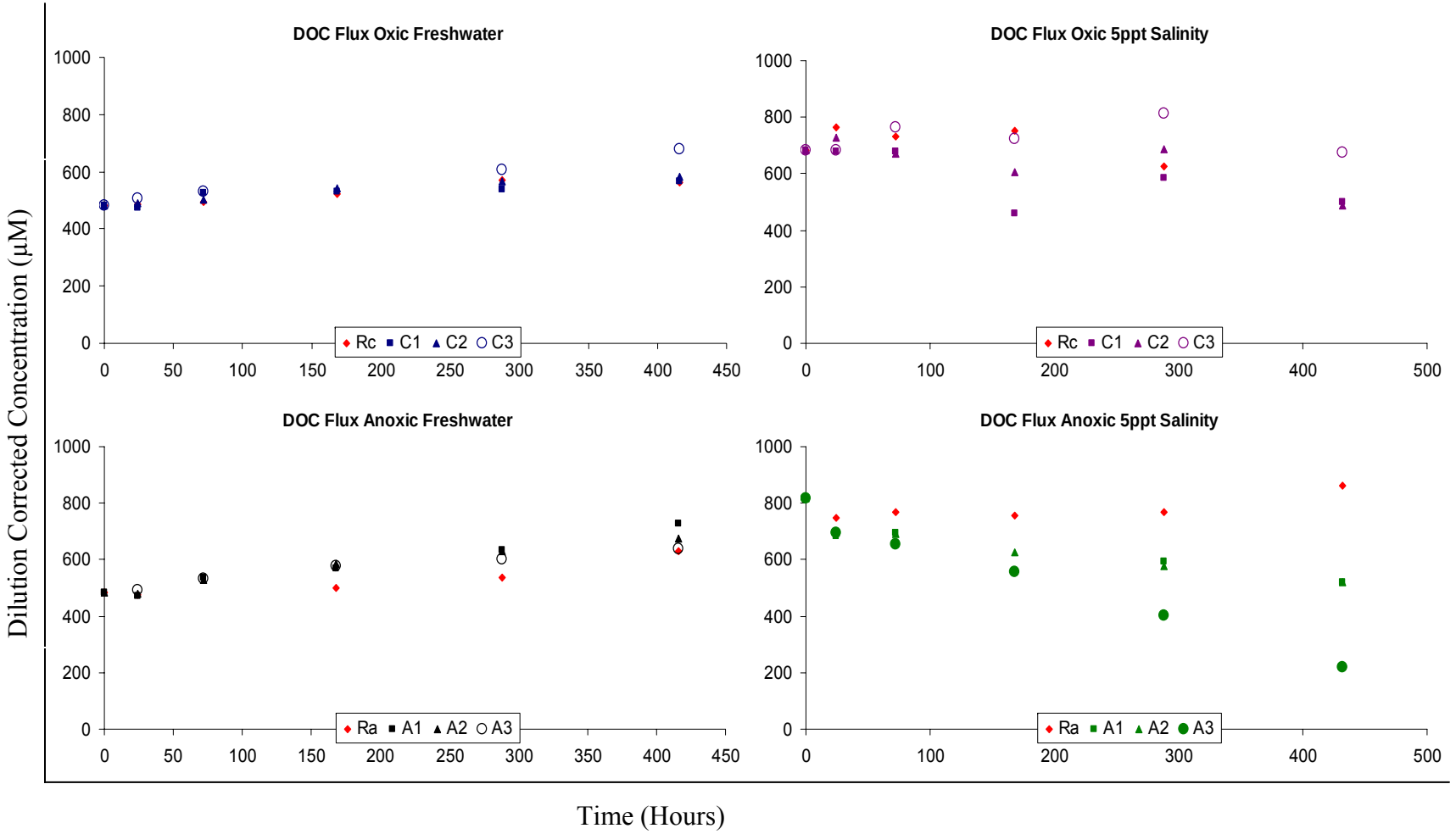

Figure 16c. Eagle Island experiment IV. Dilution-corrected concentrations of DOC in overlying water of incubated sediment cores as a function of time.

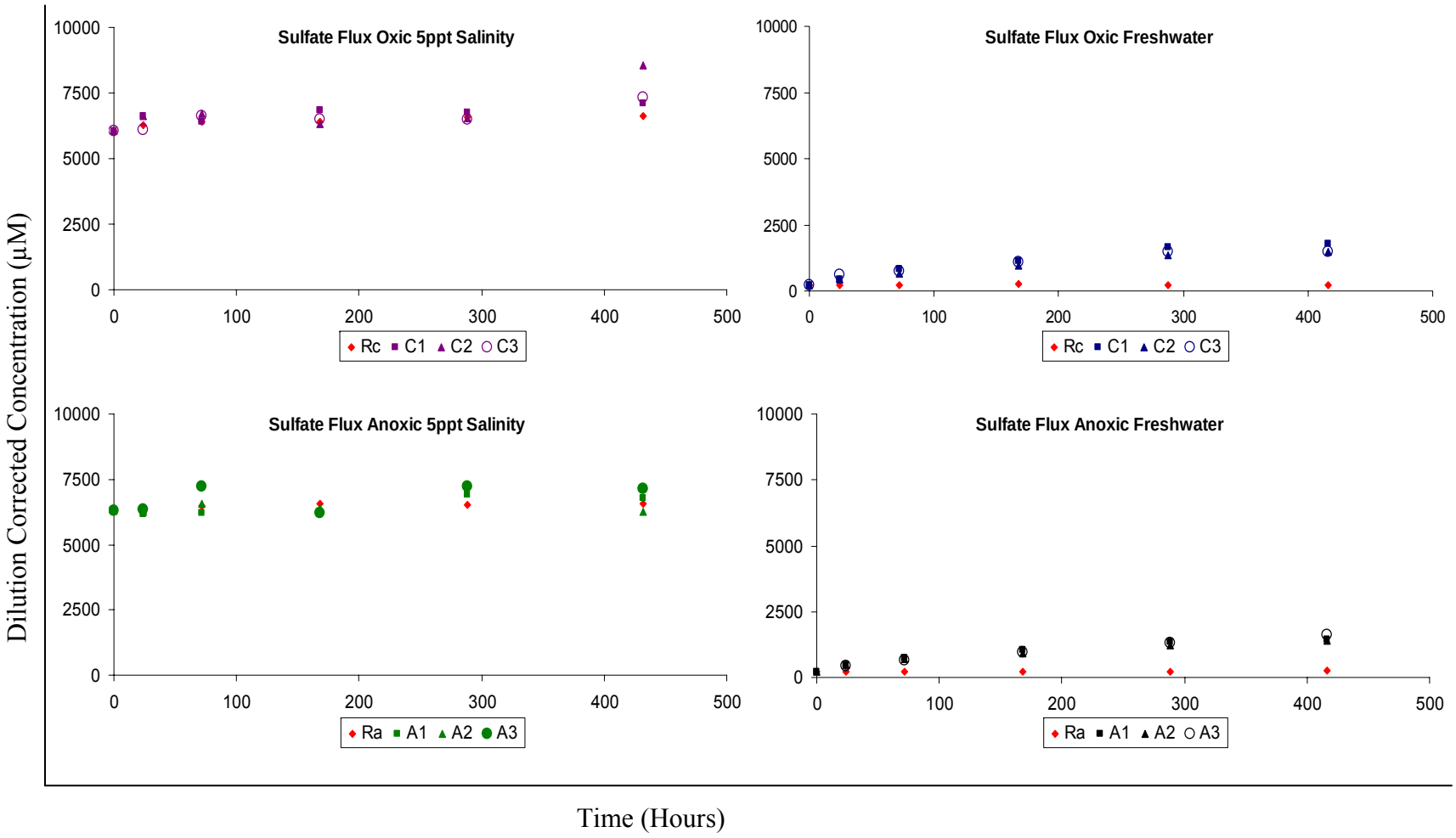

Figure 16d. Eagle Island experiment IV. Dilution-corrected concentrations of sulfate in overlying water of incubated sediment cores as a function of time.

Table 10. Flux summary of the four analytes studied in experiment IV. T-test for the slope of the regression line, using the dilution corrected concentrations, was applied to determine significance for each treatment.

Treatment	MeHg (pmol m^{-2} d^{-1})	TDHg (pmol m^{-2} d^{-1})	DOC (mmol m^{-2} d^{-1})	Sulfate (mmol m^{-2} d^{-1})
Oxic 5ppt Salinity	0.0	-56.2 ($p \leq 0.005$)	0.0	0.0
n=3	-4.8 ($p \leq 0.01$)	0.0	0.0	7.2 ($p \leq 0.05$)
	0.0	0.0	0.8 ($p \leq 0.05$)	3.0 ($p \leq 0.05$)
Anoxic 5ppt Salinity	-2.2 ($p \leq 0.02$)	0.0	-1.6 ($p \leq 0.001$)	2.4 ($p \leq 0.05$)
n=3	-3.4 ($p \leq 0.02$)	-33.6 ($p \leq 0.02$)	-1.7 (p 0.001)	0.0
	-3.4 ($p \leq 0.001$)	-49.2 ($p \leq 0.05$)	-3.4 ($p \leq 0.001$)	0.0
Oxic Fresh	0.0	0.0	0.0	9.0 ($p \leq 0.001$)
n=3	0.0	0.0	0.0	7.1 ($p \leq 0.001$)
	0.0	-52.8 ($p \leq 0.01$)	0.5 ($p \leq 0.001$)	6.9 ($p \leq 0.001$)
Anoxic Fresh	-1.0 ($p \leq 0.05$)	64.1 ($p \leq 0.05$)	0.6 ($p \leq 0.001$)	6.6 ($p \leq 0.001$)
n=3	0.0	72.7 ($p \leq 0.05$)	0.3 ($p \leq 0.005$)	6.2 ($p \leq 0.001$)
	0.0	55.7 ($p \leq 0.05$)	0.0	7.6 ($p \leq 0.001$)

pmol m^{-2} d^{-1} ($p \leq 0.02$, $p \leq 0.05$). DOC fluxes of -1.7, -1.7, and -3.4 mmol m^{-2} d^{-1} ($p \leq 0.001$, 0.001, and 0.001, respectively) were observed. One of the three cores under the anoxic low salinity conditions had a measurable sulfate flux of 2.4 pmol m^{-2} d^{-1} ($p \leq 0.05$) out of the sediment.

In the oxic freshwater cores no MeHg was seen to flux in or out of the sediment in triplicate cores. TDHg fluxed into the sediments in two of the three cores at rates of -11.9 and -6.3 pmol m^{-2} d^{-1} ($p \leq 0.001$, $p \leq 0.001$). DOC had a 0.5 mmol m^{-2} d^{-1} ($p \leq 0.001$) flux in one of the cores with no significant flux in the other two. Sulfate fluxes in this treatment were all out of the sediment at rates of 9.0, 7.1, and 6.9 mmol m^{-2} d^{-1} ($p \leq 0.001$, $p \leq 0.001$, $p \leq 0.001$, respectively).

Under anoxic freshwater conditions a single MeHg flux of -1.0 pmol m^{-2} d^{-1} ($p \leq 0.05$) was measured. TDHg had three measurable fluxes of 64, 73, and 56 pmol m^{-2} d^{-1} ($p \leq 0.05$, $p \leq 0.05$, $p \leq 0.05$, respectively). Two of three cores under these conditions had measurable fluxes of 0.6 and 0.3 mmol m^{-2} d^{-1} ($p \leq 0.001$, $p \leq 0.005$). Sulfate fluxes, in triplicate core, were observed at rates of 6.6, 6.2 and 7.6 mmol m^{-2} d^{-1} ($p \leq 0.001$, $p \leq 0.001$, $p \leq 0.001$, respectively). This positive flux of sulfate out of the sediment is likely due to the residual sulfate in the sediment from the previous low salinity 5 treatment.

Sediment Mercury Content

Fig. 13 shows the sediment depth profiles of sediment MeHg and TDHg at the beginning and end of each treatment. Overall these sediments had lower concentrations of MeHg in the sediments than the White Oak sediment with a subsurface maximum remaining below 500 pg g^{-1} in the top 8 cm. The low salinity treatment was the only

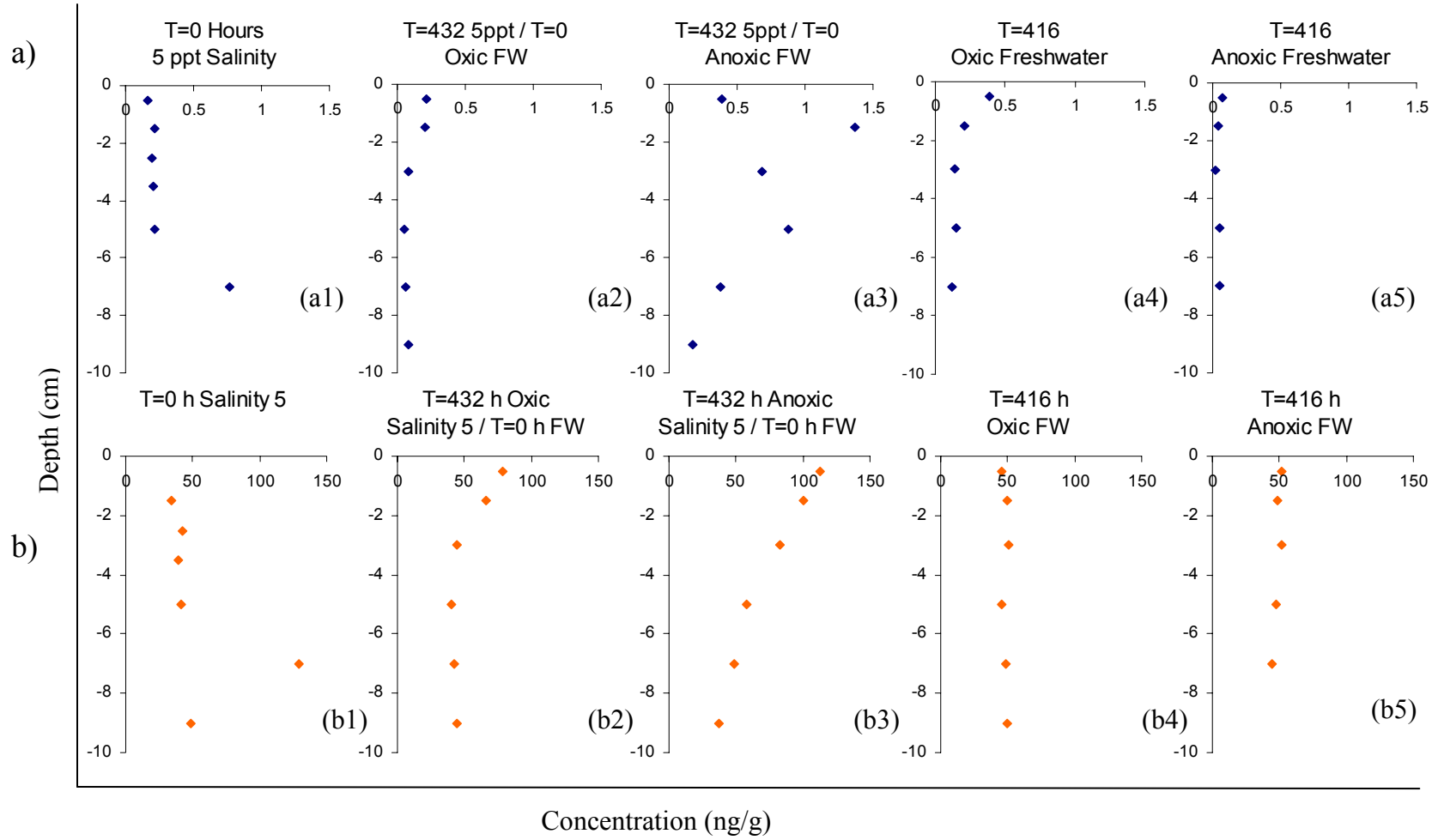

Figure 17. Sediment Hg profiles from experiment IV. a) MeHg. b) TDHg. Sediment cores were sectioned and analyzed before incubation (a1, b1), after freshwater treatment (a2-a3, b2-b3) , and after 4ppt salinity treatment (a4-a5, b4-b5).

exception which had a maximum of over 1200 pg g^{-1} at 1-2 cm depth at 432 h indicative of methylation in a zone of sulfate reduction. Surprisingly, TDHg concentrations were lower in these sediment then those measured in the White Oak river.

DISCUSSION

Sediment Biogeochemistry

Eagle Island: Experiments I & II

Monthly depth profiling of three Eagle Island sites, including the site used for this study, was carried out for approximately 12 months by Shaugnessy (2007). The dominance of reduced Mn in the sediments prior to incubation, as seen in the experiments described here, is consistent with those findings. Sediments of Eagle Island were found to be relatively heterogeneous as depicted in Fig. 14. Therefore it can not always be assumed that a profile of any given time point represents the biogeochemical "norm" of the core. As a result overall trends are examined here with less emphasis or examination of any one time point profile.

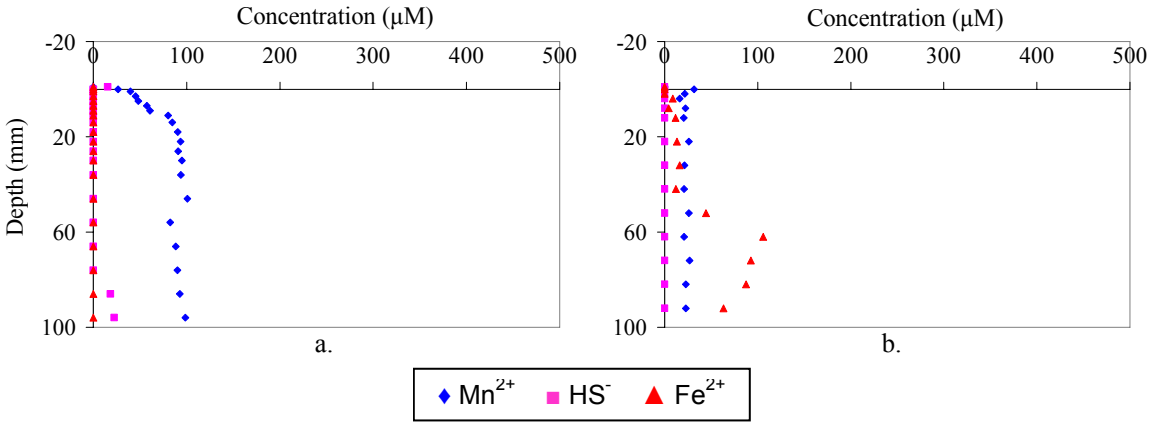

Figure 18. Two depth profiles generated by Shaugnessy (2007) of the same core taken from the same site as this study, demonstrating the extent of heterogeneity in these sediment cores.

Concentrations of dissolved pore water Mn^{2+} reached 488 μM in Eagle Island sediments indicative of a Mn-rich environment. Mn^{2+} pore water concentrations of previous studies in coastal marine sites have ranged from <250 μM in typical sites (Sørenson and Jørgenson 1987,; Luther et al. 1997) to 600 μM in a Mn-rich Scottish sea loch (Bartlett et al. 2007). Recent studies have elucidated the complexity of manganese cycling in sediments with Mn(IV) oxides capable of oxidizing Fe^{2+} (Canfield et al. 1993), sulfide (Aller 1994) as well as ammonia (Luther et al., 1997; Burdige, 1993). Burdige (2006) suggested that if Mn oxides are present in abundance a distinct zone of iron reduction may not be observable by pore water concentrations of Fe^{2+} due to its oxidation by Mn(III) & Mn(IV).

In the "oxic" freshwater sediment cores collected during the summer (experiments I and II) Mn^{2+} is seen to increase below the SWI and remain the dominant analyte throughout the core (Fig 1, 2a). The ability of Mn(III) & Mn(IV) to oxidize reduced iron and sulfide may explain, in part, the minimal detection of those analytes in the cores. In addition, there may be another factor affecting carbon remineralization in these sediments. The Eagle Island study site, as described previously, is located on the intertidal mud bank adjacent to the marsh edge. Erosion of the new marsh is visually observable and it is possible that the sediments of the mud bank are remnants of the old marsh. If this is so, despite % organics by LOI of 10-20% (Shaugnessy 2007), the labile organic content in these sediments may be low and remineralization processes may be diminished and therefore rarely proceed beyond Mn reduction. This is, however, speculative as no measurement of labile organic carbon was taken. The air source used to aerate the cores in experiment I was inconsistent and, despite not having oxygen measurements it is likely

that the SWI was anoxic, which explains the increase of Fe^{2+} and Mn^{2+} at the SWI as the reduced form of their respective oxides (Davison 1993; Beutal et al., 2008). Under anoxic freshwater conditions (Fig. 1, 2a) a similar increase at the SWI of Fe^{2+} and Mn^{2+} is seen and attributable to this same process.

Replacement of the overlying freshwater with 1.6 mM spiked sulfate water (experiment I) had little visible effect on the sediment biogeochemistry (Fig 1). These sediments were largely dominated by Mn reduction; sulfate reduction would not be expected to occur until reducible Mn was depleted (Froelich et al., 1979). In experiment II, replacement of the overlying water with low salinity water resulted in immediate increase of sulfide to maximum concentrations of 30 and 40 μM in the oxic and anoxic treatments, respectively. These concentrations are similar to concentrations of sulfide measured in surficial porewaters by microelectrode in recent studies by Merrit and Amirbahman (2008). As experiment I & II were carried out with sediment from the same site and both incubated at the same temperature, it is unclear if the differences in biogeochemical response to sulfate are a result of heterogeneity of the site or seasonality. The reduction of Fe(III) and Mn(III) & Mn(IV)oxides at the SWI continued to be observed in the anoxic treatment (Fig. 1and 2b) and likely plays an important role in MeHg cycling to be discussed later.

White Oak: Experiment III

This section of the White Oak River has previously been described by Martens and Goldhaber (1978), Kelley (1993), Chanton et al., (1989) and Kelley et al., (1995). This site was chosen for two reasons. First, it is at the extreme freshwater end of the

saline to freshwater transition zone, therefore only experiencing very low salinities during combinations of extreme high tides and drought. Second, its organic content is much higher, and the sediments are less compacted (~85% water) relative to Eagle Island sediments (~45% water) on the Cape Fear River. Despite the uniformity of these fine-grained, silty sediments, heterogeneity in the biogeochemistry was observed from one core to another. This heterogeneity can be seen in Figure 5a, where at 0 h both "oxic" and "anoxic" treatment have not yet commenced and therefore are representative of natural profiles. Note the scale in White Oak depth profiles is smaller than that for Eagle Island. Fe^{2+} and Mn^{2+} concentrations reached a maximum of 89 and 66μM, respectively in White Oak sediments compared to 450 and 490 μM, respectively in Eagle Island sediments.

Under freshwater conditions clear differences were observable between the "oxic" and "anoxic" treatments (Fig 5a). The "oxic" treatment maintained varying levels of Fe and Mn reduction throughout the core with small levels of sulfide measurable at depth. The "anoxic" treatment remained sulfidic throughout the treatment with maximum concentrations migrating toward the SWI.

Upon replacement of the overlying water with low salinity water the "oxic" core maintained varying levels of Fe and Mn reduction in the top 4 cm whereas sulfate reduction became visible at depth. Under "anoxic" conditions the magnitude of sulfate reduction was seen to increase as observed by the increase in sulfide at and above the SWI.

Unlike the Eagle Island profiles no Fe^{2+} or Mn^{2+} was detected at the surface in the anoxic treatments. Sulfide in these cores was measurable in the overlying water and based on the findings of Mason et al. (2006) a pε of < -3.3 is necessary for sulfide to

persist in the overlying water and under such conditions insoluble metal sufide complexes would form. This is supported by field data observed by Holmes and Lean (2006).

Eagle Island: Experiment IV

The last experiment was carried out in the winter with sediments from the Eagle Island site and cores incubated in a temperature controlled room at 5-6^{0}C. As is common for Eagle Island sediments the profiles revealed heterogeneity within cores. Despite this heterogeneity Mn dominance in these sediments was observed. Pore water concentrations were not as high as in experiments I & II, with maximum concentrations in experiment IV reaching only 230 μM. This concentration is representative of more typical coastal marine sites (Sørenson and Jørgenson 1987,; Luther et al. 1997) and suggests that seasonality has substantial effect on the geochemistry of these sediments. Lower temperature of these sediments upon collection as well as during incubation likely reduced bacterial metabolic rates (Shiah and Ducklow 1994) and carbon remineralization. In addition, maintaining anoxic conditions in the anoxic treatments proved difficult in freshwater at low temperature as can be seen from the overlying and pore water profiles (Fig. 9b). Burdige (2006) suggests that decreased temperatures could lead to vertical migration in the depth of redox zones. These factors combined could explain the prevalence of Mn in these sediments. No discernable changes were seen in the sediment biogeochemistry upon replacement of the overlying freshwater with low saliny water. Once again this is likely due to the abundance of thermodynamically favored Mn reduction.

Summary of Biogeochemistry

The results of the three Eagle Island sediment profiles indicate a Mn-rich environment. Consistent increase in the concentrations of Fe^{2+} and Mn^{2+} near the SWI support the contention that under reducing anoxic conditions metal oxides are reduced at the SWI via microbiological and chemical processes (Davison 1993). This reduction of the oxides at the SWI may play an important role in MeHg cycling, as will be discussed later, by releasing bound MeHg upon reduction (Beutal et al. 2008,; Merrit and Amirbahman, 2008;Chadwick et al. 2005; Mason et al. 2006). Seasonality was seen to have a significant impact on the biogeochemistry via the availability of Mn for reduction. In the February and June Eagle Island experiments (I & IV) reduced Mn^{2+} was dominant throughout the experiment at depth and treatment of the overlying water had little effect. In the September Eagle Island experiment (II) low concentrations of Mn^{2+} and Fe^{2+} were detected at depth with peak concentrations occurring at the SWI indicating depletion of Mn(III&IV) and Fe(III) at depth by the end of summer. Under these conditions the addition of sulfate stimulated immediate sulfate reduction at depth as seen by increases in pore water sulfide. As will be discused later, the combination of sulfate reduction at depth and metal oxide reduction at the SWI appears to play a significant role in the distribution of MeHg across the SWI.

The White Oak sediment profiles and previous work in these sediments (Avery et al., 2002) indicate an environment dominated by methanogenesis (Fig.5a and b). Pore waters were dominated by sulfide with sporadic Fe^{2+} and Mn^{2+} detected surficially. Addition of sulfate, by replacement of overlying water with low salinity water, resulted in

increased concentrations of pore water sulfide indicative of increased sulfate reducing activity.

Sediment-Water Fluxes

Eagle Island: Experiment I & II

Fluxes of MeHg over the course of this study appear to be directly related to conditions controlling the redox state of Fe and Mn at the SWI, as well as the presence or absence of active sulfate reduction and the depth at which it occurs. Fluxes of TDHg and DOC were more ambiguous and potentially affected by factors beyond the scope of this project. Some very general tends were occasionally observed and will be discussed briefly where relevant.

In experiments I & II from Eagle Island significant fluxes of MeHg were negative under all conditions except sulfate-containing, anoxic water (Table 2). It is now widely accepted that Hg methylation occurs primarily under anoxic conditions (Olson and Cooper, 1974; Compeau and Bartha, 1984) in the presence of active microbial sulfate reduction (Compeau and Bartha, 1985; Benoit et al., 2001; King et al., 2001). As such, it is expected that Hg methylation, under the conditions studied herein, should occur in the cores treated with sulfate containing anoxic water, once the more thermodynamically favored electron acceptors become depleted. It has been suggested that Hg is methylated in the suboxic zone just below the SWI (Gilmour et al., 1992) and that suboxic surface sediment may create a barrier against its diffusive flux across the SWI (Gagnon et al. 1996). The mechanism of this barrier is thought to involve adsorption of MeHg to Fe and Mn oxides at the SWI (Chadwick et al. 2005; Mason et al 2006; Merrit and Amirbahman

2008). It has been proposed by Gagnon et al. (1996) and Gill et al. (1999) that the flux of MeHg from sediments to water is controlled by the dissolution of these metal oxides, or by the co-transport of Hg and MeHg bound to DOC. Further evidence for this mechanism is reported by Merrit and Amirbahman (2008) who propose that vertical migration of the redoxicline and associated reduction of Fe and Mn oxides could result in the release of adsorbed MeHg. The results of this study indicate that reduction of these metal oxides plays a critical role in controlling the amount of MeHg diffusing from these sediments.

Replicate positive fluxes of MeHg were seen in experiment II under anoxic low salinity conditions. Sediment depth profiles of this treatment revealed sulfate reduction initiated within 24 h after the addition of sulfate. Concentrations of sulfide reaching 40 μM are consistent with pore water data reported by Merrit and Amirbahman (2008) in which that concentration was coincident with maximum MeHg pore water concentrations. MeHg produced by this sulfate reduction is predicted to have been bound to Fe and Mn oxides at the SWI upon diffusion through the sediments. Fe^{2+} and Mn^{2+} peaks detected at the SWI indicate the reduction of these metal oxides and resultant dissolution and release of the MeHg. These findings are consistent with similar studies using sediment flux chambers by Beutal et al. (2008) who found a positive correlation between Hg accumulations in overlying water with Mn under anaerobic conditions. Though sulfate reduction was seen to occur in the "oxic" cores as well, Fe^{2+} and Mn^{2+} peaks in this treatment were below the SWI indicating the metal-oxide barrier remained intact, effectively adsorbing MeHg and removing it from solution.

In the first experiment with Eagle Island sediment a prevalence of Mn^{2+} was seen in the pore water of both "oxic" and "anoxic" cores and remained throughout the

experiment. With an abundance of reducible Mn, sulfate reduction is not thermodynamically predicted to occur. In fact no resultant sulfide was detected in these sediments upon addition of sulfate. Without bacterial sulfate reduction, Hg is not expected to be methylated and accumulate in the sediment or adsorb to the metal oxides. Therefore, reduction of the metal oxides in the anoxic core would not be expected to release MeHg into the overlying water. Of the two replicate cores for each treatment, one of the sulfate-containing anoxic cores of experiment I did measure a positive flux. As the cores used to measure fluxes were not also used to generate depth profiles, it is possible, considering the heterogeneity of the site, that a flux core did not contain the abundance of Mn seen in the profile core. If this were the case a MeHg flux would be expected as microbial remineralization proceeded to sulfate reduction.

Chadwick et al. (2005) have reported a correlation of the cycles of Fe and Mn to DOC. The authors suggest that DOC is coprecipitated with metal oxides, the dissolution of which releases the DOC back into solution. If dissolution of metal oxides, namely those of Mn, at the SWI is responsible for MeHg flux one would expect a similar flux, at least directionally, of DOC. As mentioned previously there are many factors affecting DOC that are beyond the focus of the present study. There does, however, appear to be a relationship between MeHg Flux and DOC in these Eagle Island experiments. Positive fluxes of MeHg in each experiment were associated with positive fluxes of DOC (Tables 2 and 4). Conditions conducive to the reduction of metal oxides, based on the findings of Chadwick et al. (2005), would be favorable for positive DOC flux. A comparison of the pore water depth profiles (Fig. 1 and 3a,b) with the DOC fluxes (Tables 2 and 4), in fact, does reveal a positive flux of DOC where reduced forms of iron and manganese were

detected at the SWI. Large concentrations of DOC in overlying water relative to Mn concentrations at the SWI suggest reduction of oxides is not the sole factor affecting flux of DOC to the water column, but may be one of a number of factors.

White Oak River: Experiment III

Triplicate cores were used for each treatment in this experiment. MeHg flux results showed no significant fluxes under oxic conditions, regardless of salinity of the overlying water. Under anoxic freshwater condition two negative fluxes were measured, whereas fluxes under saline conditions were small and variable with one cores having zero flux a second having a small negative flux, and the third having a small positive flux (Table 6). It is uncertain why, under saline, anoxic conditions, these sediment did not show consistent positive fluxes of MeHg as Eagle Island sediments had. The absence of Fe^{2+} and Mn^{2+} at the SWI in the anoxic cores indicates there were no Fe or Mn oxides available to act as a diffusive barrier. With the addition of sulfate an increase in sulfide was seen at depth due to sulfate reduction. Without a metal oxide barrier one would expect MeHg produced by increased sulfate reduction to be seen in the overlying water. However, Bloom et al. (1999) and Hammerschmidt et al. (2004) describe an interaction between organic matter and mercury whereby increased organic matter increases the distribution coefficient (K_d=Hg_{sed}]/[Hg_{aq}]) of both inorganic Hg (IHg) and MeHg. Hammerschmidt et al. (2004) reported increased retention of MeHg to the solid phase with increasing organic matter content in Long Island Sound sediments. With the high concentrations of organic matter in the White Oak sediment the higher K_d of Hg is likely affecting the flux of MeHg. Furthermore, Miller et al. (2006) reported that neutral

mercury sulfide complexes may form larger complexes with certain types of dissolved organic matter, thereby inhibiting passive diffusion through the cell membranes of sulfate reducing bacteria.

DOC fluxes measured in experiment III were significantly positive for all triplicate cores of all treatments. Though no discernable trend in these fluxes was detectable, fluxes of DOC under oxic and anoxic low salinity water were slightly greater than those under freshwater. Reasons for consistently positive DOC fluxes are unclear, but are possibly related to the high levels of organic matter in these sediments. Sulfate fluxes measured in this experiment were negative for all triplicate cores (except one oxic low salinity core) of all treatments. This is not unexpected as pore water depth profiles showed varying degrees of sulfate reduction taking place in the sediments (Fig. 5a,b). The magnitude of these fluxes is visually consistent with increases in sulfide in the pore water profiles. It would have been interesting to compare rates of sulfate reduction with these sulfate flux rates, but such measurements were not logistically feasible.

Eagle Island: Experiment IV

As in experiment III triplicate cores were used for each flux treatment. Note that in this experiment incubation cores were first exposed to saline conditions (salinity 5) followed by freshwater due to initial saline conditions of the site on the day of sampling. Of the four experiments, this winter experiment with Eagle Island sediment resulted in the least pronounced MeHg flux activity. Lower temperature of these sediments upon collection, as well as during incubation, likely reduced bacterial metabolic rates (Shiah and Ducklow 1994), which in turn affect the fluxes. Seasonal variations in labile organic

matter may also have affected microbial activity As mentioned previously maintaining anoxic conditions in the anoxic freshwater treatments was difficult due to higher oxygen solubility at lower temperatures. In all treatments all significant fluxes of MeHg were small and negative (Table 8). In addition to lower temperatures, pore water depth profiles from these treatments (Fig. 9a,b) show Mn reduction dominating the redox chemistry of the sediments. Under such conditions sulfate reduction is not expected to occur and based on pore water depth profiles of sulfide it did not. Reduction of Fe and Mn oxides at the SWI appears to have been present in the anoxic low salinity treatment, but as sulfate reduction was minimal at best, it is unlikely for desorption of any MeHg to be associated with this. It is unclear why small negative MeHg fluxes were consistently measured in the anoxic treatments in this experiment. Negative fluxes measured by the flux chamber method are not uncommon and have been observed in similar studies (Choe et al. 2004; Gill et al. 1999). Choe et al. (2004) propose a number of possible explanations for negative MeHg fluxes including the lack of bioirrigation that enhances exchange of interstitial pore water, and the dominance of demethylation processes. The magnitude of these fluxes relative to other studies is on the low end of the spectrum (Table 9) and though they are statistically significant, this should be taken into consideration.

DOC flux was, again, difficult to interpret and there appear to be more factors affecting this flux than were studied here. Fluxes of DOC were insignificant or slightly positive for all treatments except the anoxic low salinity. It is unclear why this treatment had a negative flux as reduction of metal oxides had previously been associated with positive fluxes of DOC (experiments I & II). Sulfate fluxes were positive for all treatments. Fluxes under the initial treatment of low salinity were generally smaller then

they were under the treatment of freshwater. This is expected as no sulfate reduction was detected in any treatments and the replacement of the low salinity water with freshwater increased the sulfate concentration gradient from the sediment to the water which presumably increased the diffusive flux.

Solid Phase Mercury, MeHg, R-Fe, and R-Mn

Additional cores for sectioning and solid phase analysis were taken for experiments III & IV from the White Oak River and Eagle Island site, respectively. Comparison of these two sites is not ideal due to differences in seasonality, but some general conclusions, as they pertain to the pore water profiles and Hg fluxes, can be discerned. The vertical distribution of MeHg in these profiles is consistent with previous studies (Bloom et al. 1999; Choe et al. 1994; Merritt et al. 2008). The White Oak River, with variable Fe and Mn detected near the SWI of the oxic treatments, had measurably higher concentrations (>500 pg g^{-1}) of MeHg near the SWI. This is believed to be a result of reduced Fe and Mn oxidizing upon aeration and forming metal oxyhydroxides to which the MeHg is binding and accumulating which is consistent with the negative MeHg fluxes observed in these treatments. White Oak River was thought to be a relatively pristine, uncontaminated site, but sediment analysis showed higher concentrations of TDHg than in Eagle Island sediments. However, relative to the overall range of sediment Hg concentrations reported over the years (Table 10), this difference is quite small. MeHg concentrations were higher in White Oak sediments during the summer than they were in Eagle Island sediments during winter. One would expect this as sulfate reduction was active in White Oak sediments and not observed in Eagle Island

winter sediments. Interestingly, however, upon closer examination of percent of TDHg that is MeHg a higher percentage was seen in Eagle Island sediments (Fig. 18) suggesting some factor inhibting Hg methylation in White Oak sediments. Because sediment Hg concentration for Eagle Island sediment was only determined in the last experiment, it is uncertain, but suspected that during months of increased sulfate reduction (i.e. late summer-early fall), concentrations of MeHg would have been greater.

R-Fe and R-Mn concentrations were only slightly affected in the surface layer by overlying water conditions. Eagle Island sediments had two and three times the maximum concentration of R-Fe and R-Mn, respectively, than the White Oak site. The higher concentration of R-Fe and R-Mn and associated Fe and Mn oxides may be a result of the lower concentration of labile organic matter in these sediments and may be important in understanding the potential of these sediments as a source of MeHg to the overlying water under anoxic conditions.

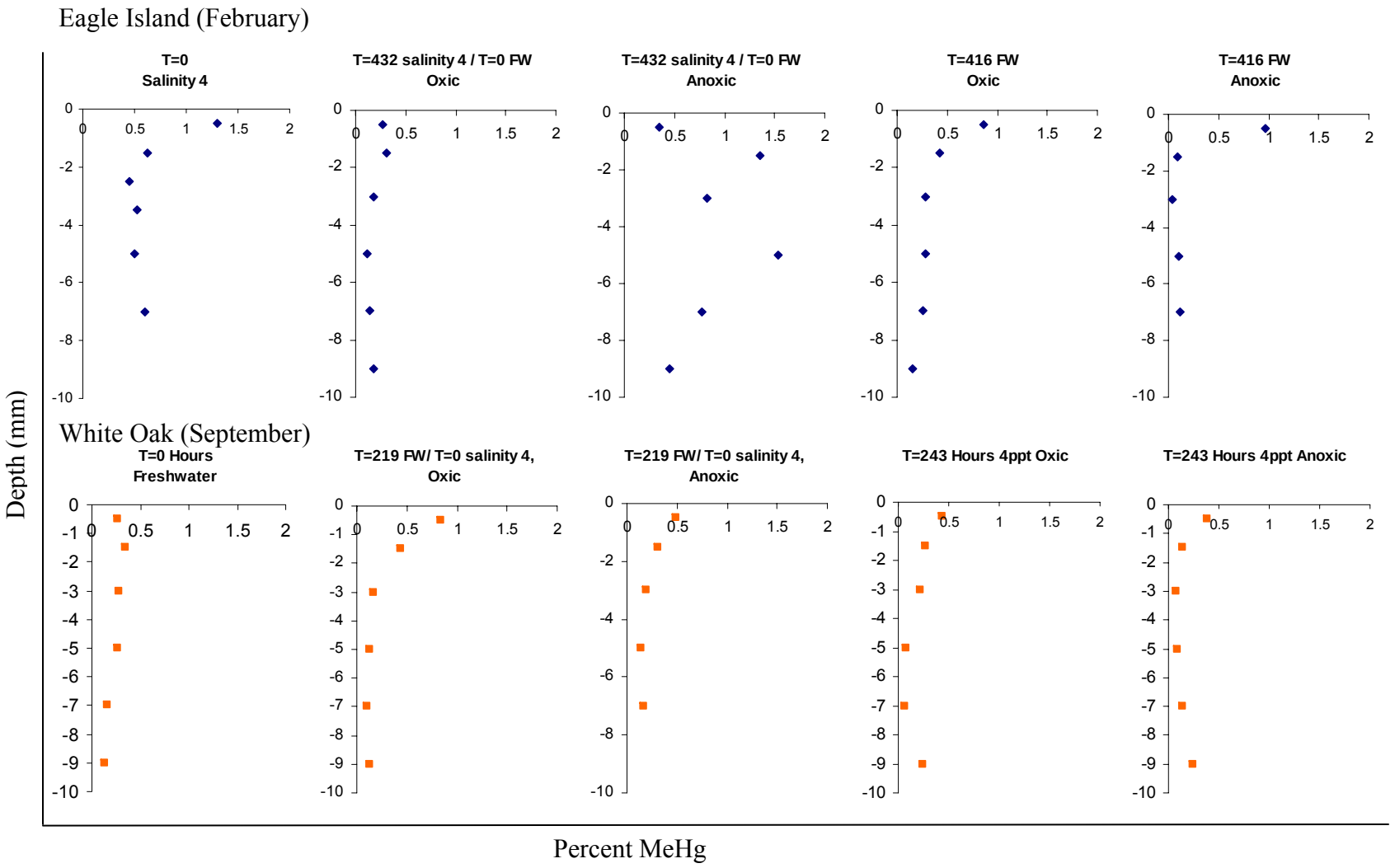

Figure 19. Sediment percent MeHg profiles at the beginning and end of each treatment for Eagle Island site (February) and White Oak River site (September)

Table 11. Comparison of MeHg flux results from a range of salinities, methods, and levels of contamination. Methods include sediment incubation chamber (SIC), diffusive flux (DF), and benthic flux chamber (BFC). diffusive fluxes are calculated using Fick's first law and pore water concentration gradients.

Location	Method	MeHg (pmol/m2/day)	Sediment MeHg (ng/g)	Sediment TDHg (ng/g)	Salinity	Reference
White Oak	SIC	-12 to 6	0.1 - 1.4	≤225	0	Vinson 2008
Eagle Island, Cape Fear River, NC	SIC	-36 to 36	0.02 - 1.4	≤125	0-6	Vinson 2008
Baltimore Harbour, MD	SIC	12 to 50	unknown	≤2,092	5 - 18	Mason et al. 2006
Lake St. Francis, Ontario, Can.	DF	-7 to 47	1 - 13	≤320	0	Holmes et al. 2006
St Lawrence River Wetland, Can.	DF	-1 to 25	0.4 - 1.7	≤54	0	Goulet et al. 2007
Lavaca Bay, TX.	BFC	75 to 770	1.4 - 6.5	≤789	15 - 25	Gill et al. 1999
San Francisco Bay Delta	BFC	-92 to 850	2.8 - 6.5	≤1000	0 - 9	Choe et al. 2004
Gulf of Trieste, Northern Adriatic	BFC	-530 to 12,000	≤72	≤3600	33 - 39	Covelli et al. 1999

IMPLICATIONS

Pore water profiling of Eagle Island sediments as a function of time showed a very gradual consumption of reducible Mn and, to some extent, Fe despite reducible Fe and Mn sediment concentrations typical of coastal marine sites. Based on the three Eagle Island experiments, Mn reduction was the dominant remineralization pathway for most of the year. This slow consumption of Mn supports the contention that surface sediments along this section of the Cape Fear River are old marsh sediments and contain little labile organic content necessary to drive the redox processes toward sulfate reduction. Upon depletion of Mn, however, these sediments were seen to switch to sulfate reduction in the presence of sulfate. In addition these experiments have shown that anoxic conditions consistently result in the reduction of metal oxides at the SWI. The two factors that were seen to affect the direction and rate of MeHg flux in these sediments were the zone at which sulfate reduction ocurrs and the redox state of Fe and Mn at the SWI.

These findings have significant implications with regard to sea level rise and salt water intrusion. Eagle Island is an example of a site that during non-drought years is predominantly freshwater. If salinity increases, sulfate reduction, likely to occur in late summer, coupled with anoxic events may result in enhanced fluxes of MeHg to the Cape Fear River estuary. With continued saltwater intrusion, due to sea level rise or river widening, current freshwater sediments may act as a new source of MeHg to the Cape Fear River. In the case of sea level rise and river widening the surface area of the river bottom is effectively increased which in turn increases the amount of MeHg fluxing into the overlying water. If we assume the sediments studied here to be low in labile organic material, then the increase of MeHg from these sediments may be compounded by a new

source of labile organic matter as the water level approaches the upper, nutrient rich, new marsh. A sudden increase in labile organic matter could result in more frequent anoxia and MeHg flux.

The experiment carried out with White Oak River sediments, showed no flux of MeHg and needs further investigation. Having carried out only one experiment at that site during one season, one can not extrapolate seasonal trends or typical sediment biogeochemical responses to saltwater inundation. Pore water profiling showed that the sediments, and bacterial populations, were responsive to introduced sulfate and immediately began or increased sulfate reduction. These sediments are typically anoxic and show little sign of maintaining a metal oxide barrier against diffusing MeHg. Despite these conducive conditions no flux was seen. Possible mechanisms resulting in organic matter complexation with neutral dissolved Hg (Miller et al. (2006), or an increase in the distribution coefficient of MeHg (Bloom et al. 1999; Hammerschmidt et al 2004) may be responsible.

DOC fluxes were often large, both into and out of the sediment, relative to previous studies (Burdige et al., 1999; Alperin et al., 1999., Mason et al., 2006). Positive fluxes were often seen to correlate directionally with the anoxic treatments suggesting that reduction of metal oxides may be a factor controlling DOC to overlying water. Concentrations of DOC in the overlying water were far greater than those of Fe^{2+}, and Mn^{2+} at the SWI suggesting that oxidation state of metal oxides is not the only source of these large DOC fluxes. Though all the factors responsible are unclear, these data indicate that variations in both salinities and oxygen content of the water overlying estuarine sediment can significantly change the rates of DOC transfer across the SWI.

Further investigations using sediment flux chambers to examine DOC and related parameters such as bioturbation rates, particle size, porosity, pH, and mineral surface area, would be necessary to better understand these DOC fluxes.

REFERENCES

Aller, R.C., 1994. The sedimentary Mn cycle in Long Island Sound: its role as an oxidant and the influence of bioturbation,O2 and Corg flux on diagenetic reaction balances. Journal of Marine Research 52, 259–295.

Alperin, M.J., Martens, C.S., Albert, D.B., Suayah, I.B., Benninger, L.K., Blair, N.E., 1999. Benthic fluxes and porewater concentration profiles of dissolved organic carbon in sediments from North Carolina continental slope. Geochim. Cosmochim. Acta, 63, 427-448.

Avery, G.B., Shannon, R.D., White, J.R., Martens, C.S., Alperin, M.J., 2002. Controls on methane production in a tidal freshwater estuary and a peatland: methane production via acetate fermentation and CO_2 reduction. Biogeochemistry, 62, 19-37.

Barkay, T., 1992. Encyclopedia of Microbiology Vol. 3 Academic Press, San Diego, pp. 65-74.

Bartlett, R., Mortimer, R.J.G,Morris, K.M., 2007. The biogeochemistry of a manganese-rich Scottish sea loch: Implications for the study of anoxic nitrification. Contin. Shelf Res. 27, 1501-1509.

Barnhill, W.L. 1992. Soil surveyof onslow county. Dep. of Agriculture, Soil Conservation Service, North Carolina, US.

Benoit, J.M, Gilmour, C.C., Mason, R.P., Heyes, A., 1999. Sulfide controls on mercury speciation and bioavailability in sediment pore waters. Environ. Sci. Technol. 33, 951-957

Benoit, J.M., Gilmour, C.C., Mason, R.P., 2001. The influence of sulfide on solid phase mercury bioavailability for methylation by pure cultures of *Desulfobulbus propionicus*. Environ Sci Technol 35,127–132.

Beutel, M.W., Leonard, T.M., Denta, S.R., Moore, B.C., 2008. Effects of aerobic and anaerobic conditions on P, N, Fe, Mn, and Hg accumulation in waters overlaying profundal sediments of an oligo-mesotrophic lake. Water Research, 42, 1953 – 1962.

Bloom, N.S., Gill, G.A., Cappellino, S., Dobbs, C., McShea, L., Driscoll, C., Mason, R., Rudd, J., 1999. Speciation and Cycling of mercury in Lavaca Bay, Texas, sediments. Environ. Sci. Technol. 33, 7-13.

Brendel, P.J., Luther, G.W., 1995. Development of a gold amalgam voltammetric microelectrode for determination of dissolved Fe, Mn, O_2, and S(-II) in pore waters of marine and freshwater sediment. Environ. Sci. Technol. 29, 751-761.

Brett, C.M.A and Brett, A.M.O (1998) Electroanalysis. Oxford University Press, Inc, New York.

Burdige, D.J., 1993. The biogeochemistry of manganese and iron reduction in marine sediments. Earth-Science Reviews 35, 249–284.

Burdige, D.J., 2006. Geochemistry of marine sediments. Princeton University Press.

Burdige, D.J., Homestead, J., 1994. Fluxes of dissolved organic carbon from Chesapeake Bay sediments. Geochim. Cosmochim. Acta, 58, 3407-3424.

Burdige, D.J., Berelson, W.M., Coale, K.H., McManus, J., Johnson, K.S., 1999. Fluxes of dissolved organic carbon from California continental margin sediments. Geochim. Cosmochim. Acta, 63, 1507-1515.

Canfield, D.E., Thamdrup, B., Hansen, J.W., 1993. The anaerobic degradation of organic matter in Danish coastal sediments: iron reduction, manganese reduction, and sulfate reduction. Geochim. Cosmochim. Acta. 57(16), 3867-83.

Chadwick, S.P., Babiarz, C.L., Hurley, J.P., Armstrong, D.E., 2005 Influence of iron, manganese and dissolved organic carbon on the hypolimnetic cycling of amended mercury. Sci. Tot. Environ. 368, 177-188.

Chanton, J.P., Martens, C.S., 1988. Seasonal variatios in ebullitive flux and carbon isotopic composition of methane in a tidal freshwater estuary. Global. Biogeochem. Cycles 2, 289-298.

Chanton, J.P., Martens, C.S., Kelley, C.A., 1989. Gas transport from methane-saturated tidal freshwater and wetland sediments. Limnol. Oceanogr. 34, 807-819.

Choe, K.Y., Gill, G.A., Lehman, R.D., Han, S., 2004. Sediment-water exchange of total mercury and monomethyl mercury in the San Francisco Bay-Delta. Limnol. Oceanogr., 49(5), 1512-1527.

Compeau, G.C., Bartha, E., 1985. Sulfate-reducing bacteria: principle methylators of mercury in anoxic estuarine sediment. Appl. Environ. Microbiol. 50, 498-502.

Compeau, G.C., Bartha, E., 1984. Methylation and demethylation of mercury under controlled redox, pH, and salinity conditions. Appl. Environ. Microbiol. 48(6), 1203-1207.

Covelli, S., Faganeli, J., Horvat, M., Brambati, A., 1999. Porewater distribution and benthic flux measurements of mercury and methylmercury in the Gulf of Triest (Northern Adriatic Sea). Estuar. Coast. Shelf Sci. 48, 415-428.

Davison,W., 1993. Iron and manganese in lakes. Earth-Sci. Rev. 34, 119–163.

Environmental Protection Agency Fact Sheet: National Listings of Fish Advisories, EPA-823-F-07-003; July 2007, http://www.epa.gov/waterscience/fish/advisories /2006/tech.html.

Environmental Protection Agency, 2002. Method 1631, Revision E: Mercury in water by oxidation, purge and trap and cold vapor atomic fluorescence spectrometry. EPA-821-R-02-019.

Environmental Protection Agency, 1998. Method 1630: Methyl mercury in water by distillation, aqueous ethylation, purge and trap, and cold vapor atomic fluorescence spectrometry.

Fitzgerald, W.F., Engstrom, D.R., Mason, R.P., Nater, E.A., 1998. The case for atmospheric mercury contamination in remote areas. Environ. Sci. Technol. 32, 1-7.

Fleming, E.J., Mack, E.E., Green,P.G., Nelson, D.C., 2006. Mercury Methylation from Unexpected Sources: Molybdate-Inhibited Freshwater Sediments and an Iron-Reducing Bacterium. Appl. Environ. Microbiol. 72(1), 457-464.

Froelich, P.N., Klinkhammer, G.P., Bender, M.L., Luedtke, N.A., Heath, G.R., Cullin, D., Dauphin, P., Hammond, D., Hartman, B., Maynard, V., 1979. Early oxidation of organic matter in pelagic sediments of the eastern equatorial Atlantic: suboxic diagenesis. Geochim. Cosmochim. Acta. 43, 1075-1090.

Gagnon, C., Pelletier, E., Mucci, A., Fitzgerald, W.F., 1996. Diagenetic behavior of methylmercury in organic-rich coastal sediments. Limnol. Oceanogr. 41(3), 428-434.

Gill, G.A., Bloom, N.S., Cappellino, S., Driscoll, C.T., Dobbs, C., McShea, L., Mason, R., Rudd, J.W.M., 1999, Sediment-water fluxes of mercury in Lavaca Bay, Texas. Eviron. Sci. Technol. 33, 663-669.

Gilmour, C.C., Henry,E.A., Mitchell, R., 1992. Sulfate Stimulation of Mercury Methylation In Freshwater Sediments. Environ. Sci. Technol. *26,* 2281-2287.

Goulet, R. R., Holmes, J., Page, B., Poissant, L., Siciliano, S.D., Lean, D.R.S., Wang, F., Amyot, M., Tessier, A., 2007. Mercury transformations and fluxes in sediments of a riverine wetland. Geochim. Cosmochim. Acta. 71, 3393–3406.

Hackney, C.T., Posey, M., Leonard, L.L., Alphin, T., and Avery, G.B., Jr. (2006) "Monitoring effects of a potential increased tidal range in the Cape Fear River ecosystem due to deepening Wilmington Harbor, North Carolina." Year 6: June 1, 2005-May 31, 2006. Report to Army Corps of Engineers, Wilmington District, Contract DACW 54-02-0009, 311p.

Hackney, C.T., Posey, M., Leonard, L.L., Alphin, T., and Avery, G.B., Jr. (2007) "Monitoring effects of a potential increased tidal range in the Cape Fear River ecosystem due to deepening Wilmington Harbor, North Carolina." Year 7: June 1, 2006-May 31, 2007. Report to Army Corps of Engineers, Wilmington District, Contract DACW 54-02-0009.

Hammerschmidt, C.R., Fitzgerald, W.F., Lamborg, C.H., Balcom, P.H., Visscher, P.T., 2004. Biogeochemistry of methylmercury in sediments of Long Island Sound. Mar. Chem. 90, 31-52.

Hammerschmidt, C.R., Fitzgerald, W.F., 2005. Methylmercury cycling in sediments on the continental shelf of southern New England. Geochim. Cosmochim. Acta. 70, 918–930.

Hines, M. E., Faganelli, J., Adatto, I., Horvat, M. 2006. Microbial mercury transformations in marine, estuarine and freshwater sediments downstream of the Idrija Mercury Mine, Slovenia. App. Geochem. 21, 1924–1939.

Holmes, J., Lean, D., 2006. Factors that influence methylmercury flux rates from wetland sediments. Science of the Total Environment. 368, 306-319.

Horvat, M., Bloom, N.S., Liang, L., 1993. Comparison of distillation with other current isolation methods for the determination of MeHg compounds in low level environmental samples. Part I. Sediment. Anal. Chim. Acta. 282, 135-152.

Horvat, M., Coveli, S., Faganeli, J., Logar, M., Mandić, V., Rajar, R., Širca, A., Žagar, D., 1999. Mercury in contaminated coastal environments; a case study: The Gulf of Triest. Science of the Total Environment. 237-238, 43-56.

Kelley, C.A. 1993. Physical controls on methane production and flux from organic-rich wetland envrinments. PhD Dissertation, Univ. of North Carolina.

Kelley, C.A., Martens, C.S., Ussler, W., 1995. Methane dynamics across a tidally flooded riverbank margin. Limnol. Oceanogr. 40, 1112-1129.

King, J.K., Kostka, J.E., Frischer, M.E., Saunders, F.M., Jahnke, R.A., 2001. A Quantitative Relationship that Demonstrates Mercury Methylation Rates in Marine Sediments Are Based on the Community Composition and Activity of Sulfate-Reducing Bacteria. Environ. Sci. Technol. 35, 2491-2496

King J. K., Saunders F. M., Lee R. F., and Jahnke R. A., 1999. Coupling mercury methylation rates to sulfate reduction rates in marine sediments. Environ. Toxicol. Chem., 18, 1362–1369.

Kostka, J.E., Luther, G.W., 1994. Partitioning and speciation of solid phase iron in saltmarsh sediments. Geochim. Cosmochim. Acta, 58, 1701-1710.

Kounaves, S.P. (1997) "Voltammetric Techniques" in Handbook of Instrumental Techniques for Analytical Chemistry. F.A.Settle (Ed.) Prentice Hall PTR, Upper Saddle River, NJ.

Lamborg, C.H., Fitzgerald, W.F., O'Donnell, J., Torgersen, T., 2002. An examination of global-scale mercury biogeochemistry using a non-steady state compartment model which features interhemispheric gradients in the atmosphere as constraints. Geochim. Cosmochim. Acta, 66, 1-14.

Luther III, G.W., Sundby, B., Lewis, B.L., Brendel, P.J., Sliverberg, N., 1997. Interactions of manganese with the nitrogen cycle: alternative pathways to dinitrogen. Geochimica et Cosmochimica Acta, 61 (19), 4043–4052.

Luther, G.W., Brendel, P.J., Lewis, B.L., Sundby, B., Lefrancois, L., Silverberg, N., Nuzzio, D., 1998. Simultaneous measurement of O_2, Mn, Fe, I^-, and S(-II), in marine pore waters with a solid-state voltammetric microelectrode. Limnol. Oceanogr. 43(2), 325-333.

Mallin, M.A., 2008. The ecology of the Cape Fear River system. University of North Carolina Wilmington. http://www.uncwil.edu/riverrun/river_tutorial/ CFRSystem.htm. (June, 2008).

Marten, C.S., Goldhaber, M.B., 1978. Early diagenesis in transitional sedimentary environments of the White Oak River Estuary, North Carolina. Limnol. Oceanogr. 233, 428-441.

Mason, R.P., Kim, E., Cornwell, J., Heyes, D., 2006. An examination of the factors influencing the flux of mercury and methylmercury and other constituents from esuarine sediment. Mar. Chem. 102(1-2), 96-110.

Mason, R.P., Reinfelder, J.R., Morel, F.M.M., 1996. Uptake, toxicity, and trophic transfer of mercury in a coastal diatom. Environ. Sci. Technol. 30, 1835-1845.

Meites, L. (1965) Polarographic Techniques, 2nd edition. Wiley Interscience, New York.

Merrit, K.A., Amirbahman, A. 2007. Methylmercury cycling in estuarine sediment pore waters (Penobscot River estuary, Maine, USA). Limnol. Oceanogr. 53(3), 1064-1075.

Miller, C.L., Mason, R.P., Gilmour, C.C., Heyes, A., 2007. Influence od sissolved organic matter on the complexation of mercury under sulfidic conditions. Environ. Toxicol. Chem., 26(4), 624-633.

Morel, F.M.M., Kraepiel, A.M.L, Amyot, M. 1998. The chemical cycle and bioaccumulation of mercury. Annu. Rev. Ecol. Syst. 29, 543-566.

Olson, B.H.; Cooper, R.C., 1974. In situ methylation of mercury in estuarine sediment. Nature, 252, 682.

Shaughnessy, G.A., 2007. Surface and scale processes of biogeochemical cyclingof organic matter in tidal marsh sediments. Masters Thesis, Univ. North Carolina at Wilmington.

Shia, F., Ducklow, H.W., 1994. Temperature and substrate regulation of bacterial abundance, production and specific growth rate in Chesapeake Bay, USA. Mar. Ecol. Prog. Ser. 103, 297-308.

Skrabal, S.A., Donat, J.R., Burdige, D.J., 1997. Fluxes of copper-complexing ligands from estuarine sediments. Limnol. Oceanogr., 42, 1803-1813.

Sørensen, J., Jørgensen, B.B., 1987. Early diagenesis in sediments from Danish coastal waters: microbial activity and Mn–Fe geochemistry. Geochim. Cosmochim. Acta 51, 1583-1590.

Spry, D.J., Wiener, J.G.,1991. Metal bioavailability and toxicity in fish in low-alkalinity lakes: A critical review. Environ. Pollut. 71 (2-4), 243-304.

Stumm, W., Morgan, J.J.,1996. Aquatic Chemistry: Chemical equilibria and rates in natural waters, 3rd ed. Wiley-Interscience.

Zar, J.H., 1984. Biostatistical Analysis, 2nd ed. Prentice-Hall, Inc